COMPRESSIBILITY AND STRENGTH CHARACTERISTICS OF A PARTIALLY SATURATED BLACK COTTON SOIL OF NORTH-EASTERN NIGERIA

BY

OJURI OLUWAPELUMI OLUMIDE

CVE / 97 / 9901

A THESIS IN THE DEPARTMENT OF CIVIL ENGINEERING SUBMITTED TO THE SCHOOL OF POSTGRADUATE STUDIES TOWARDS THE DEGREE OF MASTER OF ENGINEERING IN TRANSPORTATION ENGINEERING

DEPARTMENT OF CIVIL ENGINEERING

SCHOOL OF ENGINEERING AND ENGINEERING TECHNOLOGY

FEDERAL UNIVERSITY OF TECHNOLOGY, AKURE, ONDO STATE NIGERIA.

JANUARY, 2001

CERTIFICATION

This is to certify that this research work was carried out and written by **Ojuri Oluwapelumi Olumide**

Prof J. B. Adeyeri
Supervisor

Signature and Date 27-02-20

DEDICATION

To my parents, whose investments in the education of their children are invaluable.

ACKNOWLEDGEMENT

I must confess that I am indeed overwhelmed by the rare attention and fatherly encouragement of my supervisor, **Prof. J.B. Adeyeri.** I am greatly indebted to him for his drive and support in carrying out this work.

I acknowledge the keen interest and co-operation of **Dr A.M. Oguntuase** and all members of staff of the department of Civil Engineering Federal University of Technology Akure.

I also acknowledge the contributions of my colleagues **Mr. B.J. Abiodun, Mr. Walter Osedeme** and Mr. Adams to the success of this project.

Finally, the author cannot overlook the love, care, help and moral support of his best friend **Omoleye,** during the period of this project.

Jesus Christ the author's source of strength and being must above all be acknowledged.

O.O. Ojuri

August, 2000

TABLE OF CONTENTS

LIST OF FIGURES

LIST OF TABLES

LIST OF PHOTOGRAPHS

NOMENCLATURE

U_w	-	Pore Water Pressure
U_a	-	Pore air Pressure
e	-	Void ratio
C_v	-	Coefficient of Consolidation
M_v	-	Coefficient of Volume Compressibility
H	-	Height
γ_w	-	Unit weight of water
γ_a	-	Unit weight of air
γ	-	γ_w / γ_a
τ_{ff}	-	Shear Strength
C_u	-	Cohesion (undrained condition)
ϕ_u	-	Angle of Shearing resistance (undrained condition)
σ_{ff}	-	Total Stress
X	-	Effective Stress parameter
σ^1	-	Effective Stress
Ψ	–	Total Suction
$U_a - U_w$	-	Matric Suction
π	-	Osmotic Suction
a_r	-	Coefficient of Compressibility

S_r	-	Degree of Saturation
w	-	Moisture content
C_c	-	Compression index
C_s	-	Swell index

ABSTRACT

The consolidation and strength characteristics of a partially saturated clay soil are studied theoretically and experimentally.

The Terzaghi's one-dimensional consolidation equation for saturated soils has been extended to embrace unsaturated soils using unsaturated soil principles and theories. The model equation obtained has been solved using the implicit method of numerical analysis for the assumed initial and boundary conditions. The proposed differential equation for one-dimensional consolidation of a partially saturated soil was used to predict the rate of dissipation of excess pore pressure for partially saturated black cotton soil at various degrees of saturation. It was found that except at the initial stage the profiles of pore water pressure U_w, pore air pressure U_a and void ratio e follow a parabolic pattern during the process of consolidation. The rate of reaching complete saturation was found to be decreasing with height from the bottom of the clay layer as expected depending on the degree of saturation, also the lower the degree of saturation, the faster is the rate of change of the pore pressures.

Oedometer, triaxial compression and suction tests were performed in the laboratory on samples of Black Cotton soil compacted by static compaction to various degrees of saturation and moisture content. The investigation indicated that significant changes in the volume and shear strength of a partially saturated soil would accompany slight variations in the moisture content of the soil when the degree of saturation is below 80%. This can also be inferred from the theoretical considerations which shows that the rate of change of the pore pressures is quite remarkable with degree of saturation, especially when this is below 80%. Equations 5.4 and 5.6 relate the pore pressures with compression index 'C_c' and shear strength 'τ_f'. The data

obtained from the experimental programme also emphasize that, for design of pavements, especially in arid and semi-arid regions, one must consider not only material changes but also potential significant changes in soil suction for the same material.

From the results, a more accurate prediction of the magnitude and rate of consolidation settlement, in advance of construction for Black Cotton soil at a specific state of soil moisture can now be determined. It is recommended that minimum variations in soil moisture and equilibrium moisture conditions should be maintained for highways with Black Cotton soil subgrade. It is also suggested that periodic measurement of soil suction for such highways can be used as a means of evaluating pavement performance.

CHAPTER ONE

INTRODUCTION

1.1 GENERAL

Current soil mechanics theory and practice have mainly been developed in those areas of North America and Europe where high water table and freeze-thaw conditions are usual and soils are predominantly saturated or near saturation for many months of the year. Consequently, the simplifying assumptions made are applicable only to saturated soils, composed only of the solid and liquid phases. Geometric relationships are therefore simple, and as both phases are relatively incompressible, the soil can be assumed to be incompressible under undrained conditions. Furthermore, the effective stress law holds for practical purposes which can lead to simpler laboratory test procedures.

Since semi-arid to arid climate conditions predominate in many of the newer developing nations, such as in Africa, Australia etc., as indicated in Figure 1.1. Thus the soils are usually unsaturated throughout most of the year and pose many problems to soil engineers.

Erroneous predictions and incorrect decisions often result from the use of current codes of practice, which are not applicable to unsaturated soils. A good example is the lack of appreciation of water flow through unsaturated soils. In many instances, granular layers, which work as drainage layers in saturated soils will actually lead to the wetting up of the unsaturated soil and cause serious heave and failure problems.

Significant areas of the earth's surface are arid zones. The annual evaporation from the ground surface in these regions often exceeds the annual precipitation. Figure 1.1 shows the climatic classification of the extremely arid, arid and semi-arid areas of the world. Meigs (1953) used the Thornthwaite moisture index to map these zones. He excluded the cold deserts. Regions with a Thornthwaite index between – 20 and - 40 are classified as semi-arid areas. A Thornthwaite index less than – 40 indicates arid areas. About 33% of the earth's surface is considered arid and semi-arid.

Arid and semi-arid areas usually have a deep groundwater table, soils located above the water table have negative pore-water pressures. The soils are generally unsaturated due to the excessive evaporation and evapo-transpiration. Upon wetting the pore-water pressures increase tending towards positive values. As a result, changes occur in the volume and shear strength of the soil. Many soils exhibit extreme swelling or expansion when wetted. Other soils show a significant loss of shear strength upon wetting. Reductions in the bearing capacity and resilient modulus of soils are also associated with increase in the negative pore-water pressure. These phenomena indicate the important role of negative pore-water pressures in controlling the mechanical behaviour of unsaturated soils.

When the degree of saturation of a soil is greater than approximately 85% saturated soil mechanics principles can be applied with reasonable success provided the negative pore-water pressure can be measured. However, when the degree of saturation goes below about 85%, it becomes necessary to extend saturated soil mechanics principles to embrace unsaturated soils. Soils used in the construction of highways fall into this latter category particularly in arid areas.

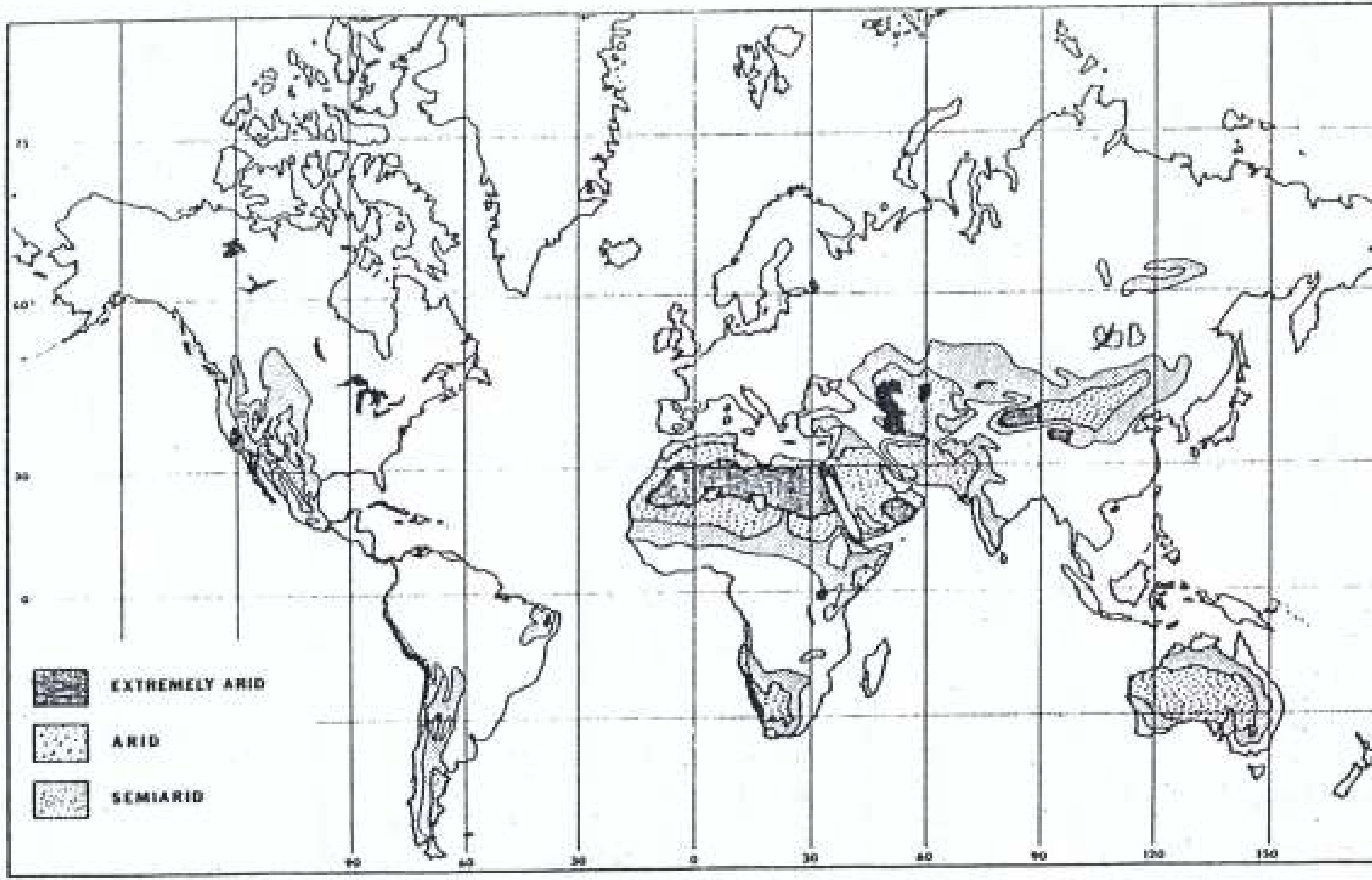

Figure 1.1: Extremely arid, arid and semi-arid areas of the World (1 and 2) (Fredlund and Rahardjo, 1987)

Therefore, it is important that unsaturated soil mechanics be incorporated into engineering principles associated with highway design.

1.2 OBJECTIVES OF STUDY

The Objectives of the study are:

i. To study the shear strength and volume change behaviour of partially saturated clay soils under simple states of stress.

ii. To extend the theory of one-dimensional consolidation based on saturated soil assumptions to the analysis of partially saturated soils.

iii. To find out the influence/effects of soil suction on the engineering properties of soils.

iv. To apply partially saturated soil theories to the analysis of black cotton soils as a highway construction material in a semi-arid region.

1.3 SCOPE OF WORK

a. Theoretical Studies:

One-dimensional consolidation theory based on fully saturated soil conditions was studied and extended to partially saturated soils. This led to the derivation of a basic differential equation for one-dimensional consolidation of partially saturated soils. Based on assumed initial and boundary conditions, a numerical solution of the resulting differential equation was obtained using the implicit scheme for diffusion.

b. Experimental Programme

Black cotton soil samples were obtained from a section of existing road with Black cotton soil subgrade from Numan to Guyuk off Yola-Gombe road in Adamawa State of Nigeria,

Identification and classification tests were performed on the samples notably, grain size distribution, Atterberg limits, spercific gravity and compaction tests.

Compressibility and strength characteristics were determined using Oedometer and Triaxial compression tests, while suction measurements were performed on samples compacted to specific water contents and degrees of saturation.

A relationship between soil suction and the consolidation parameters would be established for the soil.

The theoretical results are compared with the experimental findings and appropriate conclusions drawn.

1.4 JUSTIFICATION

The principles of unsaturated soil mechanics can be visualized as an extension of saturated soil mechanics. The understanding of unsaturated soil behaviour is important to many problems relevant to highway engineering in arid and semi-arid areas. Problems associated with volume change and shear strength can be analysed and resolved within consistent theoretical context. These eliminate the need for many empirical approximations which often depend on local practices.

Black cotton soils are problematic soils. Their geotechnical properties, particularly as they affect pavement design, are not well known. The proposed study is therefore a welcome development as it would provide technical information that could be used in the design of highway pavements on Black cotton soils, prevalent in North-Eastern, Nigeria.

CHAPTER TWO

LITERATURE REVIEW

2.1 Fundamentals of Compressibility and Strength

2.1.1 Fundamentals of Consolidation

When a saturated soil layer is subjected to a stress increase, the pore water pressure is suddenly increased. In sandy soils that are highly permeable, the drainage caused by the increase of pore water pressure is completed immediately. Pore-water drainage is accompanied by a volume reduction of the soil mass, resulting in settlement. As a result of rapid drainage of pore water in sandy soils, immediate settlement and consolidation take place simultaneously.

When a saturated compressible clay layer is subjected to a stress increase, elastic settlement occurs immediately. Since the coefficient of permeability of clay is significantly smaller than that of sand, the excess pore water pressure generated due to loading gradually dissipates over a long period of time. Thus the associated volume change (that is the consolidation) in soft clay may continue long after the immediate settlement. The settlement due to consolidation in soft clay may be several times larger than the immediate settlement.

The time-dependent deformation of saturated clayey soils can best be understood by first considering a simple rheological model consisting of a linear elastic spring and dashpot connected in parallel (Kelvin model Figure 2.1) (Das, 1990). The stress-strain relationship of the spring and the dashpot can be given by:

$$Spring : \sigma = \bar{k}\varepsilon \qquad (2.1)$$

$$Dashpot : \sigma = \eta \frac{d\varepsilon}{dt} \qquad (2.2)$$

where σ = stress

ε = strain

k = spring constant

η = dashpot constant

t = time

The visco-elastic response for the stress σ_0 in Figure 2.1 can be written as:

$$\sigma_0 = \bar{k}\varepsilon + \eta \frac{d\varepsilon}{dt} \qquad (2.3)$$

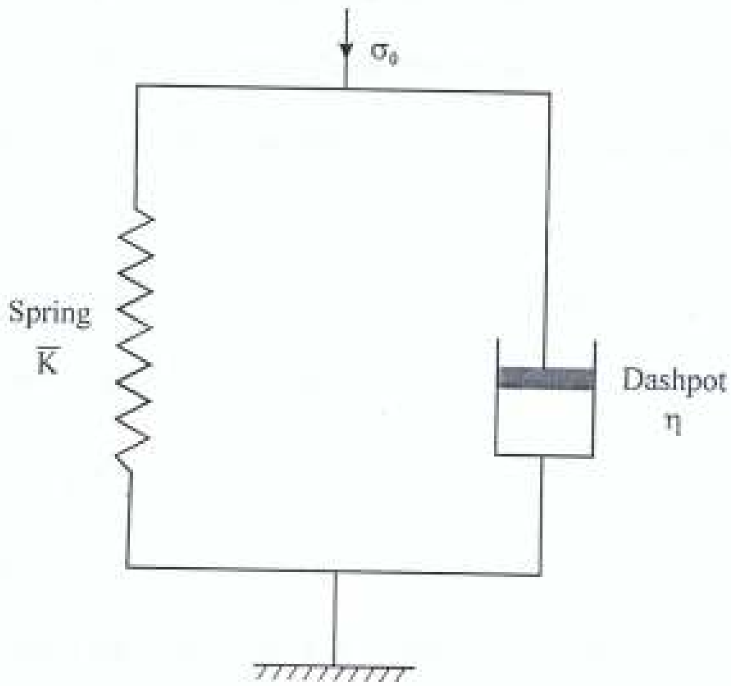

Figure 2.1 The Kelvin model

If stress, σ_0 is applied at time t = 0 and remains constant thereafter the equation for strain at any time t can be found by solving the preceding differential equation. Thus

$$\varepsilon = \frac{\sigma_0}{\bar{k}}(1 - e^{-(\bar{k}/\eta)t}) + \varepsilon_0 e^{-(\bar{k}/\eta)t}$$

where ε_0 = strain at time t =0

If ε_0 is taken to be zero, then

$$\varepsilon = \frac{\sigma_0}{\bar{k}}(1 - e^{-(\bar{k}/\eta)t}) \qquad (2.4)$$

The nature of variation of strain with time represented by eqn (2.4) is shown in Figure 2.2. At time $t = \infty$, the strain will approach the maximum value $\frac{\sigma_0}{\bar{k}}$. This is the strain that the spring alone would have immediately undergone with the application of the same stress σ_0, without the dashpot having been attached to it.

The distribution of stress at any time t between the spring and dashpot can be evaluated from eqns (2.5) and (2.6).

$$\sigma_s = \bar{k}\varepsilon = \sigma_0(1 - e^{-(\bar{k}/\eta)t}) \qquad (2.5)$$

Portion of stress carried by the dashpot:

$$\sigma_d = \eta\frac{d\varepsilon}{dt} = \sigma_0 e^{-(\bar{k}/\eta)t} \qquad (2.6)$$

(Note: $\sigma_0 = \sigma_s + \sigma_d$)

Figure 2.3 shows the variation of $\sigma_s + \sigma_d$ with time. At time t=0, the stress σ_0 is totally carried by the dashpot. The share of stress carried by the spring gradually increases with time. The stress carried by the dashpot decreases at an exponential rate. At time $t = \infty$, the stress σ_0 is carried entirely by the spring.

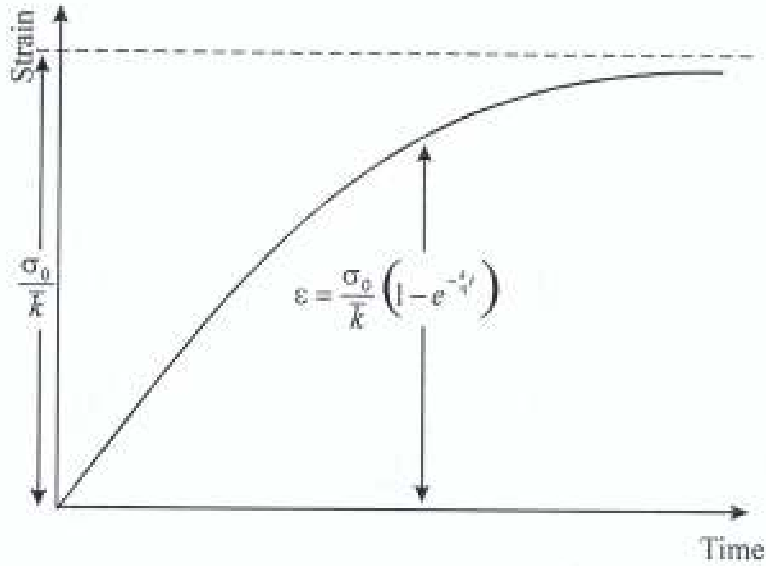

Figure 2.2 Strain-time diagram for the Kelvin model

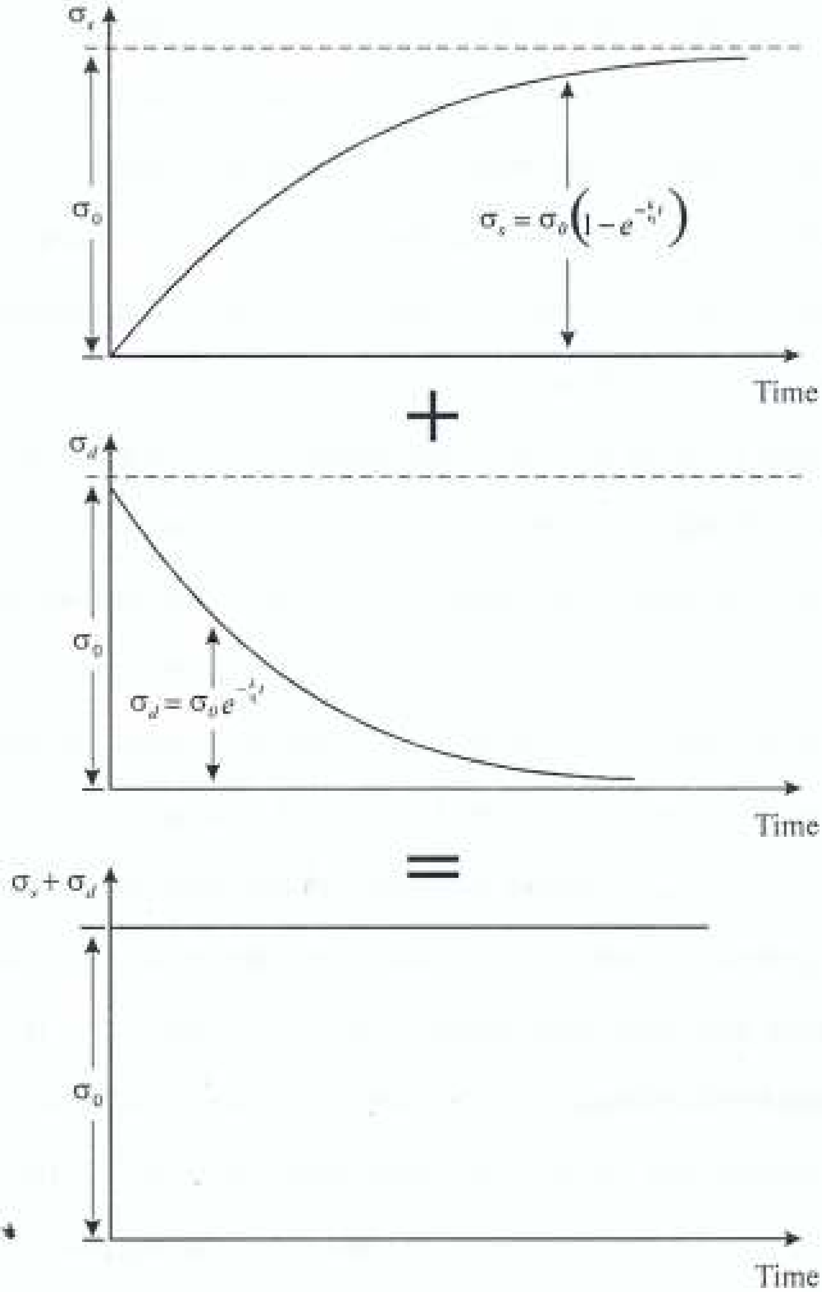

Figure 2.3: Stress-time diagram for spring and dashpot in Kelvin model

2.1.2 One-Dimension Consolidation Laboratory Test:

The one-dimensional consolidation testing procedure was first suggested by Terzaghi (1943). This test is performed in a consolidometer (sometimes referred to as an Oedometer). The schematic diagram of a consolidometer is shown in Figure 2.4. The soil sample is placed inside a metal ring with two porous stones, one at the top of the sample and another at the bottom. The samples are usually 63.5mm (2½in) in diameter and 25 .4mm (1 in) thick. The load on the sample is applied through a lever arm, and compression is measured by a micrometer dial gauge. The sample is kept under water during the test. Each load is usually kept for 24 hours. After that the load is usually doubled thus doubling the pressure on the sample and compression measurement is obtained. At the end of the test, the dry weight of the test sample is determined.

The general shape of the plot of deformation of the sample against time for a given load increment is shown in Figure 2.5. From the plot, it can be observed that there are three distinct stages, which may be described as follows:

Stage I: Initial compression, which is mostly due to preloading.

Stage II Primary consolidation, during which excess pore water pressure is gradually transferred into effective stress because of the expulsion of pore water.

Stage III Secondary consolidation which occurs after complete dissipation of excess pore water pressure, when some deformation of the sample takes place owing to plastic adjustment of the soil fabric.

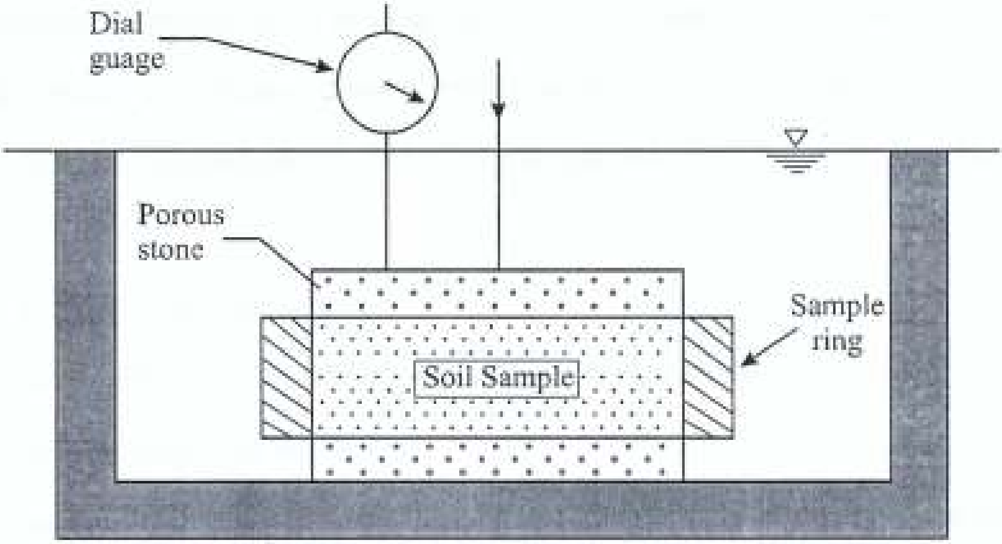

Figure 2.4 Consolidometer (Oedometer)

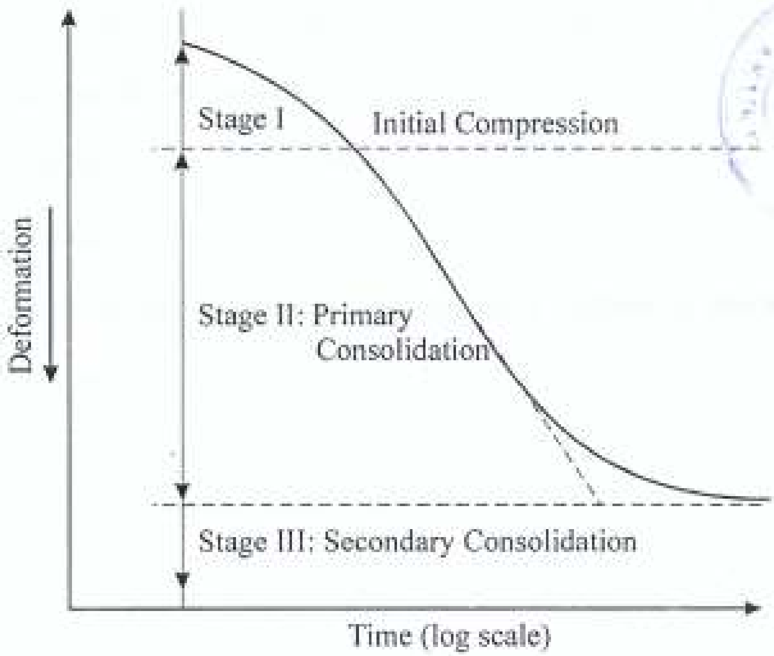

Figure 2.5 Time-deformation plot during consolidation for a given load increment

It is usually necessary to calculate both the magnitude and the rate of the consolidation settlement and in practice, use is generally made of the Terzaghi theory of one-dimensional consolidation which considers the situation shown in Figure 2.6.

The main assumptions on which the Terzaghi theory are based are (Simons and Menzies, 1977):

i. The soil is saturated.

ii. The water and the clay particles are incompressible.

iii. Daicy's law is valid.

iv. For a change in voids ratio corresponding to a given increment in effective stress, the permeability k, and the coefficient of volume change m_v remain constant.

vi. The time taken for the clay to consolidate depends entirely on the permeability of the clay.

vii. The clay is laterally confined.

viii. The flow of water is one-dimensional.

ix. Effective and total stresses are uniformly distributed over any horizontal section.

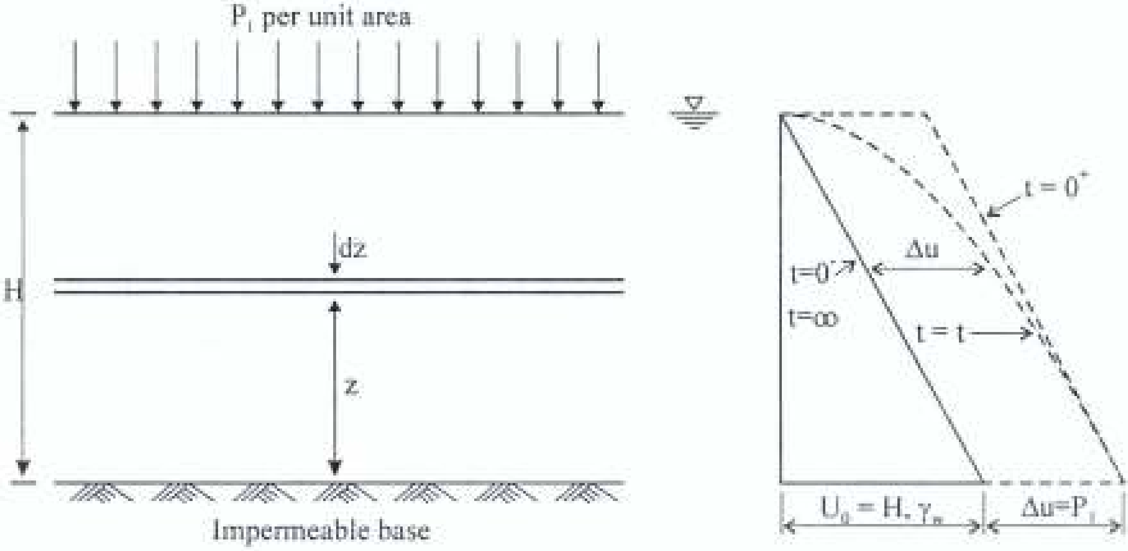

Figure 2.6 Key figure for one-dimensional consolidation

These assumptions correspond to the Oedometer test in the laboratory and to a clay layer in the field subjected to uniform strip loading, that is, a uniformly distributed loading applied over an infinite area.

Based on these assumptions, the governing differential equation relating excess pore-water pressure u, position z, and time t, can be derived as follows (Schiffmann, 1959).

$$\frac{\partial u}{\partial t} = C_v \frac{\partial^2 u}{\partial z^2} \qquad (2.7)$$

where

$$C_v = \frac{k}{m_v \gamma_w} = \text{Coefficient of consolidation}$$

and

$$m_v = \frac{\Delta V}{V} / \Delta P$$

$$= \frac{\Delta H}{H} / \Delta P = \text{Coefficient of volume compressibility}$$

Equation 2.7 must be solved for the following boundary conditions

$\Delta u = P_1$ for t = 0 and $0 \le Z \le H$

$\Delta u = 0$ for t>0 and Z = H

$\Delta u = 0$ for $t = \infty$ and $0 \le Z \le H$

The solution may be expressed in the form:

$$\Delta u = \frac{4P_1}{\pi}\sum_{N=0}^{N=\infty}\frac{(-1)^N}{2N+1}.e^{-(2N+1)^2 \pi^2 (Tv/4)}.Cos[(2N+1)\pi z/2H] \quad (2.8)$$

where

$T_v = \frac{C_v t}{H^2}$, which is an independent dimensionless variable known as Time Factor

It follows that the degree of consolidation U, at any time, (equal to the settlement at that time, δ, expressed as a percentage of the total final settlement, δ_c at the end of consolidation) is given by:

$$u = \frac{\delta_t}{\delta_c} = 1 - \frac{8}{\pi^2}\Sigma\frac{1}{(2N+1)^2}.e^{-(2N+1)^2 \pi^2 \frac{Tv}{4}} \quad (2.9)$$

Using these solutions, it should be noted that the total thickness of the consolidation layer is always used in the computations. The solution relating U and T_v is then taken corresponding to the drainage conditions of the particular problem.

2.1.3 FUNDAMENTALS OF SHEAR STRENGTH

Undrained shear occurs in practical problems whenever external loads change at a rate much faster than the rate at which the induced pore pressures can dissipate. Excess pore pressures dissipate relatively slowly from a clay and relatively rapidly from sand.

The condition of undrained shear is thus of great practical importance in the case of clays. With sands, undrained strength is relatively unimportant for static loadings but may be very important for problems involving dynamic loadings.

The shear strength of partially saturated soils is related to effective stress and this may be evaluated by Eq 2.10b. Clearly, the $\phi = 0$ concept does not in general apply to partially saturated soils. Figure 2.7a shows the typical relation between confining stress and strength during UU (unconsolidated undrained) tests. For the lower range of confining stresses, the soil remains partially saturated and effective stress increases as the confining stress is increased. Once the confining stress becomes large enough to cause full saturation, further increases in confining stress do not cause the effective stress to increase and from this point, the $\phi = 0$ concept does apply; sometimes a relationship between undrained strength and total stress is used:

$$\tau_{ff} = C_u + \sigma_{ff} \tan\phi_u \qquad (2.10a)$$

where C_u and ϕ_u are the total stress parameters. Values for C_u and ϕ_u depend very much upon the range of σ_{ff} which is of interest. Great care must be taken to duplicate expected field conditions (total stress, pore water pressure, and pore air pressure) when performing tests to evaluate the undrained strength of partially saturated soils.

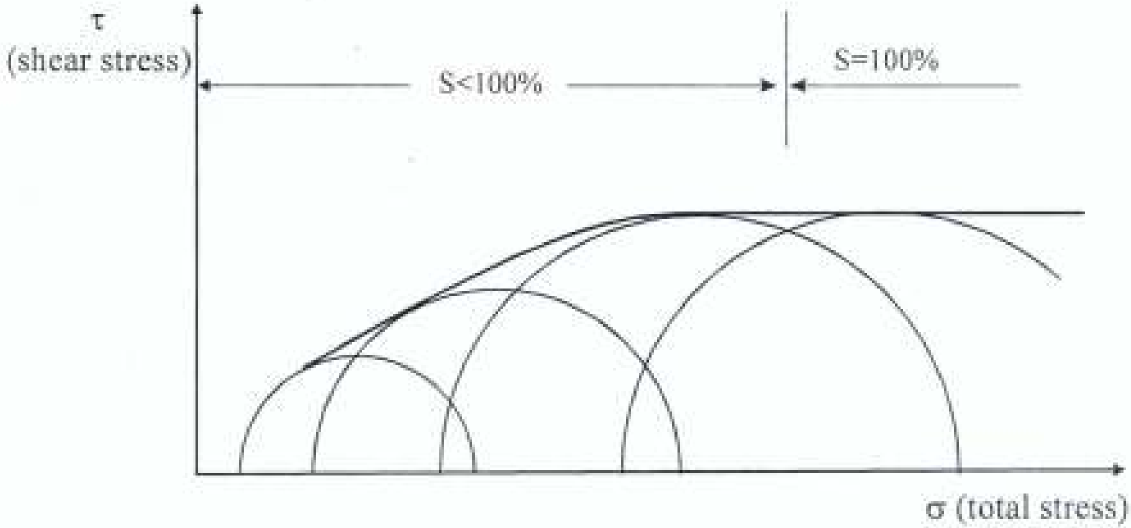

Fig. 2.7a Unconsolidated undrained tests on partially saturated soil.

2.2 BEHAVIOUR OF UNSATURATED SOILS

Soils can be considered to be composed of three phases i.e, solid, liquid and gaseous. When the pore pressure in the liquid phase is positive (e.g in a soil below the water table), any gaseous phase present in the soil can only exist as trapped gas at a higher pressure than the ambient air pressure on the soil. This gas will tend to diffuse out of the system and the soil will tend to reach a fully saturated condition where all the pore spaces are completely filled with water. Therefore, except for a few instances as in the case with the rapid inundation of any unsaturated soil, positive pore pressures will tend to cause the soil to become saturated. On the other hand, when pore pressures become negative, the air-water interfaces tend to become concave and recede into soil pores; large pores may be empty and air bubbles may not only form but also grow in size. Therefore, when negative pore pressure exist, the soil will tend to be unsaturated.

However, even up to significant values of negative pore pressure (as high as $1000kNm^{-2}$) in many clay soils (Holmes, 1955), soils remain essentially saturated and for practical purposes, their behaviour can still be assumed as being saturated. This has been defined as "quasi-saturated" state, (Aitchison, 1956). In general, however by measuring water pressure, the soil can simply and conveniently be assessed as being saturated or unsaturated.

Although present-day practice is as yet more or less unaffected by the research that has been carried out into the behaviour of unsaturated soil and the development of new theories and techniques, the prospect for the future are most promising, particularly in the field of road and air field pavements, building foundations, retaining walls and natural man-made slopes.

2.2.1 WATER PRESSURE IN A CAPILLARY TUBE OR IN UNSATURATED SOIL

If the tip of a capillary tube is inserted in a beaker of water, the attraction of water between glass and water molecules (adhesion) causes water molecules to migrate up the interior wall of the capillary tube. The cohesive force between water molecules causes other water molecules to be drawn up the capillary tube. Now we need to ask, "What are the pressure relationships in the capillary tube?" and "Why is this knowledge important?"

We need to bear in mind that water pressure decreases from the bottom to the top of a beaker filled with water, and that at the top of the water surface, the water pressure is zero. Beginning at the water surface of the beaker and moving upward into the capillary tube, the water pressure continues to decrease. Thus, the water pressure in a capillary tube is less than zero i.e it is "negative". From Fig. 2.7b, one can observe that the water pressure decreases with height above the water in a beaker. At a height of 20cm above the water surface in a beaker, the water pressure in a capillary tube is equal to – 20grams per square centimetre. Figure. 2.7b also shows that at this same height above the water surface, the water pressure in "unsaturated" soil is the same – 20 grams per square centimetre at the 20cm height. The two pressures are the same at any one height and there is no net flow of water from the soil or capillary after an equilibrium condition is established.

Applying the considerations of water in a capillary tube to an unsaturated soil, we can make the following statements:

i. Water in unsaturated soil has a "negative" pressure or is under "tension";

ii. the water pressure in unsaturated soil decreases with increasing distance above the surface of a water table; and

iii. water in unsaturated soil, compared to saturated soil has a lower pressure and lower energy level.

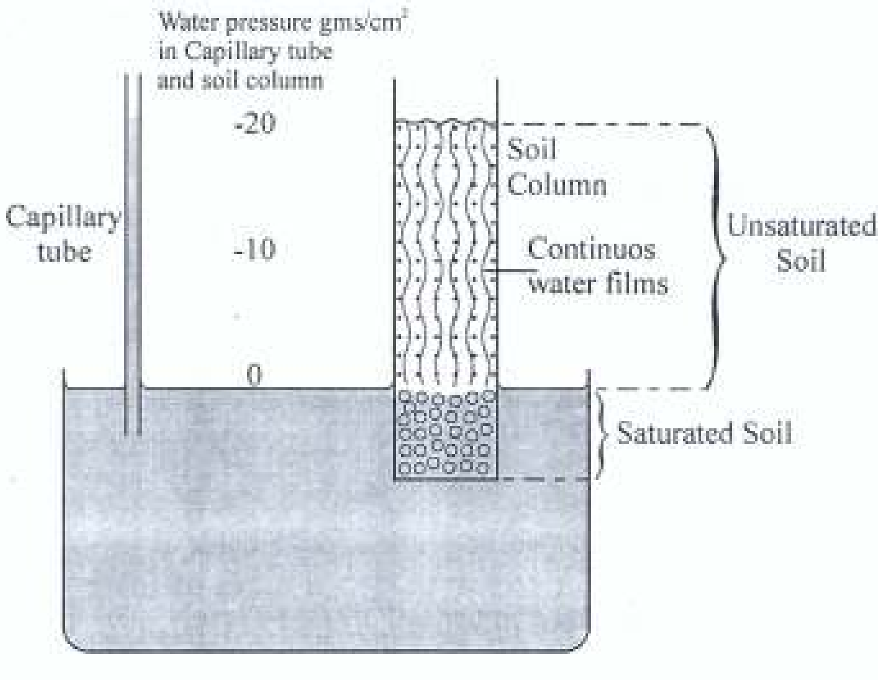

Fig. 2.7b Water pressure in a capillary tube.

2.2.2 EFFECTIVE STRESS IN PARTIALLY SATURATED SOIL

In partially saturated soil, water in the void spaces is not continuous, and it is a three-phase system, i.e., solid, pore water, and pore air (Figure 2.8). Hence the total stress at any point in a soil profile consist of intergranular pore air, and pore water pressures. From laboratory test results, Bishop, et. Al. (1960) gave the following equation for effective stress in partially saturated soils.

$$\sigma^1 = \sigma - U_a + X(U_a - U_w) \qquad (2.10b)$$

where

σ^1 = effective stress

σ = total stress

U_a = pore air pressure

U_w = pore water pressure

X = effective stress parameter

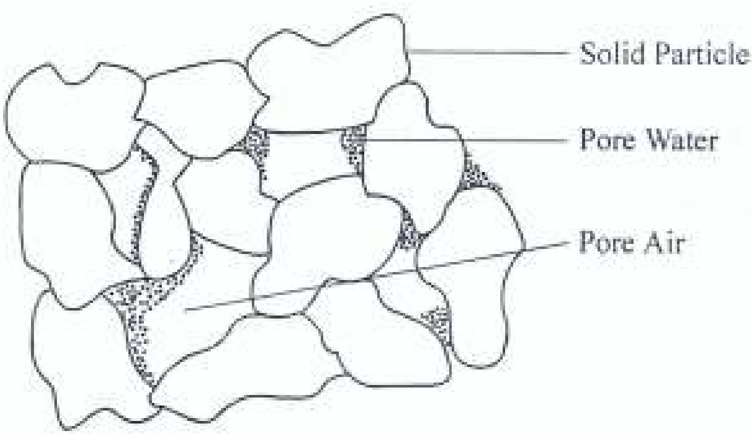

Figure 2.8 Partially Saturated Soil

In Eq. (2.10b), X represents the fraction of a unit cross-sectional area of the soil occupied by water. For dry soil X=0, and for saturated soil X=1.

Bishop et al (1960) have pointed out that the intermediate X will depend primarily on the degree of saturation S. However, these values will also be influenced by other factors such as soil structure.

2.2.3 DEFINITION OF SOIL SUCTION

The behaviour of compacted and natural unsaturated soil is strongly influenced by the state of stress in the pore-water. The pore-water pressure is negative (relative to atmospheric pressure) and varies according to the surrounding micro-climate. A change in the negative pore-water pressure, in turn produces a change in the volume and shear strength of the soil. An understanding of the effect of changing negative pore-water pressure is important from an engineering stand point.

The negative pore-water pressure relative to the pore-air pressure (i.e generally atmospheric conditions) is referred to as matric suction (Croney. and Colemm, 1961). Another component of suction called solute or "osmotic" suction is a function of the salt content of the pore fluid. The sum of the matric suction and solute (osmotic) suction is called total suction. The slowness in the development of a technology for understanding the behaviour of unsaturated soils can be largely traced to the difficulties associated with measuring soil suctions and in particular the negative pore-water pressure.

When pore-water pressure is positive, there is no conceptual difficulty in understanding the presence of water in the soil. However, when pore-water pressures become negative, such as in soil above a water table, the problem of understanding the mechanism become much more difficult. In soil science this problem is now treated thermodynamically, where the mechanism of soil water retention need not be considered in developing a rational understanding and theory of behaviour (Richards, 1974).

When an unsaturated soil comes in contact with a pool of free water as shown in Figure 2.9, it absorbs water; the soil exerts a suction i.e the soil suction on the free water. This can be considered to be a convenient reference state. One way to quantitatively define this soil suction is to apply a suction of the same value to the pool of free water. When the suction on the free water is such that flow between soil and water ceases, then we have a quantitative measurement of soil suction. Using this concept, we can define soil suction as quoted by the International Society of Soil Science as follows:

"Soil suction (h) is the negative gauge pressure relative to the external air pressure on the soil water (normally atmospheric pressure), to which the pool of pure water at the same elevation and temperature must be subjected in order to be in equilibrium with the soil water"

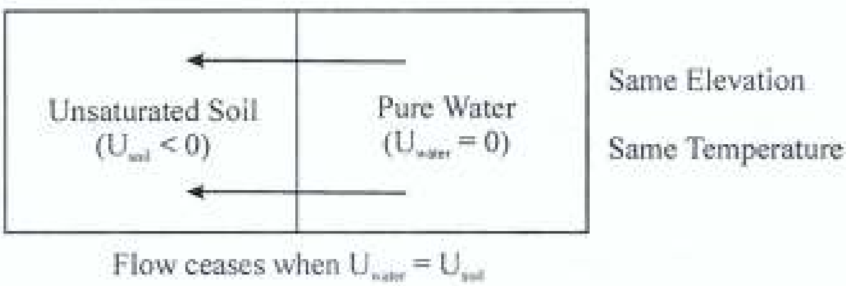

Figure 2.9 Diagrammatic representation for soil suction (Richards, 1974)

The application of negative gauge pressure on the pool of free water is quite conceivable up to 100kNm^{-2} suction e.g., it can readily be applied by standard vacuum pump. When negative gauge pressure or soil suction exceed one atmosphere (values of over 100,000 kNm^{-2} are often measured), the simple concept of negative gauge pressure is no longer valid. Effective suction, however, can be applied to free water by thermal gradient (thermo-osmosis), electric fields (electro-osmosis), solute concentration differences (chemical or solute osmosis) or by elevating reference gas pressure above atmospheric pressure. Although an actual negative gauge pressure is not used on the pool of free water, it is quite correct to define an equivalent or effective gauge pressure.

2.2.4 MEASUREMENT OF SOIL SUCTION

From a thermodynamic standpoint, the total suction of the soil consists of two components, namely matric suction and osmotic suction (Fredlund and Rahardjo, 1987)

$$\psi = (U_a - U_w) + \pi \qquad (2.11)$$

where

ψ = total suction

$U_a - U_w$ = matric suction

π = osmotic suction

Several devices commonly used for measuring soil suction and their range of measurement are listed in Table 2.1.

Suction, which is the stress-free negative pore water pressure of a specimen of soil is conveniently expressed on the pF scale. On this scale, the logarithm to the base 10 of the suction in cm of water is the pF value e.g., 100cm water is pF2. The use of logarithmic scale rather than linear scale of moisture content has advantages in dealing with large changes in strength for small changes in moisture content at low moisture contents. (Suction can be expressed in any unit of pressure e.g, in the S.I system pF2 is 9.81kNm^{-2}).

In the measurement of the uniaxial compressive strength of soil specimen placed in controlled atmospheric environment of known relative humidities, the results were plotted as graphs of strength against suction, by converting the relative humidity (H) to suction using the following expression (Croney, 1977):

$$pF = 6.502 + \log_{10}(2 - \log_{10}H) \qquad (2.12)$$

2.2.5 CLASSICAL PRINCIPLES AND EQUATIONS

Classical equations for describing the mechanical behaviour of unsaturated soils can be presented as an extension of the equations commonly applied to saturated soils The extension must be consistent with the number of stress state variables required for an unsaturated soil (Fredlund and Rahardjo, 1987).

Table 2.2 summarizes and compares some of the saturated and unsaturated soil mechanics equations. The variables used in these equations are described in Table 2.3. When a soil approaches saturation, the unsaturated soil equations undergo a smooth transition to the saturated soil equations.

2.2.6 SHEAR STRENGTH OF UNSATURATED COHESIVE SOILS

The relationship among total stress, effective stress, and pore-water pressure for unsaturated soils was briefly introduced in Eq (2.10) as:

$$\sigma^{1} = \sigma - U_a + X(U_a - U_w)$$

When the value of σ^{1} from (2.10b) is substituted in the shear strength equation, which is based on effective stress parameters we get (Das, 1987)

$$\tau_f = c + [\sigma - U_a + X(U_a - U_w)]\tan\phi \qquad (2.13)$$

As pointed out before, the values of X primarily depends on the degree of saturation. With ordinary triaxial equipment used for laboratory testing, it is not possible to accurately determine effective stresses in unsaturated soil samples. So the common practice is to conduct undrained triaxial tests on unsaturated samples and measure only the total stress.

Table 2.1 Devices for measuring suction (Fredlund and Rahardjo, 1987)

Name of device	**Suction component Measured**	**Range (kPa)**	**Comments**
Tensiometers	Negative pore-water pressures or matric suction when pore-air pressure is atmospheric	0 to ~ 90	Difficulties with cavitation and air diffusion through ceramic cup.
Thermal conductivity sensors	Matric	0 to ~ 400+	Indirect measurement on a porous ceramic sensor.
Psychrometers	Total	100* to ~ 8,000	Constant temperature environment required.
Filter paper	Total	(Entire range)	May measure matric suction when in contact with moist soil.
Pore fluid squeezer	Osmotic	(No limit)	Used in conjunction with a pyschrometer or electrical conductivity measurement.

*Controlled temperature environment to ± 0.001°C

Table 2.2 Summary of classic saturated and unsaturated soil mechanics principles and equations (Fredlund and Rahardjo, 1987).

Principle or equation	Saturated soil	Unsaturated soil
Stress state variables	$(\sigma - U_w)$	$(\sigma - U_a)$ and $(U_a - U_w)$
Resilient modulus	$E_r = f[(\sigma_3 - U_w),(\sigma_1 - \sigma_3)]$	$E_r = f[(\sigma_3 - U_a),(U_a - U_w),(\sigma_1 - \sigma_3)]$
Shear strength	$\tau = c' + (\sigma - U_w)\tan\phi'$	$\tau = c' + (U_a - U_w)\tan\phi^b + (\sigma - U_a)\tan\phi'$ $c = c' + (U_a - U_w)\tan\phi^b$
Ultimate bearing Capacity of clay	$q_{ult} = cN_c$	$q_{ult} = cN_c$
Constitutive equations for Ko loadings.	**Soil structure and water phase** $de = G_s d_w = a_v d(\sigma_y - U_w)$	**Soil structure:** $de = a_t d(\sigma_y - U_a) = a_m d(U_a - U_w)$ **Water phase:** $dw = b_t d(\sigma_y - U_a) = b_m d(U_a - U_w)$
Flow law for water (Darcy's law)	$V_w = -k_s \frac{\partial h_w}{\partial y}$ $h_w = y + \frac{U_w}{\rho_w g}$	$V_w = -k_w(U_a - U_w)\frac{\partial h_w}{dy} = 0$ $h_w = y + \frac{U_w}{\rho_w g}$
Steady state seepage	**One-dimensional:** $\frac{\partial^2 h_w}{\partial y^2}$ **Two-dimensional:** $\frac{\partial^2 h_w}{\partial \chi^2} + \frac{\partial^2 h_w}{\partial y^2} = 0$	**One-dimensional:** $k_w \frac{\partial^2 h_w}{\partial y^2} + \left(\frac{\partial k_w}{\partial y}\right)\frac{\partial h_w}{\partial y} = 0$ **Two -dimensional:** $k_w \frac{\partial^2 h_w}{\partial x^2} + \left(\frac{\partial k_w}{\partial x}\right)\frac{\partial h_w}{\partial x} +$ $k_w \frac{\partial^2 h_w}{\partial y^2} + \left(\frac{\partial k_w}{\partial y}\right)\frac{\partial h_w}{\partial y} = 0$

All variables are defined in Table 2.3

Table 2.3: Symbols and variable used in the equations (Fredlund and Rahardjo, 1987)

E_r	=	resilient modulus
$(\sigma_3 - U_w)$	=	effective confining stress
$(\sigma_1 - \sigma_3)$	=	deviator stress
σ_1	=	major principal stress
σ_3	=	minor principal stress (or total confining stress)
$(\sigma_3 - U_a)$	=	net confining stress
τ	=	shear stress
c'	=	effective cohesion intercept
ϕ'	=	effective angle of internal friction
ϕ^b	=	angle of shear strength increase with an increase in matric suction
c	=	cohesion intercept
q_{ult}	=	ultimate bearing capacity
N_c	=	bearing capacity factor for clays soils
de	=	change in void ratio
e	=	void ratio
dw	=	change in water content
w	=	water content
a_v	=	coefficient of compressibility
$d(\sigma_y - U_w)$	=	change in effective vertical stress
σ_y	=	total vertical stress
a_t	=	coefficient of compressibility with respect to a change in $(U_a - U_w)$
$d(\sigma_y - U_a)$	=	change in net vertical normal stress
a_m	=	coefficient of compressibility with respect to a change in $(U_a - U_w)$
$d\ (U_a - U_w)$	=	change in matric suction
b_t	=	coefficient of water content change with respect to a change in $(\sigma_y - U_a)$
b_m	=	coefficient of water content change with respect to a change

in $(U_a - U_w)$

v_w = flow rate of water

k_s = water saturated coefficient of permeability

$\frac{\partial h_w}{\partial y}$ = hydraulic head gradient in the y-direction

h_w = hydraulic head

y = gravitational (or elevation) head

$\frac{U_w}{\rho_w g}$ = pore-water pressure head

ρ_w = water density

g = gravitational acceleration

$k_w(U_a-U_w)$ = unsaturated coefficient of permeability which is a function of $(U_a - U_w)$

$\frac{\partial k_w}{\partial y}$ = change in water coefficient of permeability in the y-direction

$\frac{\partial k_w}{\partial x}$ = change in water coefficient of permeability in the x-direction

$\frac{\partial h_w}{\partial x}$ = Hydraulic head gradient in the x-direction

ρ = total density of a soil

ρ_d = dry density of a soil

G_s = specific gravity of a soil

2.3 PRESENT STATUS OF SCIENTIFIC RESEARCH ON BLACK COTTON SOILS

The black cotton soils are dark coloured expansive clays, characterized by the phenomena of swelling on absorption of water and shrinkage on drying (Adeyeri, 1988). These characteristics make them highly problematic as foundation for both building and road structures. Such soils are common products of tropical weathering and are encountered in several parts of the world.

In general, the black cotton soils derive their origin from basic igneous rocks such as basalts, rich in feldspars and mafic minerals such as montmorillonites, (Ibrahim, 1983). In Nigeria, these soils are found predominantly in the North-Eastern region of the country, lying within the Chad Basin and partly within the Benue trough (Figure 2.10). It is believed that these soils derive their origin in Nigeria from basalts in the upper Benue trough which cover several hundred square kilometers extending North and East of the Jos Plateau, and from quaternary sediments of the lacustrine origin from the Chad Basin consisting mainly of shales, clays and sandy sediments.

Black cotton soils generally occur in poorly drained areas, with alternating wet and dry seasons and with an annual rainfall generally less than 120cm. Such physiographical features and climatic conditions are typified in the Chad Basin where sediments were deposited as the old lake expanded and shrank during the alternating wet and dry periods. Other conditions conducive to their formation include the cumulative effects of leaching, alkaline environment and retention of Calcium and Magnesium in the soil.

The bulk of the black cotton soil deposits in Nigeria are found in the North-Eastern States of Borno, Adamawa, Taraba, Gombe and Bauchi. These soils generally occur in discontinuous stretches as superficial deposits usually not more than 2 meters in thickness, overlain or underlain by sandy sediments (NBRRI, 1983).

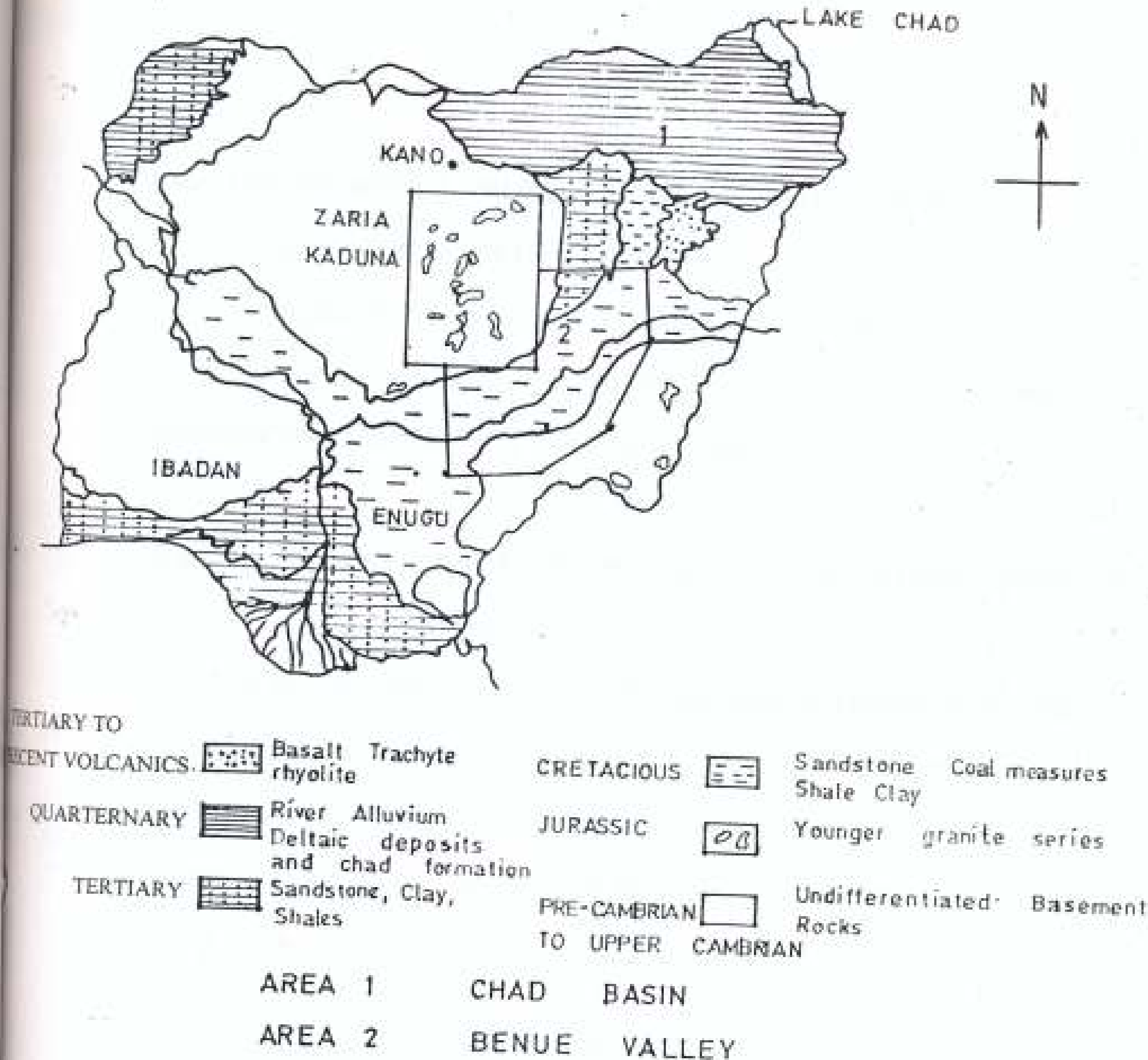

FIG. 2.10: GEOLOGICAL SKETCH MAP OF NIGERIA (NBRRI, 1983)

2.3.1 GEOTECHNICAL PROPERTIES OF THE BLACK COTTON SOIL OF NORTH-EASTERN NIGERIA

Some geotechnical properties of the black cotton soil in the North eastern Nigeria were obtained by Ola (1983). He performed a series of tests on stabilized and unstabilised black cotton soil samples and analysed the results.

2.3.1.1 GEOTECHNICAL PROPERTIES OF UNSTABILISED NIGERIAN BLACK COTTON SOIL

The grain size distribution curve for the black cotton soil used in the investigation, as a result of wet sieving is shown in Figure 2.11. More than 90% of the sample passed No. 200BS sieve and the clay fraction was about 45%. The specific gravity of the soil was 2.56. Details of the result of tests conducted on unstabilised black cotton soil samples can be seen on Table 2.4.

Table 2.4: Physical properties of the unstabilised black cotton soil (Ola, 1983)

Tests	Results
Liquid limit (%)	78.0
Plastic limit (%)	31.0
Plasticity index (%)	47.0
Linear shrinkage (%)	11.0
Standard Proctor density (kg/m^3)	1412.8
Optimum moisture content(%)	27.0
Specific gravity	2.56
Free swell (%)	50.0
Swelling pressure (PVC) at optimum moisture content (kN/m^2).	126.9

Comparison of the differential thermal analysis curves for the black cotton soil (Ola, 1983) with the standard curves developed by various authors, (Grim and Rowland, 1942), (Lambe, 1952), (Mackenzie, 1957) suggest that the soil is a mixture of montmorillonite and kaolinite. Because of the large endothermic peak at 150^0C relative to the dehydroxylation peak at 600^0C, it is suspected that montmorillonite is in greater proportion. The view is confirmed by the X-ray diffraction analysis on the fraction of the soil passing No. 200 sieve. The presence of kaolinite was confirmed by the presence of a 7.19^0 peak in the Air Dried Preferred Orientation (ADPO), which disappears after heat treatment. The presence of montmorillonite was confirmed by the expansion of the lattice from $15.41A^0$ in the ADPO to $17.49A^0$ in the Glycol Preferred Orientation (GPO). The lattice readily collapsed to $9.71A^0$ after heat treatment. The proportion of kaolinite in the clay mineral was about 30% whereas that of montmorillonite was about 70% (Ola, 1983). Similar results were also obtained by Lyon Associates, (1971).

2.3.1.2 COEFFICIENT OF COMPRESSIBILITY

The result of the Oedometer test conducted by Ola (1983) on the black cotton soil samples is shown in Figure 2.12. Analysis of this gave a compression index (C_c) of 0.53.

Skempton's relationship $C_c = 0.007(LL - 10)$ gives a C_c for this soil of 0.48. Showing that Skempton's curve is a good approximation of the compressibility of the soil close to the liquid limit. A similar relationship was also found to be true for India's black cotton soils (Mohan, 1957). Also of significance for the black cotton soil is the permeability. Table 2.5 shows the results of the coefficient of permeability from Oedometer tests for Nigerian black cotton soil.

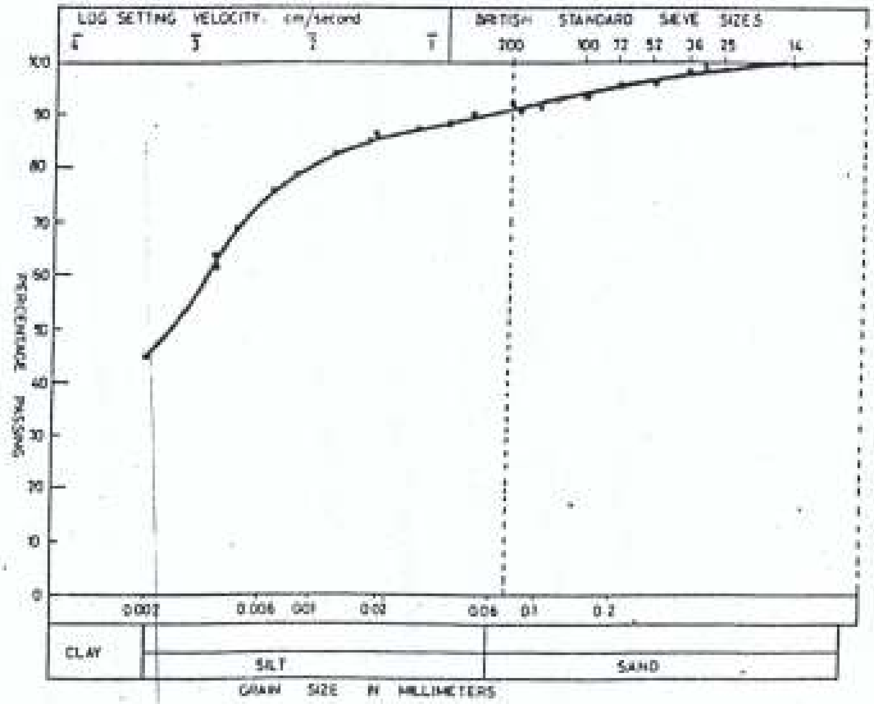

Fig. 2.11: PARTICLE SIZE DISTRIBUTION (SOIL UNSTABILISED) (Ola, 1983)

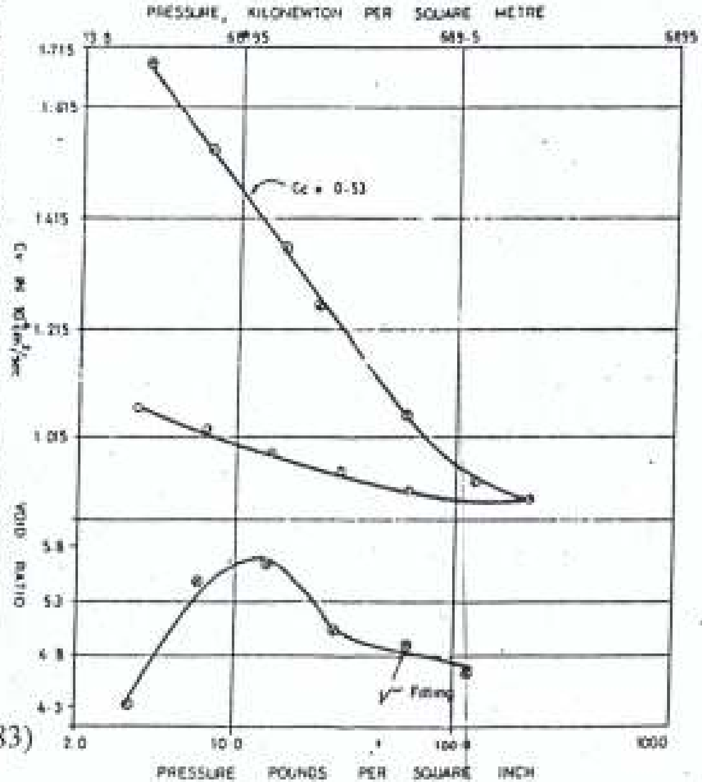

Fig. 2.12: CONSOLIDATION TEST (OLA, 1983)

Table 2.5: Coefficient of permeability from consolidation test (Ola, 1983)

a. Sample consolidated at Liquid limit

Pressure (kN/m^2)	Coefficient of permeability (k) (cm/sec. 10^{-10})
26.8	35.1
53.6	8.9
107.3	5.3
214.5	1.3
429.0	0.2

b. Sample Consolidated at optimum moisture content

Pressure (kN/m^2)	Coefficient of permeability (k) (cm/sec. 10^{-10})
429.0	0.1

The low permeability of the order of 10^{-10} cm/sec governs most of the drainage properties and causes most of the problems as shown on the table. For instance, for a loading pressure of 429.0kN/m^2 (4tsf), the coefficients of permeability for samples consolidated at liquid limit and optimum moisture contents are $2x10^{-11}$ and $1x10^{-11}$cm/sec respectively. For the same load, permeabilities of the order of 10^{-10} cm/sec were obtained by (Ranganatham, 1961) when working on an Indian black cotton soil.

2.3.1.3 SHEAR STRENGTH

Table 2.6 gives a summary of the strength characteristics of the unstabilised black cotton soil. Both the unconfined compression test and the vane test gave consistent results both for samples at optimum moisture content and at liquid limit. It is obvious from these results that the major problem of this soil is the moisture content. For instance, the shear strength at liquid limit (78%) for both unconfined compression test and vane test is negligible.

Table 2.6: Result of shear strength tests on unstabilised Nigerian Black Cotton Soil. (Ola, 1983).

Test	**Optimum moisture content (27%)**	**Liquid limit (78%)**
Unconfined compression test (kN/m^2)	124.1	-
Vane test (kN/m^2)	120.0	3.2
<u>Simple direct shear strength</u>		
Effective peak cohesion, C'_p (kN/m^2)		6.9
Effective peak angle of shearing resistance, ϕ'_p (degrees)		16^0
Residual cohesion C'_r (kN/m^2)		3.9
Residual angle of shearing resistance, ϕ'_r (degrees)		12^0

At the optimum moisture content (27%), shear strength for both unconfined compression test and vane test has increased to about 120.0kN/m^2 (2500psf). After drying to constant weight in the wet-dry test, the unconfined compression strength has further increased to 9500KN/m^2 (88.69tsf). The other properties of the unstabilised black cotton soils as reported by (Ola, 1983) are shown in Table 2.4. The free swell was 50%

and swelling pressure at optimum moisture content was 126.88kN/m^2 (2650PSF) showing that the soil is of high swelling capacity.

2.3.1.4 GEOTECHNICAL PROPERTIES OF STABILIZED NIGERIAN BLACK COTTON SOIL

The effect of lime and cement stabilization on the properties depend on the various mechanisms of stabilization. These mechanisms have been discussed by many investigators (Moh, 1962) and (Ola, 1975).

From the results of lime and cement stabilization by (Ola 1983), it was shown that lime primarily prevents road base swelling while the primary function of cement is to increase the strength of the base. For durability test, only samples with 9% lime and 8% cement were utilized. The values got are below the maximum allowable weight loss and volume increase of 1.5% each. What is perhaps most impressive is the increase in compressive strength of the stabilized soil after the 12th cycle of wetting and drying. The compressive strength increases from 1370kN/m^2 to 9500 kN/m^2. From the analysis of the three criteria used in determining the adequacy of soil stabilization (CBR, unconfined compressive strength and durability test), a mixture of lime and cement stabilization is best for black cotton soil and a combination of 6% lime and 8% cement was recommended for field trial in the first instance if economically feasible.

2.32 ENGINEERING PROPERTIES OF BLACK COTTON SOIL OF NIGERIA AND RELATED PAVEMENT DESIGN

The National Building and Road Research Institute (NBRRI, 1983) carried out an extensive investigation on the Black Cotton soils of North-Eastern, Nigeria and supplied relevant information that could aid in the design of highway pavements on Black Cotton soil subgrade. The programme of sampling the Black Cotton soils was chalked out in such a manner to cover the wide variety of Black Cotton soils encountered in the country. The locations of the 21 samples collected from the North-Eastern States of Borno, Adamawa, Taraba, Bauchi and Gombe are shown in Figure 2.13.

The locations of samples was well spread over the black cotton soil areas of the N-E region and the tests were performed on "representative" samples. The depth of the sampling was generally within 0-2meters below the top soil. The samples were collected from near the roadside taking 1 to 3 samples from each of the following roads:

i. Maiduguri – Bama Road, Borno State

ii. Dikwa – Marte Road, Borno State

iii. Chad Basin Development Authority (CBDA), Pumping Station Road, Borno State.

iv. Maiduguri - Gamboru Road, Borno State.

v. Potiskum – Nefads Road, Borno State

vi. Maiduguri - Damboa Road, Borno State

vii Gwoza - Bama Road, Borno State

viii. Numan – Gombe Road, Borno State

ix. Yola – Gombe Road, Borno State

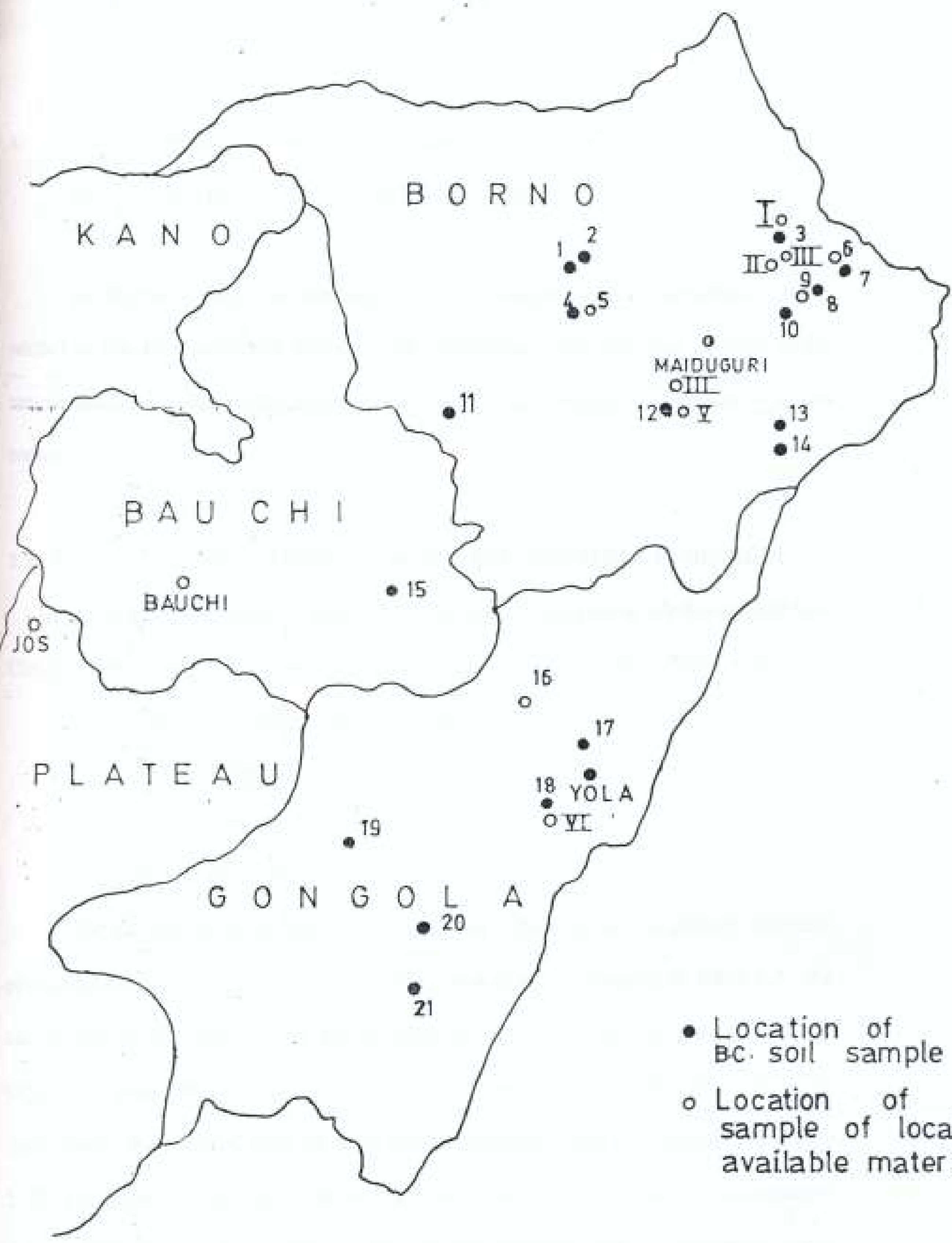

FIG 2.13: LOCATION OF SAMPLES COLLECTED (NBRRI, 1983)

x. Yola – Mayo Balewa Road, Gongola State.

xi Mayo Balewa – Ganye Road, Gongola State.

Additional information like depth of groundwater and its fluctuations, annual rainfall in the area, pavement thickness and composition were collected at some of the sample locations where insitu tests were conducted for subgrade equilibrium moisture content.

2.3.2.1 CLASSIFICATION OF BLACK COTTON SOILS IN NIGERIA

To be able to classify the various black cotton soil samples as per the Unified Soil Classification System, the following laboratory tests were conducted (NBRRI, 1983):

i. Mechanical sieve analysis, using the standard set of BS sieves, up to 63 micron mesh size.

ii. Liquid limit test and

iii. Plastic limit test

All the above three tests were conducted according to the British Standard procedures detailed in BS 1377 (1975). The result data are tabulated in Table 2.7. As can be seen from Table 2.7, the percent passing BS sieve 63 micron (i.e silt and clay combined), varies from 37 to 95, with most of the values ranging from 60 to 90. The liquid limit values ranged from 23 to 78 and the Plasticity Index Plot is shown in Figure 2.14. For Nigerian black cotton clays, it is remarkable that the values plot as a straight line, running more or less parallel to the "A" line (NBRRI, 1983). According to the Unified Soil Classification System all the 21 values fall in CL and CH groups.

The silt and clay content and the relative swelling potential of the black cotton soil samples were also determined using the sedimentation test and the free swell test. The result obtained from these two laboratory tests are tabulated in Table 2.8. Also included in Table 2.8 is the "Activity" ratio of each sample, defined as the ratio of plasticity index to percent smaller than 2 micron. The data in Table 2.8 shows a general trend of increase in the Plasticity Index with increasing percent smaller than 63 micron size (i.e, silt and clay content) and also with percent smaller than 2 micron (clay content). These trends are shown in Figures 2.15 and 2.16.

Table 2.7: Mechanical Sieve analysis and Atterberg Limits (NBRRI, 1983)

Sample No.	Percent Passing B.S. Sieve			Liquid Limit	Plastic Limit
	2mm	425micron	63 micron		
1.	100	95	83	45	16
2.	99.5	97	82	46	19
3.	100	100	93	55	23
4.	100	98	52.5	32	12
5.	100	98.5	50	36	17
6.	100	100	95	78	36
7.	100	94	38	26	16
8.	100	99.5	79.5	38	13
9.	100	99	79	50	14
10.	100	100	95	67	23
11.	99.5	98.5	86.5	53	27
12.	100	89	50.5	23	17
13.	99.5	94.5	85	51	24
14.	99	87.5	76	44	20
15.	95	80.5	67.5	61	25
16.	97.5	80	61.5	57	27
17.	97	96	81	58	25
18.	99.5	99	93	58	24
19.	95	79.5	67	37	19
20.	99	82	37	28	18
21.	92	73	59	54	23

It is quite apparent from the laboratory test data that all Black Cotton soils are not the same (NBRRI, 1983). The variations in their particles, size distribution, clay and silt contents, Liquid and Plastic limits and swell potential are so wide that black cotton soil cannot be considered as just one type of soil. These soils need to be sub-divided further. In regard to the design of pavements on Black Cotton soil subgrades, any one set of blanket specifications can neither be considered scientific nor economical. It is therefore of utmost importance that design specifications should be developed for each category or group or type of Black Cotton soil encountered in a particular area. Such a classification or grouping is of immense value due to the need for quality control on road works involving colossal amounts of earthwork.

With the above points in view, the following categorization of Black Cotton Soils has been proposed for the purpose of pavement design (NBRRI, 1983)

Category I	**(Low Swell Potential)**
Plasticity index	Below 20
Free swell	Less than 50%
Percent smaller than 1 micron	Less than 20

Category II	**(Medium Swell Potential)**
Plasticity index	15-30
Free swell	50-80%
Percent smaller than 1 micron	15-30

Category III **(High Swell Potential)**

Plasticity index	over 30
Free swell	over 80%
Percent smaller than 1 micron	over 30.

The proposed categorization of the black cotton soils of Nigeria as outlined above is diagrammatically shown in Figure 2.17.

Table 2.8: Laboratory Classification Test Data for Swelling Clays (NBRRI, 1983)

Sample No.	Plasticity Index	Percent smallelr than 2 micron	Activity ratio	Percent smaller than 1 micron	Free Swell %
1.	29	18.5	1.57	13	70
2.	25	25	1.00	20	80
3.	32	25	1.28	22	100
4.	20	28	0.71	21.5	90
5.	19	14	1.36	12	50
6.	42	58.5	0.72	52.5	140
7.	10	20	0.50	19	30
8.	25	15	1.67	12	40
9.	36	26	1.38	25	90
10.	44	28.5	1.54	23.5	110
11.	26	27.5	0.95	23	80
12.	6	19	0.32	11	30
13.	27	32	0.84	30	80
14.	24	20	1.20	17	70
15.	36	24	1.40	21	100
16.	30	21.5	1.40	17.5	100
17.	33	31	1.07	27.5	80
18.	34	33	1.03	27	70
19.	18	13.5	1.33	11	60
20.	10	8	1.25	7	40
21.	31	17.5	1.77	10.5	100

It is apparent from the foregoing review that the principle of effective stress alone is inadequate to explain the volumetric behaviour of partially saturated soils subjected to external stresses. This study has therefore attempted to treat applied stress and suction as two independent variables, and to relate this with variations in void ratio and degree of saturation.

Since the problem perculiar to design of road pavements on black cotton soil subgrades arises from the swelling and shrinkage characteristics of these soils, with changes in moisture content (Adeyeri and Mawadi, 1995), it was decided to use the black cotton soil prevalent in north-eastern Nigeria as a case study, in the experimental programme.

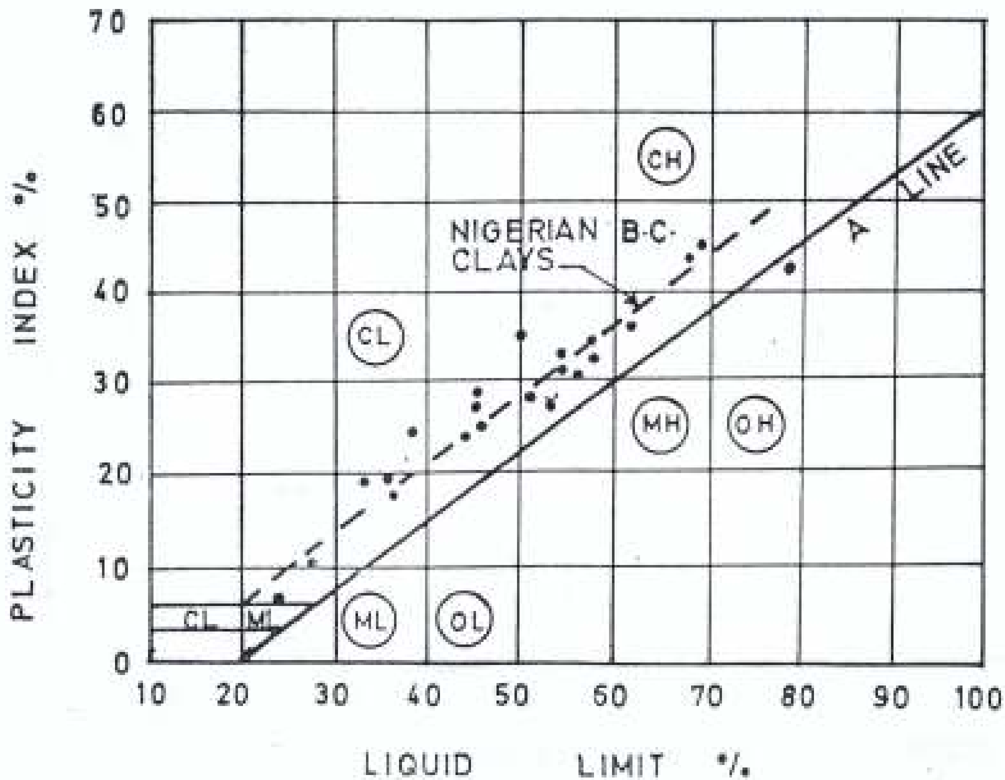

FIG2.14: LIQUID LIMIT VS PLASTICITY INDEX FOR NIGERIA B.C .SOIL S ACCORDING TO UNIFIED CLASSIFICATION METHOD (NBRRI, 1983)

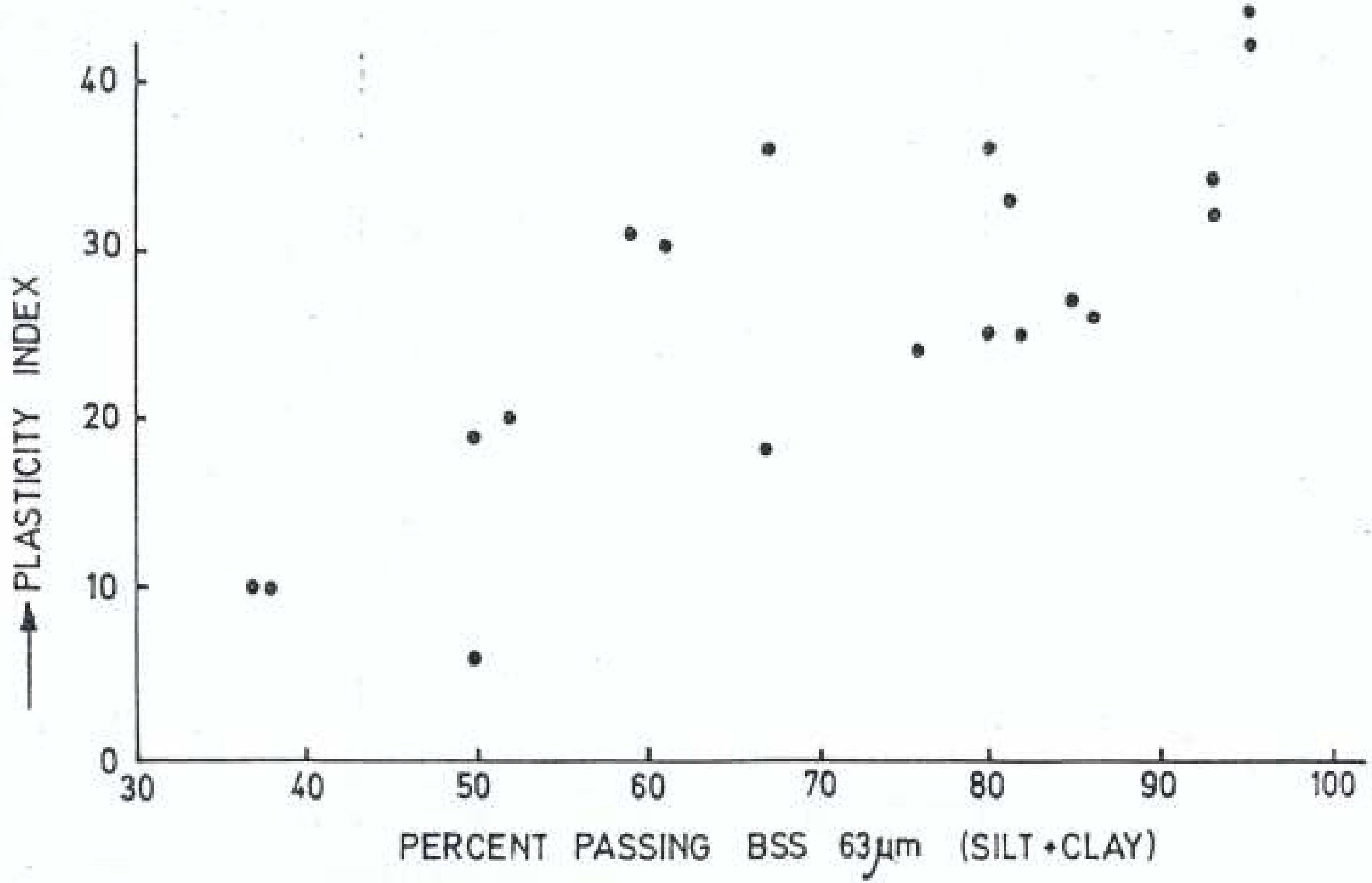

FIG 2.15: RELATIONSHIP BETWEEN PLASTICITY INDEX AND PERCENT PASSING 63-MICRON MESH (SILT&CLAY) FOR NIGERIAN B.C. SOILS (NBRRI, 1983)

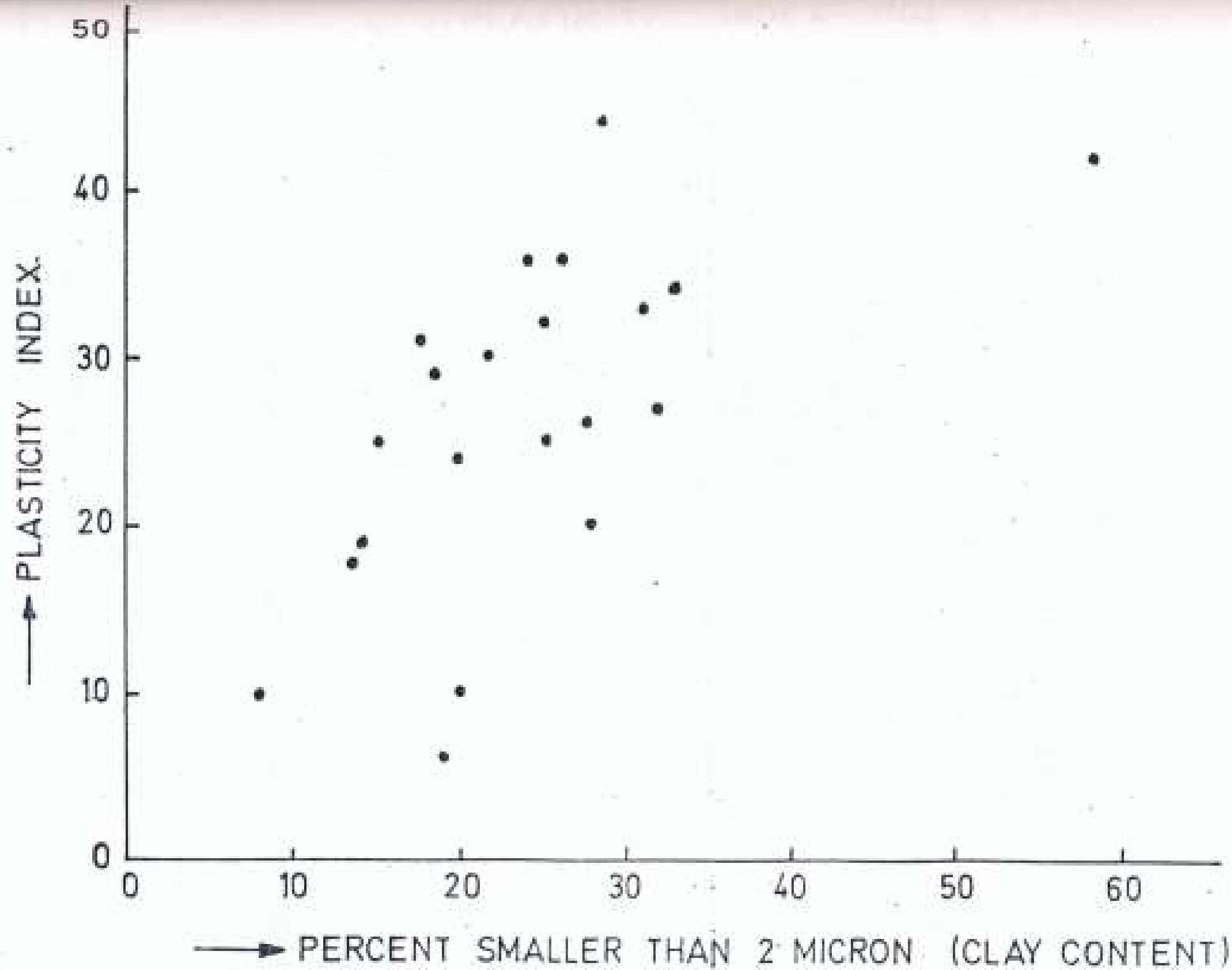

FIG 2.16: RELATIONSHIP BETWEEN PLASTICITY INDEX AND PERCENT SMALLER THAN 2 MICRON (CLAY CONTENT) FOR NIGERIAN B.C. SOILS (NBRRI, 1983)

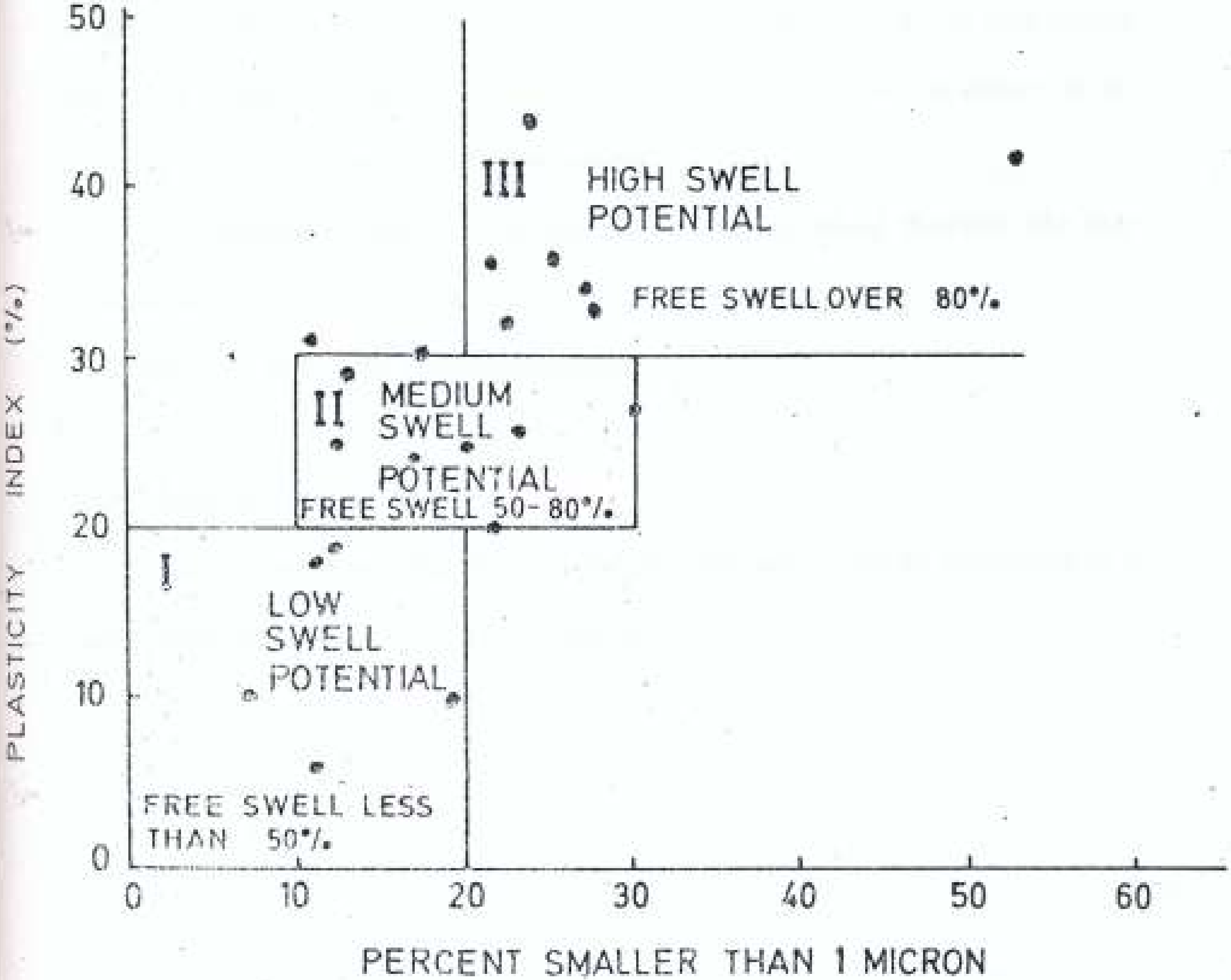

FIG 2.17: PROPOSED CATEGORISATION FOR BLACK COTTON SOILS OF NIGERIA (NBRRI, 1983)

CHAPTER THREE

THEORETICAL CONSIDERATIONS

3.1 ONE-DIMENSIONAL CONSOLIDATION THEORY FOR PARTIALLY SATURATED SOILS

3.1.1 INTRODUCTION

The prediction of consolidation during hydrodynamic period in partially saturated soils is more difficult than in saturated soils, due to the presence of a second fluid namely the air. It's presence modifies the phenomenon of consolidation due to changes in (a) effective stress, and (b) coefficient of permeability.

A consolidation theory for partially saturated soils should therefore take into account the modified effective stress law, modified coefficient of permeability and flow of air and water from voids during consolidation.

3.1.2 RHEOLOGICAL MODEL

The process of consolidation for a partially saturated soil can be represented by a simple rheological model, (Shrivastava, 1969) as in Figure 3.1

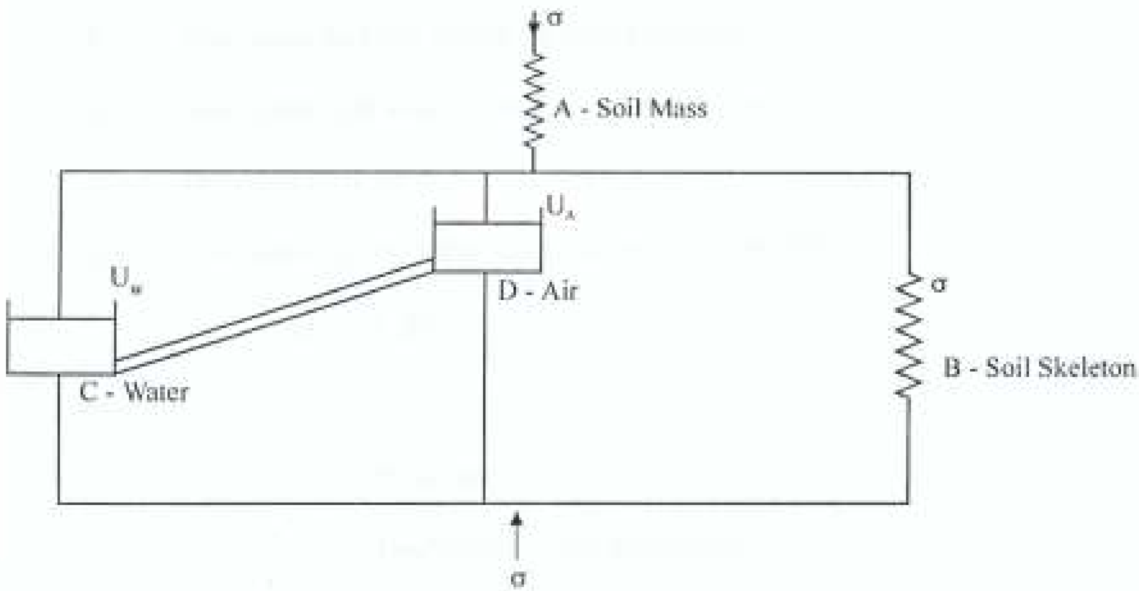

Figure 3.1: Rheological Model of a Partially Saturated Soil (Shrivastava, 1969)

When a load is applied to the soil mass, certain deformation takes place immediately depending on the degree of saturation. This corresponds to the deformation of spring A. The load is then taken by the pore fluid resulting in excess pore pressure. The pore fluid flows out under this pressure, and the effective stress on the soil grains increase. The soil mass under increased stress deforms. In the model, the viscous dashpots C,D and spring B corresponds to water, air and soil skeleton respectively. The period during which the escaping of fluid takes place is called the hydrodynamic period (more correctly the fluid-dynamic period) of consolidation.

3.1.3 MATHEMATICAL FORMULATIONS

The following assumptions are made in the formation of the theory:

i. The flow of air and water is in one direction only. (that is, in the direction of compression). This corresponds to confined compression of the soil mass.

ii. Pore water and soil grains are incompressible.

iii. The quantity of water in vapour state is negligible.

iv. Darcy's law is valid.

v. Void ratio and effective stress are linearly correlated, i.e

$$de = -a_v . d\sigma^1$$

where

e	=	Void ratio
a_v	=	Coefficient of compressibility
σ^1	=	effective stress

Figure 3.2a shows a layer of partially saturated clay of thickness H that is located between two highly permeable sand layers. If the clay layer is subjected to an increased pressure σ_1 , the pore pressure at any point "A" in the clay layer will increase. For one-dimensional consolidation, the fluid will be squeezed out in the vertical direction toward the sand layer. Figure 3.2b shows the flow of water through a prismatic element at "A" Similarly Figure 3.2C shows the flow of air through a prismatic element at "A".

For the soil element shown:

(Rate of outflow of water + Rate of outflow of air)

– (Rate of inflow of water + Rate of inflow of air)

= Rate of volume change

i.e.,

$$\left[(V_w + \frac{\partial V_w}{\partial z}dz)dxdy + (V_a + \frac{\partial V_a}{\partial z}dz)dxdy\right] - \left[(V_w dxdy + V_a dxdy)\right] = \frac{\partial V}{\partial t} \quad ......(3.1a)$$

where

V = volume of soil element

V_w = velocity of flow water in Z direction

V_a = velocity of flow air in Z direction

or

$$\frac{\partial V_w}{\partial z}dx.dy.dz + \frac{\partial V_a}{\partial z}dx.dy.dz = \frac{\partial V}{\partial t} \qquad (3.1b)$$

Using modified Darcy's law for unsaturated soil (Fredlund and Rahardjo, 1987), we have;

$$V_w = -k_{w(Ua-Uw)}.\frac{\partial h_w}{\partial z}; \qquad h_w = z + \frac{U_w}{\rho_w g}$$

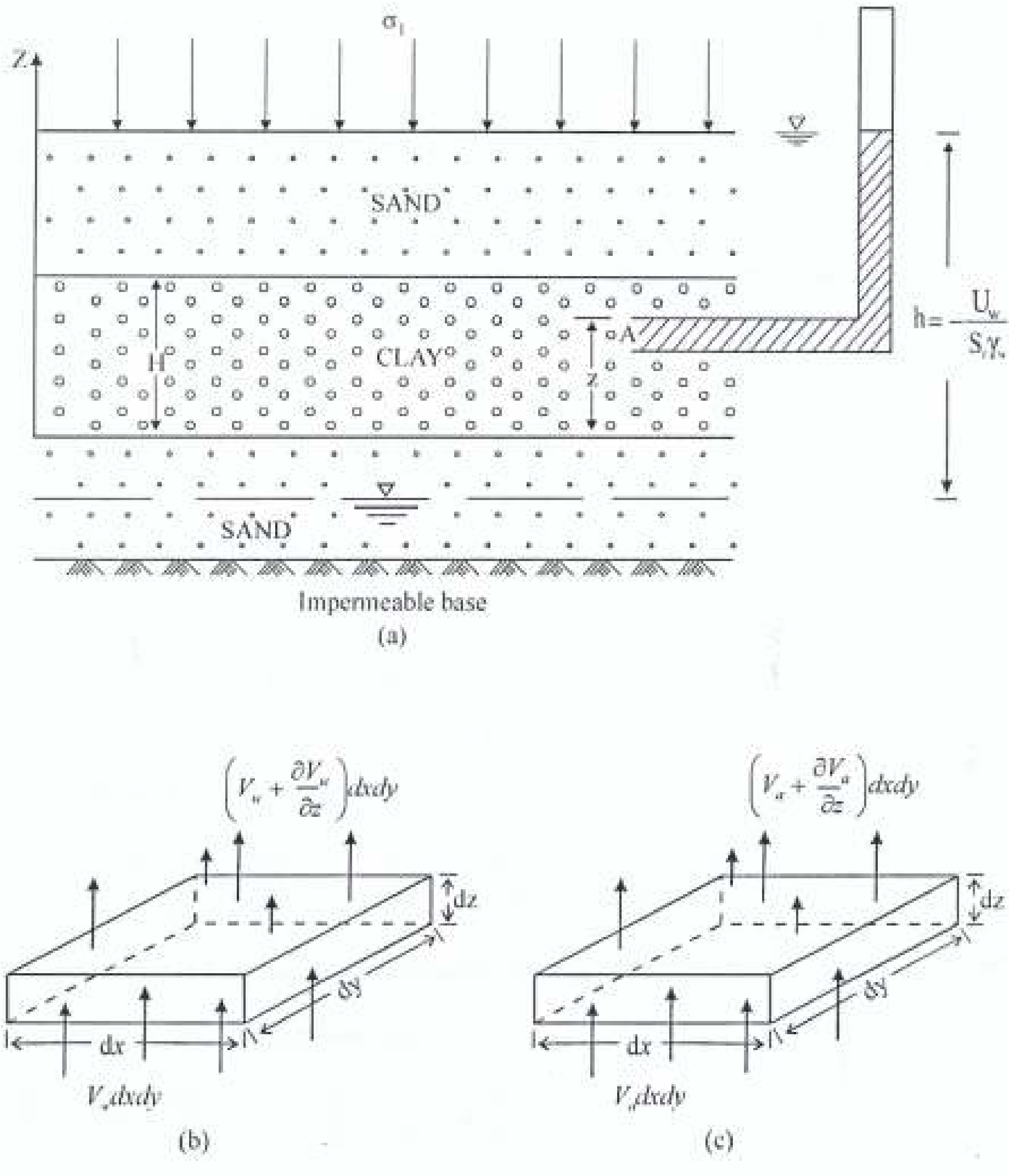

a. Partially saturated clay layer undergoing consolidation.

b. Flow of water at "A" during consolidation.

c. Flow of air at "A" during consolidation.

Figure 3.2: One-dimensional consolidation for a partially saturated clay layer

hence;

$$V_w = -\frac{k_{w(U_a-U_w)}}{\gamma_w} \cdot \frac{\partial U_w}{\partial z} \tag{3.2}$$

where:

$K_{w(U_a-U_w)}$ = Unsaturated coefficient of permeability which is a function of $(U_a - U_w)$

$\frac{U_w}{\rho_w g}$ = Pore-water pressure head

γ_w = unit weight of water

Similarly

$$V_a = -\frac{k_{w(U_a-U_w)}}{\gamma_a} \cdot \frac{\partial U_a}{dz} \tag{3.3}$$

Substituting (3.2) and (3.3) into (3.1)

$$-\frac{K_{w(U_a-U_w)}}{\gamma_w} \cdot \frac{\partial^2 U_w}{dz^2} + \left(\frac{-K_{w(U_a-U_w)}}{\gamma_a} \cdot \frac{\partial^2 U_a}{dz^2}\right) = \frac{1}{dx.dy.dz} \cdot \frac{\partial V}{\partial t} \tag{3.4}$$

During consolidation, the rate of change of volume of the soil element is equal to the rate of change of the volume of the voids, so;

$$\frac{\partial V}{\partial t} = \frac{\partial V_v}{\partial t} = \frac{\partial (V_s + eV_s)}{\partial t} = \frac{\partial V_s}{\partial t} + \frac{V_s \partial e}{\partial t} + e\frac{\partial V_s}{\partial t} \tag{3.5}$$

where

V_s = Volume of soil solids

V_v = Volume of voids

e = Void ratio

But (assuming that soil solids are incompressible),

$$\frac{\partial V_s}{\partial t} = 0$$

and

$$V_s = \frac{V}{1+e_o} = \frac{dx.dy.dz}{1+e_o}$$

Substitution for $\frac{\partial V_s}{\partial t}$ and V_s in (3.5) yields

$$\frac{\partial V}{\partial t} = \frac{dx.dy.dz}{1+e_o}.\frac{\partial e}{\partial t} \tag{3.6}$$

where

e_o = initial void ratio

Combining (3.4) and (3.6)

$$\frac{-k_{w(Ua-Uw)}}{\gamma_w}.\frac{\partial^2 U_w}{\partial z^2} + (\frac{-k_{w(Ua-Uw)}}{\gamma_a}.\frac{\partial^2 U_a}{\partial z}) = \frac{1}{1+e_o}.\frac{\partial e}{\partial t} \tag{3.7}$$

The change of void ratio is due to the increase of effective stress (that is decrease of excess pore pressure). Assuming that they are linearly related, we have,

$$\partial e = a_v(\Delta\sigma^1) = a_v \partial[U_a - X(U_a - U_w)] \tag{3.8}$$

where

$\Delta\sigma^1$ = the change in effective pressure

a_v = coefficient of compressibility (a_v can be considered to be constant for a narrow range of pressure increase)

Since, according to Bishop (1959)

$$\sigma^1 = \sigma - [U_a - X(U_a - U_w)]$$

where

σ^1 = effective stress

X = effective stress parameter (determined experimentally)

$U_a - U_w$ = soil suction

U_a = pore air pressure

combining (3.7) and (3.8) gives;

$$-\frac{k_{w(U_a-U_w)}}{\gamma_w}.\frac{\partial^2 U_w}{\partial z}+\left[\frac{-k_{w(U_a-U_w)}}{\gamma_a}.\frac{\partial^2 U_a}{dz^2}\right]=\frac{-a_v}{1+e_o}.\frac{\partial[U_a - X(U_a - U_w)]}{\partial t}$$

i.e

$$-k_{w(U_a-U_w)}\left[\frac{1}{\gamma_w}.\frac{\partial^2 U_w}{\partial z^2}+\frac{1}{\gamma_a}.\frac{\partial^2 U_a}{\partial z^2}\right]=-m_v.\partial\frac{[U_a - X(U_a - U_w)]}{\partial t}$$

$$\therefore \frac{\partial[U_a - X(U_a - U_w)]}{\partial t}=\frac{k_{w(U_a-U_w)}}{m_v}\left[\frac{1}{\gamma_w}.\frac{\partial^2 U_w}{\partial z^2}+\frac{1}{\gamma_a}.\frac{\partial^2 U_a}{\partial z^2}\right]$$

i.e,

$$\frac{\partial[U_a - X(U_a - U_w)]}{\partial t}=\frac{k_{w(U_a-U_w)}}{\gamma_w m_v}\left[\frac{\partial^2 U_w}{\partial z^2}+\frac{\gamma_w}{\gamma_a}.\frac{\partial^2 U_a}{\partial z^2}\right] \quad (3.9)$$

or

$$\frac{\partial[U_a - X(U_a - U_w)]}{\partial t}=C_{V(Ua-Uw)}\left[\frac{\partial^2 U_w}{\partial z^2}+\frac{\partial^2 U_a}{\partial z^2}.\frac{\gamma_w}{\gamma_a}\right] \quad (3.10)$$

where

X = Effective stress parameter related to degree of saturation

$C_{V(Ua-Uw)}$ = Unsaturated coefficient of consolidation which is a function of $(U_a - U_w)$

Rewriting equation 3.10, we have

$$\frac{\partial}{\partial t}[U_a - X(U_a - U_w)] = C_{V(Ua-Uw)}\left[\frac{\partial^2 U_w}{\partial z^2} + \gamma.\frac{\partial^2 U_a}{\partial z}\right]$$

where

$$\gamma = \frac{\gamma_w}{\gamma_a}$$

or

$$\frac{\partial}{\partial t}[U_a(1 - X) + XU_w] = C_{V(Ua-Uw)}\left[\frac{\partial^2 U_w}{\partial z^2} + \gamma\frac{\partial^2 U_a}{\partial z}\right]$$

$$(1 - X)\frac{\partial U_a}{\partial t} + X\frac{\partial U_w}{\partial t} = C\left[\frac{\partial^2 U_w}{\partial z^2} + \gamma\frac{\partial^2 U_a}{\partial z^2}\right] \qquad (3.11)$$

where

$$C = C_{v(U_a - U_w)}$$

For simplification, X for all practical cases may be taken as equal to degree of saturation, S_r (Shrivastava, 1969).

:. Substituting for X in (3.11), we have

$$(1 - S_r)\frac{\partial U_a}{\partial t} + S_r\frac{\partial U_w}{\partial t} = C\left[\gamma\frac{\partial^2 U_a}{\partial z^2} + \frac{\partial^2 U_w}{\partial z^2}\right] \qquad (3.12)$$

Consider a model of a partially saturated soil as in Figure (3.3)

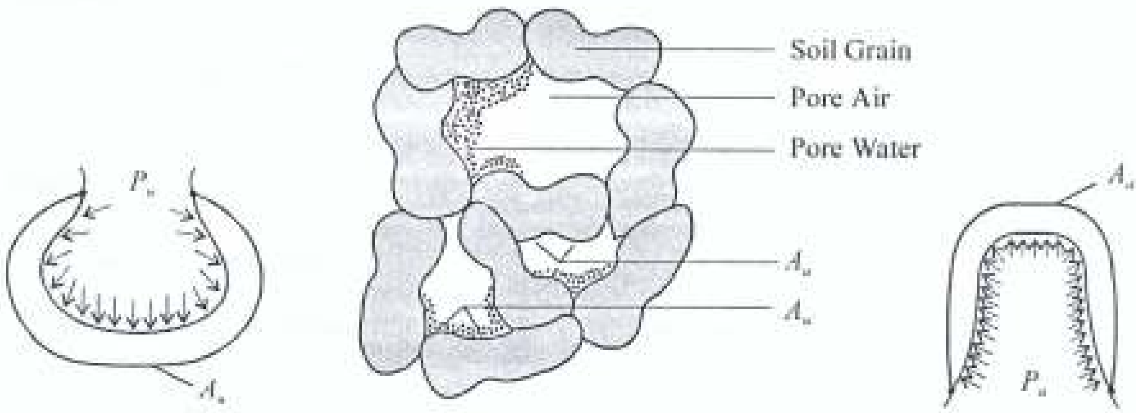

Figure 3.3: Model of a partially saturated soil (Matyas and Radhakrishna, 1968)

P_a = force exerted by air on air-solid contact

P_w = force exerted by water on water-solid contact

A_a = area of air-solid contact

A_w = area of water-solid contact

g = acceleration due to gravity

Now, we have that

$$U_a = \frac{P_a}{A_a} \text{ and } U_w = \frac{P_w}{A_w}$$

A_w is a measure of pore space saturation and is mainly a function of the degree of saturation (Matyas and Radhakrishna, 1968). From the results of the work by Sauer and Monismith (1968), it can be deduced that the degree of saturation of a soil varies inversely as the suction of the soil. This has led to the following assumption relating pore water pressure "U_w" to pore air pressure U_a;

$$U_a = \frac{\alpha}{U_w} \qquad \text{(i)}$$

Similarly;

$$U_w = \frac{\alpha}{U_a} \qquad \text{(ii)}$$

where

$\alpha \quad = \text{constant}$

∴ Substituting the transformation (i) in eqn (3.12), we have:

$$(1-S_r).\alpha.\frac{\partial\left(\frac{1}{U_w}\right)}{\partial t} + S_r.\frac{\partial U_w}{\partial t} = C\left[\gamma.\alpha.\frac{\partial^2\left(\frac{1}{U_w}\right)}{\partial z^2} + \frac{\partial^2 U_w}{\partial z^2}\right]$$

i.e

$$(1-S_r).\alpha.\frac{\partial}{\partial t}\left[\frac{1}{U_w}\right] + S_r.\frac{\partial U_w}{\partial t} = C\left[\gamma.\alpha.\frac{\partial^2}{\partial z^2}\left[\frac{1}{U_w}\right] + \frac{\partial^2 U_w}{\partial z^2}\right] \qquad (3.13)$$

Recall

$$\frac{d}{dt}\left(\frac{1}{U_w}\right) = \frac{d}{dU_w}\left(\frac{1}{U_w}\right).\frac{dU_w}{dt} = -\frac{1}{U_w^{\,2}}.\frac{dU_w}{dt}$$

$$\therefore \frac{\partial}{\partial t}\left[\frac{1}{U_w}\right] = -\frac{1}{U_w^{\,2}}.\frac{\partial U_w}{\partial t} \qquad \text{(iii)}$$

Also

$$\frac{d^2}{dz^2}\left[\frac{1}{U_w}\right] = \frac{d}{dz}\left[\frac{d}{dz}\left(\frac{1}{U_w}\right)\right] = \frac{d}{dz}\left[-\frac{1}{U_w^{\,2}}.\frac{dU_w}{dz}\right]$$

$$\frac{d^2}{dz^2}\left[\frac{1}{U_w}\right] = -\frac{d}{dz}\left(\frac{1}{U_w^{\,2}}\right).\frac{dU_w}{dz} - \frac{1}{U_w^{\,2}}.\frac{d^2U_w}{dz^2} \qquad \text{(iv)}$$

but;

$$\frac{d}{dz}\left(\frac{1}{U_w^{\,2}}\right)=\frac{d}{dU_w}\left(\frac{1}{U_w^{\,2}}\right)\cdot\frac{dU_w}{dz}=-\frac{2}{U_w^{\,3}}\cdot\frac{dU_w}{dz}$$

substituting in (iv), we have

$$\frac{d^2}{dz^2}\left(\frac{1}{U_w}\right)=\frac{2}{U_w^{\,3}}\left(\frac{dU_w}{dz}\right)^2-\frac{1}{U_w^{\,2}}\cdot\frac{d^2U_w}{dz^2} \qquad \text{(v)}$$

$$\left(\frac{dU_w}{dz}\right)^2=U_w\cdot\frac{d^2U_w}{dz^2}$$

substituting in (v), we have;

$$\frac{d^2}{dz^2}\left(\frac{1}{U_w}\right)=\frac{2}{U_w^{\,2}}\cdot\frac{d^2U_w}{dz^2}-\frac{1}{U_w^{\,2}}\cdot\frac{d^2U_w}{dz^2}=\frac{1}{U_w^{\,2}}\cdot\frac{d^2U_w}{dz^2}$$

$$\therefore \frac{\partial^2}{\partial z^2}\left(\frac{1}{U_w}\right)=\frac{1}{U_w^{\,2}}\cdot\frac{\partial^2U_w}{\partial z^2} \qquad \text{(vi)}$$

substituting (iii) and (vi) in (3.13) we have;

$$-\frac{1}{U_w^{\,2}}\cdot(1-S_r)\cdot\alpha\cdot\frac{\partial U_w}{\partial t}+S_r\frac{\partial U_w}{\partial t}=C\left[\gamma\cdot\alpha\cdot\frac{1}{U_w^{\,2}}\frac{\partial^2U_w}{dz^2}+\frac{\partial^2U_w}{dz^2}\right]$$

or

$$S_r\frac{\partial U_w}{\partial t}-\frac{1}{U_w^{\,2}}\cdot(1-S_r)\cdot\alpha\cdot\frac{\partial U_w}{\partial t}=C\left[\frac{\partial^2U_w}{\partial z^2}+\gamma\cdot\alpha\cdot\frac{1}{U_w^{\,2}}\cdot\frac{\partial^2U_w}{\partial z^2}\right]$$

i.e

$$\left[S_r-\frac{\alpha}{U^2{}_w}\cdot(1-S_r)\right]\cdot\frac{\partial U_w}{\partial t}=\left[C+\gamma\cdot\alpha\cdot\frac{C}{U_w^{\,2}}\right]\cdot\frac{\partial^2U_w}{\partial z^2}$$

$$\frac{\partial U_w}{\partial t}=\frac{\left[C+\gamma\cdot\alpha\cdot\frac{C}{U_w^{\,2}}\right]}{\left[S_r+\frac{\alpha}{U_w^{\,2}}\cdot(1-S_r)\right]}\cdot\frac{\partial^2U_w}{\partial z^2}$$

multiply R.H.S by $\frac{U_w^2}{U_w^2}$

$$\frac{\partial U_w}{\partial t} = \left[\frac{C.U_w^2 + C.\gamma.\alpha}{S_r U^2_w + \alpha(1-S_r)}\right] = \frac{\partial^2 U_w}{\partial z^2} \tag{3.14}$$

Similarly substituting the transformation $U_w = \alpha.\frac{1}{U_a}$ in (3.12)

We have;

$$S_r.\alpha.\frac{\partial\left(\frac{1}{U_a}\right)}{\partial t} + (1-S_r)\frac{\partial U_a}{\partial t} = C\left[\alpha.\frac{\partial^2\left(\frac{1}{U_a}\right)}{\partial z^2} + \gamma.\frac{\partial^2 U_a}{\partial z^2}\right]$$

$$S_r.\alpha.\frac{\partial}{\partial t}\left[\frac{1}{U_a}\right] + (1-S_r)\frac{\partial U_a}{\partial t} = C\left[\alpha.\frac{\partial^2}{\partial z^2}\left[\frac{1}{U_a}\right] + \gamma.\frac{\partial^2 U_a}{\partial z^2}\right] \tag{3.15}$$

Recall from (iii) and (iv)

$$\frac{\partial}{\partial t}\left[\frac{1}{U_a}\right] = -\frac{1}{U_a^2}.\frac{\partial U_a}{\partial t} \tag{vii}$$

also

$$\frac{\partial^2}{\partial z^2}\left[\frac{1}{U_a}\right] = -\frac{1}{U_a^2}.\frac{\partial^2 U_a}{\partial z^2} \tag{viii}$$

substituting (vii) and (viii) in (3.15)

$$-S_r.\alpha.\frac{1}{Ua^2}.\frac{\partial U_a}{\partial t} + (1-S_r)\frac{\partial Ua}{\partial t} = C\left[\alpha.\frac{1}{U_a^2}.\frac{\partial^2 U_a}{\partial z^2} + \gamma.\frac{\partial^2 U_a}{\partial z^2}\right]$$

or

$$\left[(1-S_r) - \frac{\alpha}{U_a^2}.S_r\right].\frac{\partial U_a}{\partial t} = C\left[\left(\frac{\alpha}{U_a^2} + \gamma\right)\frac{\partial^2 U_a}{\partial z^2}\right]$$

$$\frac{\partial U_a}{\partial t} = \frac{\left[\alpha.\frac{c}{U_a^{\ 2}} + c.\gamma\right]}{\left[(1-S_r) - \frac{\alpha}{U_a^{\ 2}}.S_r\right]}.\frac{\partial^2 U_a}{\partial z^2}$$

multiply R.H.S by $\frac{U_a^{\ 2}}{U_a^{\ 2}}$

$$\therefore \frac{\partial U_a}{\partial t} = \frac{\left[\alpha.C + C.\gamma.U_a^{\ 2}\right]}{\left[(1-S_r)U_a^{\ 2} - \alpha.S_r\right]}.\frac{\partial^2 U_a}{\partial z^2} \qquad (3.16)$$

Relationship between Void Ratio and Pore Pressure

From eqn (8)

$$\partial e = -a_v \partial\left[U_a - X(U_a - U_w)\right]$$

$$\partial e = -a_v \partial\left[(1-X)U_a + XU_w\right]$$

or

$$\frac{\partial e}{\partial t} = -a_v \frac{\partial}{\partial t}\left[(1-X)U_a + XU_w\right]$$

$$\frac{\partial e}{\partial t} = -a_v (1-X)\frac{\partial U_a}{\partial t} - a_v.X.\frac{\partial U_w}{\partial t}$$

For simplification X for all practical cases may be taken as equal to Sr

$$\therefore \frac{\partial e}{\partial t} = -a_v (1-S_r).\frac{\partial U_a}{\partial t} - a_v.S_r.\frac{\partial U_w}{\partial t}$$

$$\frac{\partial e}{\partial t} = -a_v\left[(1-S_r).\frac{\partial U_a}{\partial t} + S_r.\frac{\partial U_w}{\partial t}\right]$$

N.B: Coefficient of compressibility $a_v = \frac{\Delta e}{\Delta p}$ (usually disregard negative sign)

$$\therefore \frac{\partial e}{\partial t} = a_v\left[(1-S_r).\frac{\partial U_a}{\partial t} + S_r.\frac{\partial U_w}{\partial t}\right] \qquad (3.17)$$

The proposed basic differential equations for the theory of one-dimensional consolidation for partially saturated soils, are as follows:

$$\frac{\partial U_w}{\partial t} = \frac{\left[C.U_w^{\,2} + C.\gamma.\alpha\right]}{\left[S_r.U_w^{\,2} + \alpha(1-S_r)\right]}.\frac{\partial^2 U_w}{\partial z^2} \qquad (3.14)$$

$$\frac{\partial U_a}{\partial t} = \frac{\left[\alpha.C + C.\gamma.U_a^{\,2}\right]}{\left[(1-S_r)U_a^{\,2} - \alpha.S_r\right]}.\frac{\partial^2 U_a}{\partial z^2} \qquad (3.16)$$

$$\frac{\partial e}{\partial t} = a_v\left[(1-S_r).\frac{\partial U_a}{\partial t} + S_r.\frac{\partial U_w}{\partial t}\right] \qquad (3.17)$$

Equations (3.14) and (3.16) are parabolic equations with variable coefficients and can be written in a general form as:

$$\frac{\partial U}{\partial t} = K\frac{\partial^2 U}{\partial z^2} \qquad (3.18)$$

where

K ≠ a constant

This diffusion equation can be solved by various schemes/methods, but the implicit scheme has been used because it is more stable.

3.1.4 IMPLICIT SCHEME FOR DIFFUSION

The finite difference equivalent of equation (3.18) can be written as

$$\frac{U_i^{j+1} - U_i^j}{\Delta t} = a.k\left[\frac{U^j{}_{i+1} - 2U^j{}_i + U^j{}_{i-1}}{(\Delta z)^2}\right] + b.k\left[\frac{U^{j+1}{}_{i+1} - 2U^{j+1}{}_i + U^{j+1}{}_{i-1}}{(\Delta z)^2}\right] \quad .....(3.19)$$

where

a+b = 1

The pattern shown in figure 3.4 is used to form the finite difference equation.

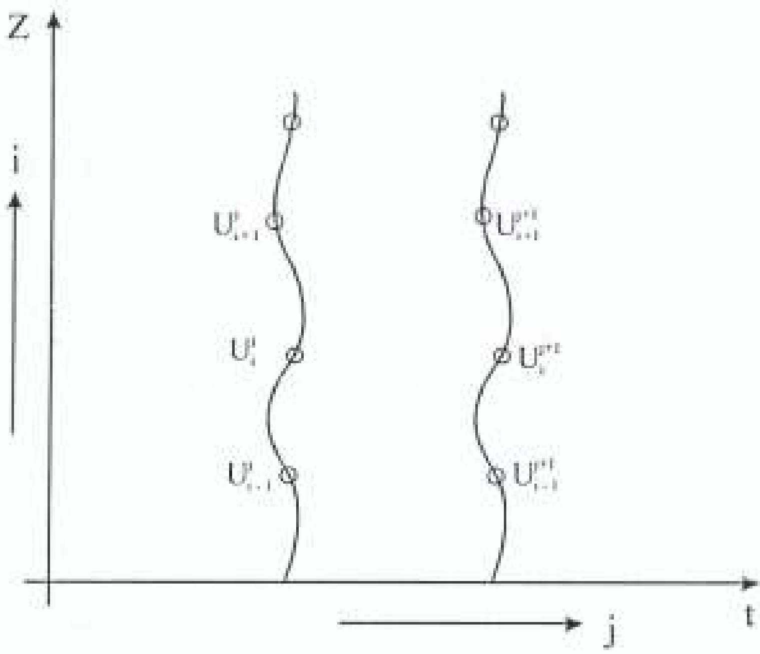

Figure 3.4: Finite-difference Grid pattern

From (3.19)

$$U_i^{j+1} = U_i^j + a.\frac{k\Delta t}{(\Delta z)^2}\left[U^j{}_{i+1} - 2U_i^j + U^j{}_{i-1}\right] + b.\frac{k\Delta t}{(\Delta z)^2}\left[U^{j+1}{}_{i+1} - 2U^{j+1}{}_i + U^{j+1}{}_{i-1}\right]$$

Let

$$r = \frac{k.\Delta t}{(\Delta z)^2}$$

$$U_i^{j+1} = U^j{}_i + arU^j{}_{i+1} - 2arU^j{}_i + arU^j{}_{i-1} + brU^{j+1}{}_{i+1} - 2brU_i^{j+1} + brU^{j+1}{}_{i-1}$$

collecting like terms

$$U_i^{j+1} + 2brU_i^{j+1} - brU^{j+1}{}_{i+1} - brU^{j+1}{}_{i-1} = U^j{}_i + arU^j{}_{i+1} - 2arU^j{}_i + arU^j{}_{i-1}$$

i.e

$$-brU^{j+1}{}_{i-1} + (1+2br)U_i^{j+1} - brU^{j+1}{}_{i+1} = U^j{}_i + ar\left(U^j{}_{i+1} - 2U^j{}_i + U^j{}_{i-1}\right) \tag{3.20}$$

Equation (3.20) can be written as;

$$-AU^{j+1}{}_{i-1} + BU^{j+1}{}_i - CU^{j+1}{}_{i+1} = D^j \tag{3.21}$$

where

A = br

B = 1 + 2br

C = br

$$D^j = U^j{}_i + ar\left(U^j{}_{i+1} - 2U^j{}_i + U^j{}_{i-1}\right)$$

Suppose

$$U_i^{j+1} = \alpha_i U^{j+1}{}_{i-1} + \beta_i \tag{3.22}$$

$$\Rightarrow U_{i+1}^{j+1} = \alpha_{i+1} U^{j+1}{}_i + \beta_{i+1} \tag{3.23}$$

Then equation (3.21) becomes

$$-A\alpha_{i+1}U_i^{j+1} - \beta_{i+1}A + BU_i^{j+1} - CU_{i-1}^j = D^j$$

$$\Rightarrow (B - A\alpha_{i+1})U_i^{j+1} - CU_{i-1}^j = D^j + \beta_{i+1}.A$$

$$\Rightarrow U_i^{j+1} = \frac{C}{B - A\alpha_{i+1}} U_{i-1}^{j+1} + \frac{D^j + \beta_{i+1}.A}{B - A\alpha_{i+1}} \tag{3.24}$$

Now compare equations (3.22) and (3.24)

$$\alpha_i = \frac{C}{B - A\alpha_{i+1}} \tag{3.25}$$

$$\Rightarrow \beta_i = \frac{D^j + \beta_{i+1}.A}{B - A\alpha_{i+1}} \tag{3.26}$$

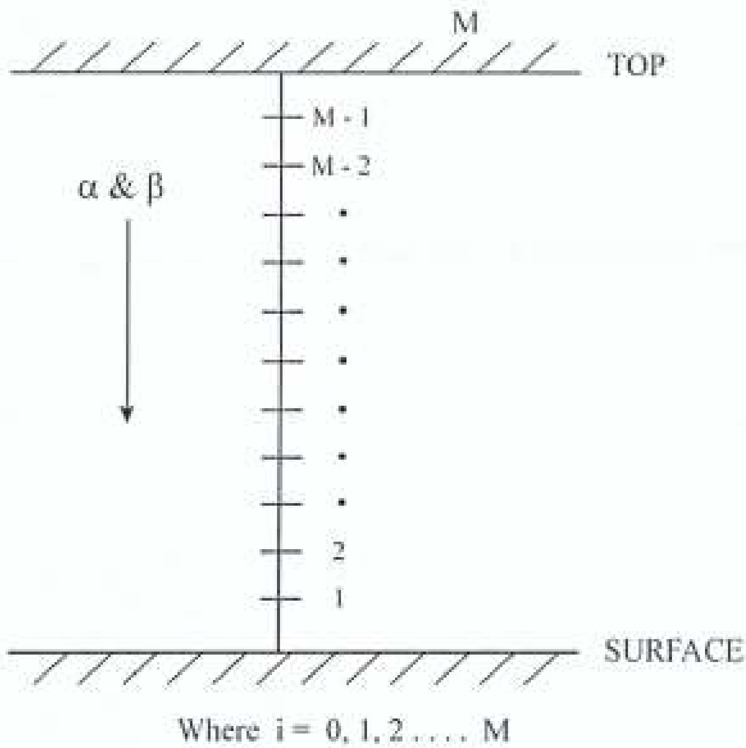

Figure 3.5: Grid points and Boundary values

Using any given boundary condition at the top, we can obtain the value of α_{m-1} from equations (3.22), hence calculate the parameters (α, β) at all levels from the top to the surface using equations (3.25) and (3.26)

The assumed initial and boundary conditions are as follows:

(i) $U = U_0 = -S_r\gamma_w z$ for $0 \le z \le 1$ at t = 0

(ii) U = 0 when z = 0 and 1 for all 't'

In our case, the boundary conditions are given as;

U = 0 when z = 0 and 1 for all "t"

Since

$$U_i^{j+1} = \alpha_i U_{i-1}^{j+1} + \beta_i \qquad (3.22)$$

if U = 0 at the top

$$\Rightarrow U_m = 0$$

i.e $\quad \alpha_m = 0, \qquad \beta_m = 0$

Hence we compute our parameters (α, β) from top to bottom and the values of U from bottom to top.

To solve equation (3.17)

Recall:

$$\frac{\partial e}{\partial t} = a_v\left[(1-S_r).\frac{\partial U_a}{\partial t} + S_r\frac{\partial U_w}{\partial t}\right]$$

$$\Rightarrow \frac{\partial e}{\partial t} = a_v(1-S_r).\frac{\partial U_a}{\partial t} + a_v S_r.\frac{\partial U_w}{\partial t}$$

Equation (3.18) can be written in a general form as

$$\frac{\partial e}{\partial t} = N_a.\frac{\partial U_a}{\partial t} + N_w.\frac{\partial U_w}{\partial t} \qquad \ldots\ldots\ldots\ldots \qquad (3.27)$$

The finite difference equivalent for (3.27) is as follows:

$$\frac{e_i^{j+1} - e_i^j}{\Delta t} = N_a\left[\frac{U_a{}^{j+1}{}_i - U_a{}^j{}_i}{\Delta t}\right] + N_w\left[\frac{U_w{}^{j+1}{}_i - U_w{}^j{}_i}{\Delta t}\right]$$

i.e $\quad e^{j+1}{}_i = e^j{}_i + N_a\left[U_a{}^{j+1}{}_i - U_a{}^j{}_i\right] + N_w\left[U_w{}^{j+1}{}_i - U_w{}^j{}_i\right] \quad \ldots\ldots\ldots(3.28)$

This numerical technique has been applied to a problem with the following assumed and experimental data for the solutions of equations (3.14), (3.16) and (3.17)

$\gamma_w = 10KN/m^3$, $\gamma_a = 0.013\ KN/m^3$

$$\gamma = \frac{\gamma_w}{\gamma_a} = \frac{10}{0.013} = 770, \qquad \alpha = 1.0 \text{ (assumed)}$$

H = 100 units, $\Delta Z = 1$, $\Delta t = 2secs$

A summary of the input data is shown in Table 3.1, with details printed out on Table 3.1.

Table 3.1: Summary of Input data for the model

Case No	S_r	C (cm^2/sec)	a_v (KN^{-1})
1	0.2	5.3×10^{-3}	0.7×10^{-4}
2	0.4	4.6×10^{-3}	1.29×10^{-4}
3	0.6	4.3×10^{-3}	1.72×10^{-4}
4	0.8	9.98×10^{-3}	1.76×10^{-4}
5	1.0	1.07×10^{-2}	2.7×10^{-4}

The computer programme is written in Fortran 90, and the plotting of the results was done with the MATLAB package. The Computer Programme and the Flow Charts are available in the appendix.

Figures 3.6 – 3.11 (a), shows the plots for the profiles of U_w, U_a and e. It can be seen that, except at the initial stage, the plots follow a parabolic pattern during the process of consolidation. The rate of reaching complete saturation is also seen to be decreasing with increasing height from the bottom as expected, depending on the degree of saturation.

As the negative pore water pressure (suction) decreases and tend towards zero, the voids ratio 'e' is seen to be increasing implying that essentially suction is responsible for the swell in black cotton soil when it comes into contact with water.

Figure 3.6 – 3.11 (b), shows the time series of U_w, U_a and 'e' at the bottom, mid height and surface of the soil layer. The curves are plotted for different degrees of saturation. As it is expected, the lower the degree of saturation, the faster is the rate of change of the pore water and pore air pressures. This explain the devastating effect, exposure to little rain can have on highway pavements with black cotton soil subgrade and the high swell-shrink characteristics of the soil.

A special case, having essentially the same input data as case 5 except that the simulation period was increased from 2 days to 20 days, tagged case 5s, reveals that for the case of 100% saturation, complete consolidation take as longer period than in a partially saturated soil.

Table 3.1a. Indata ~~and~~ for the I-D Consolidation Model

```
100   = Nx,Ny,Nz. Number of x,y,z Dimension. For now maximum(1,1,100)
 = dx,dy,dz. Increment in x,y,z Dimension.
00 120   = dt(sec),ftime(sec),rtime(min) Time increment,the simulation preriod (in
nd result time
   = c
 sr.
     = alpha.
13    = gammaW gammaA
      = uwA,uwB,uaA,uaB.  Bondary value of uw and ua.
       = av


100   = Nx,Ny,Nz. Number of x,y,z Dimension. For now maximum(1,1,100)
 = dx,dy,dz. Increment in x,y,z Dimension.
00 120   = dt(sec),ftime(sec),rtime(min) Time increment,the simulation preriod (in
nd result time
   = c
 sr.
     = alpha.
13    = gammaW gammaA
      = uwA,uwB,uaA,uaB.  Bondary value of uw and ua
        = av


100   = Nx,Ny,Nz. Number of x,y,z Dimension. For now maximum(1,1,100)
 = dx,dy,dz. Increment in x,y,z Dimension.
00 120   = dt(sec),ftime(sec),rtime(min) Time increment,the simulation preriod (in
nd result time
   = c
 sr.
     = alpha.
13    = gammaW gammaA
      = uwA,uwB,uaA,uaB.  Bondary value of uw and ua
        = av


100   = Nx,Ny,Nz. Number of x,y,z Dimension. For now maximum(1,1,100)
 = dx,dy,dz. Increment in x,y,z Dimension.
800 43200   = dt(sec),ftime(sec),rtime(min) Time increment,the simulation preriod (
) and result time
    = c
 sr.
     = alpha.
13    = gammaW gammaA
      = uwA,uwB,uaA,uaB.  Bondary value of uw and ua
        = av


100   = Nx,Ny,Nz. Number of x,y,z Dimension. For now maximum(1,1,100)
25    = dx,dy,dz. Increment in x,y,z Dimension.
72800  120   = dt(sec),ftime(sec),rtime(min) Time increment,the simulation preriod (
) and result time
    = c
 sr.
     = alpha.
13    = gammaW gammaA
      = uwA,uwB,uaA,uaB.  Bondary value of uw and ua
       = av


100   = Nx,Ny,Nz. Number of x,y,z Dimension. For now maximum(1,1,100)
 = dx,dy,dz. Increment in x,y,z Dimension.
8000 720   = dt(sec),ftime(sec),rtime(min) Time increment,the simulation preriod (in
```

```
w/ and result time
7e-2     = c
 = sr.
        = alpha.
.013    = gammaW gammaA
0 0     = uwA,uwB,uaA,uaB.  Bondary value of uw and ua
e-4      = av
```

Case 1

Key: o o o o - Initial plot

+ + + + - Plot during consolidation

* * * * - Final plot

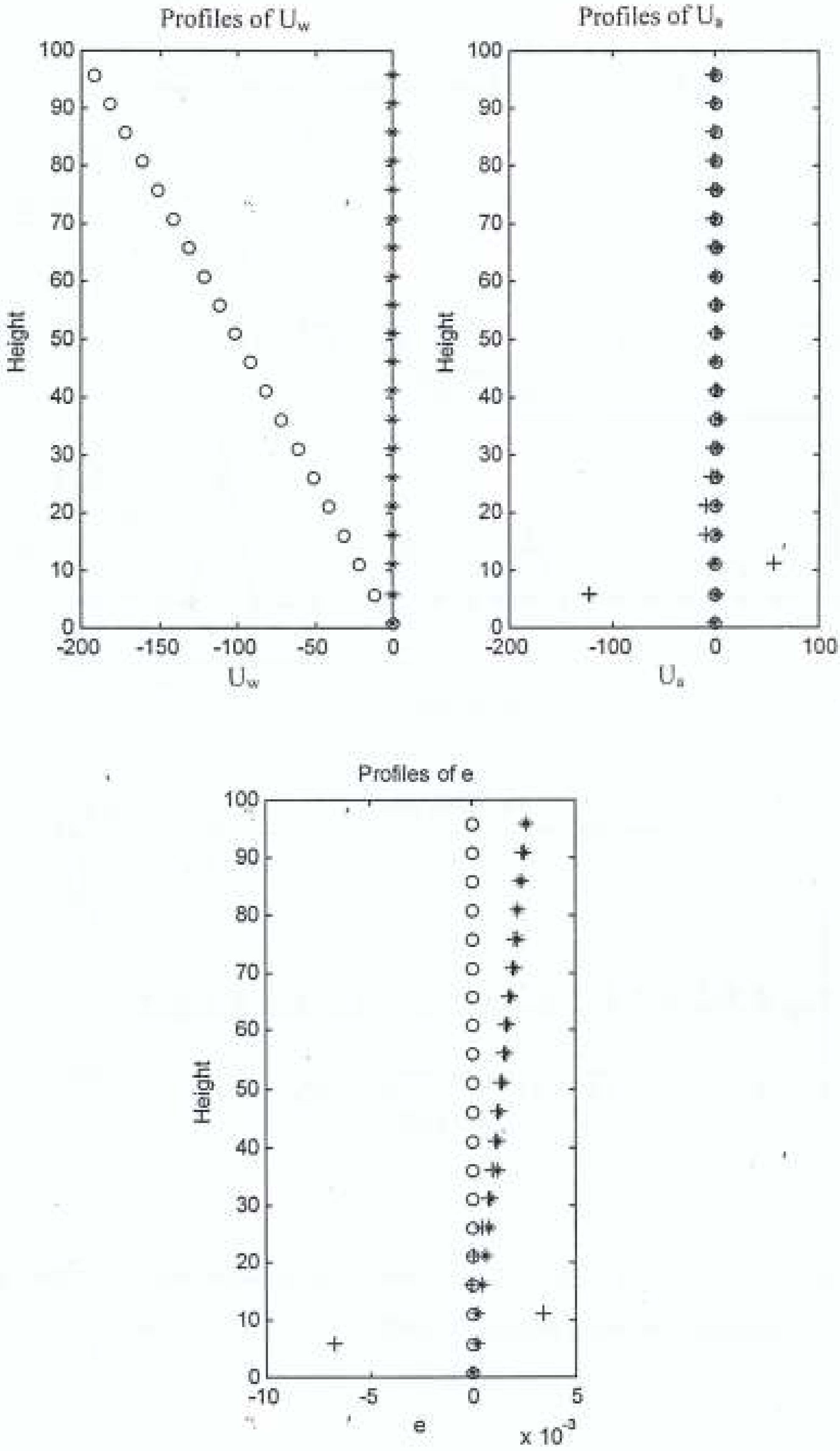

Fig. 3.6a: Profiles of U_w, U_a and e for: S_r = 20%, $C = 5.3 \times 10^{-3}$ cm^2/sec, $a_v = 0.7 \times 10^{-4} kN^{-1}$ ftime, simulation period = 172800secs

Case1

Key: + + + + - Surface plot

* * * * - Mid height plot

—— - Bottom plot

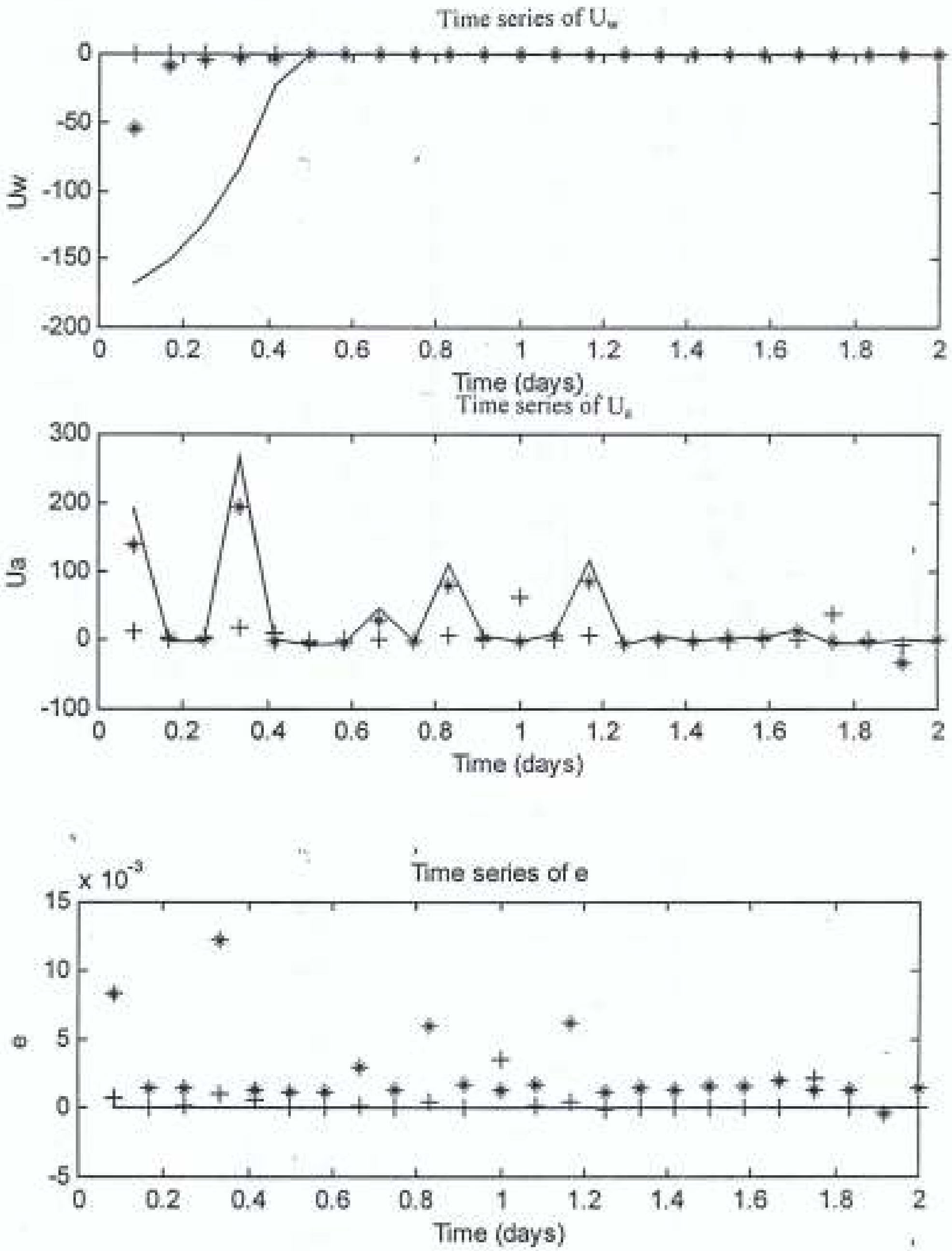

Fig. 3.6b: Time series of U_w, U_a and e for: $S_r = 20\%$, $C = 5.3 \times 10^{-3}$ cm^2/sec, $a_v = 0.70 \times 10^{-4}$kN^{-1} ftime, simulation period = 172800secs

Case2.

Key: o o o o - Initial plot

\+ + + + - Plot during consolidation

* * * * - Final plot

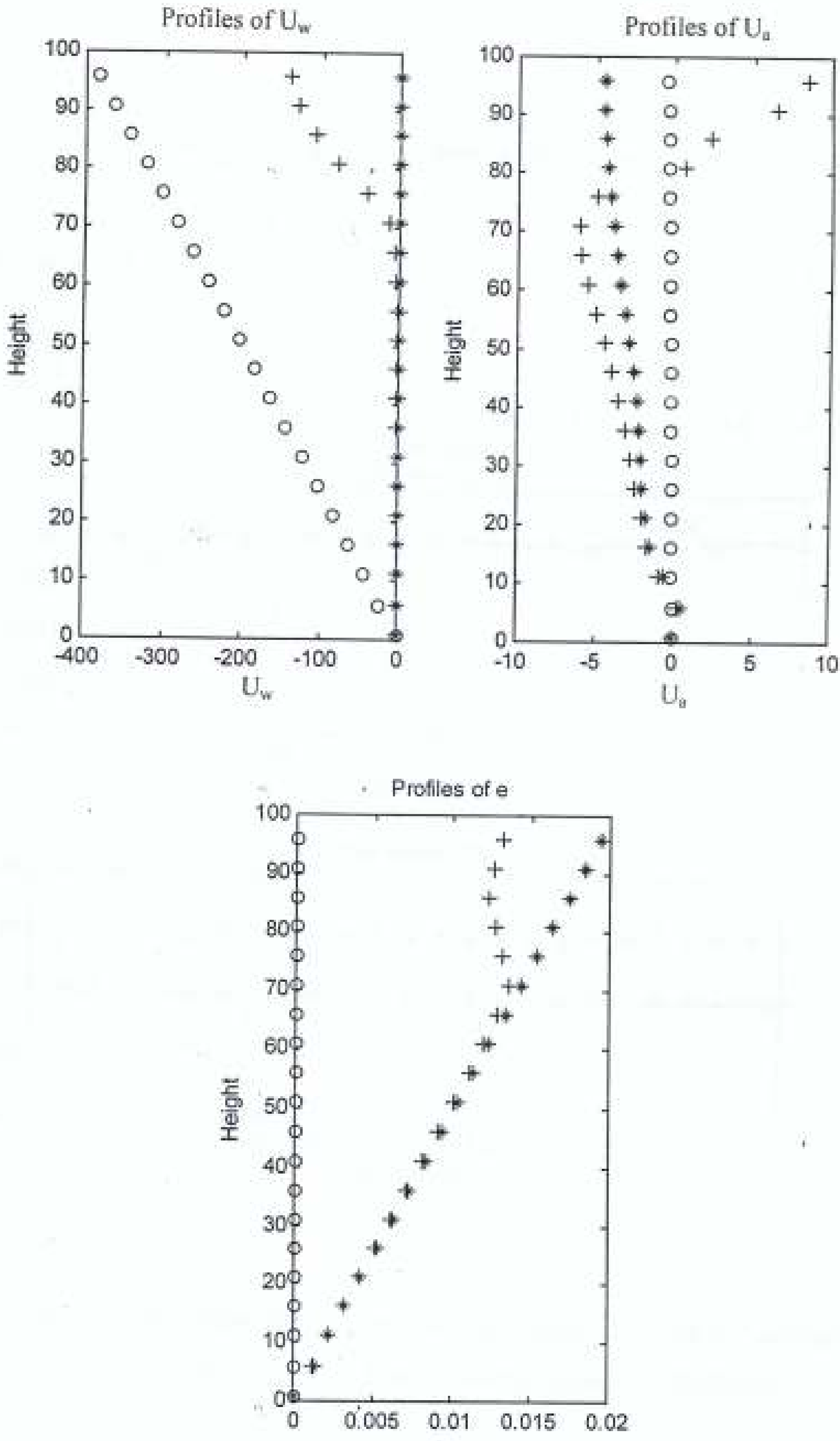

Fig. 3.7a: Profiles of U_w, U_a and e for: $S_r = 40\%$, $C = 4.6\text{x } 10^{-3}\ cm^2/sec$,

Case 2.

Key: + + + + - Surface plot

* * * * - Mid height plot

______ - Bottom plot

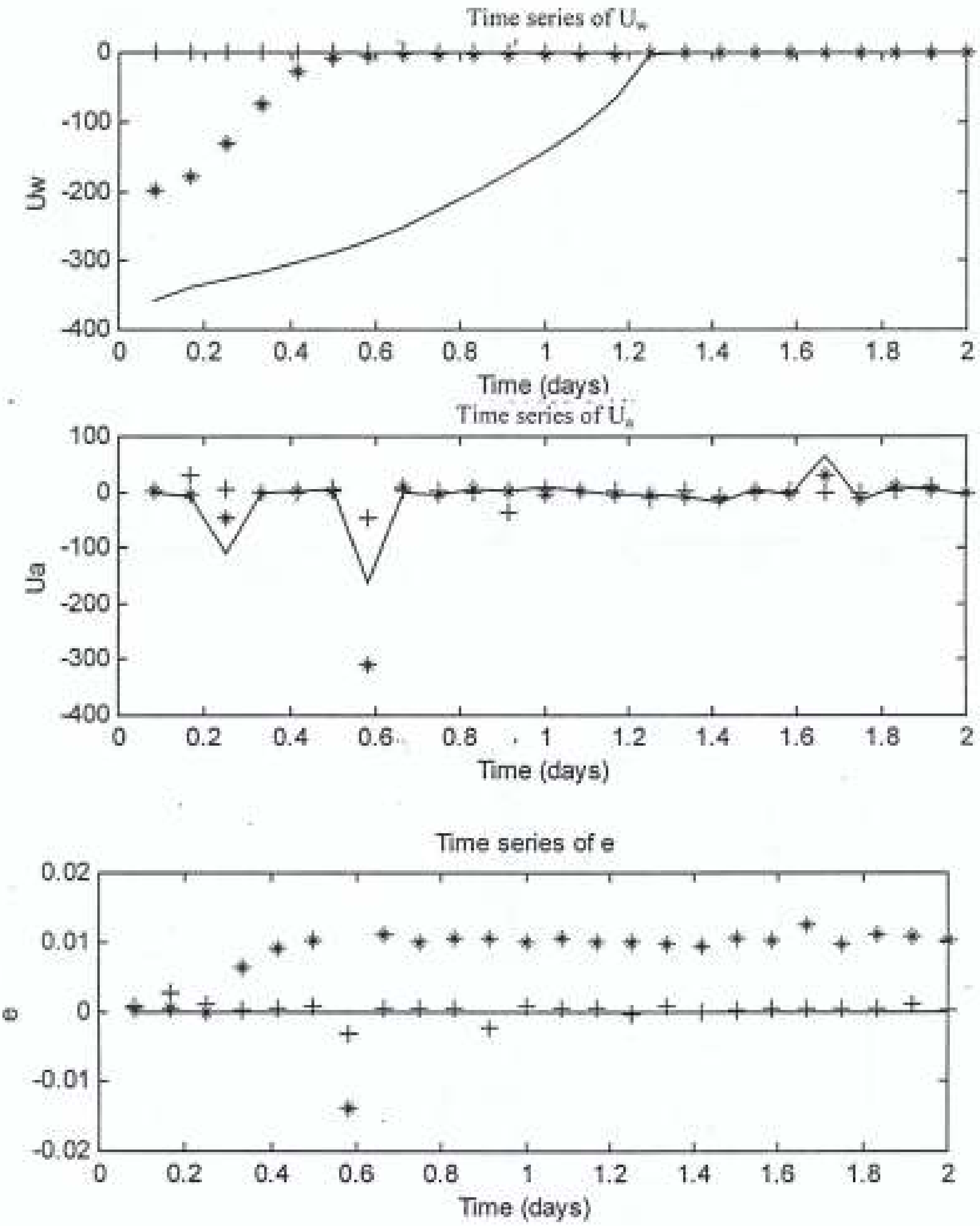

Fig. 3.7b: Time series of U_w, U_a and e for: $S_r = 40\%$, $C = 4.6 \times 10^{-3}\ cm^2/sec$, $a_v = 1.29 \times 10^{-4} kN^{-1}$ ftime, simulation period = 172800secs

Case 3

Key: o o o o - Initial plot

+ + + + - Plot during consolidation

* * * * - Final plot

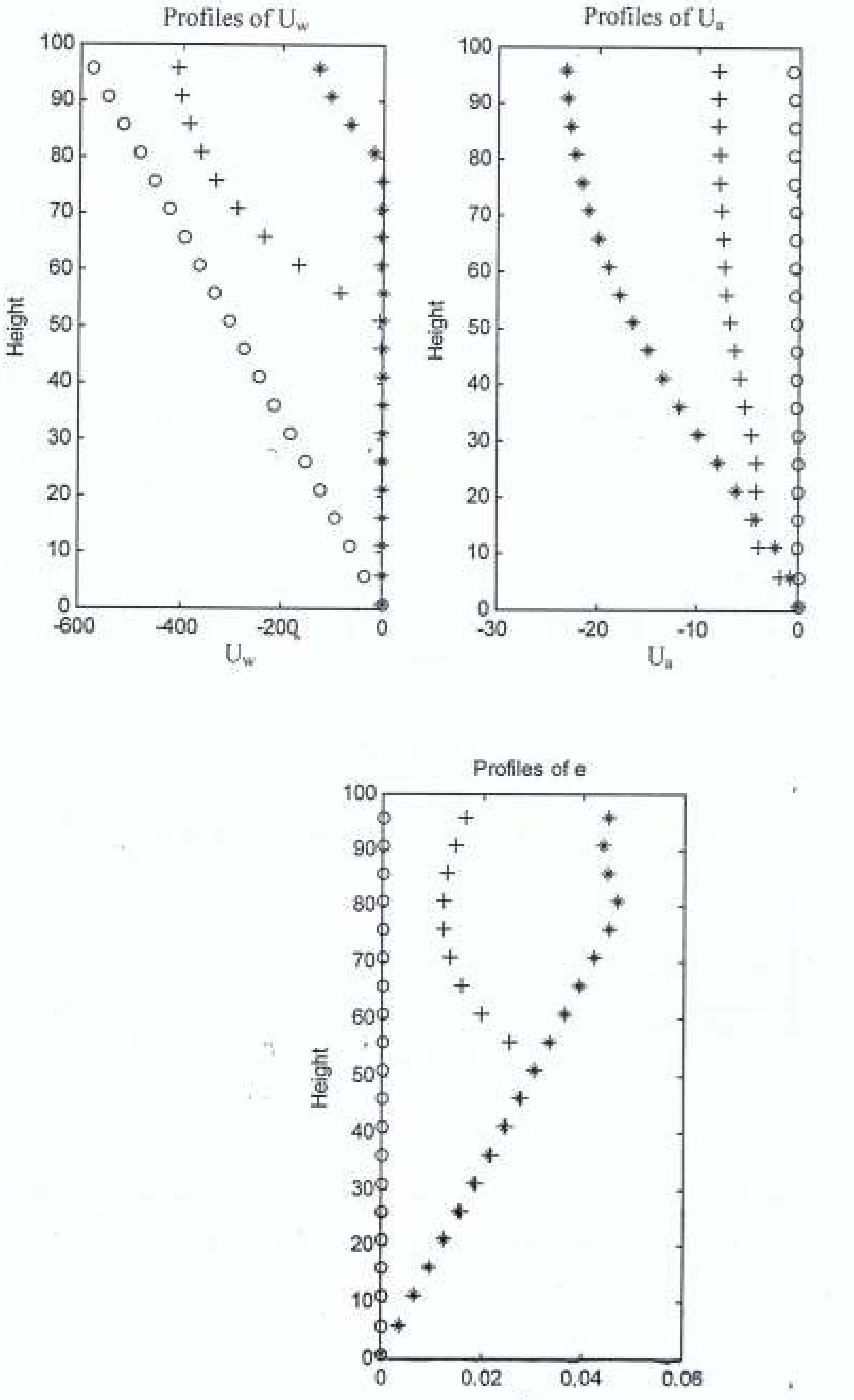

Fig. 3.8a: Profiles of U_w, U_a and e for: $S_r = 60\%$, $C = 4.3 \times 10^{-3}\ cm^2/sec$, $a_v = 1.72 \times 10^{-4} kN^{-1}$ ftime, simulation period = 172800secs

Case 3

Key: + + + + - Surface plot

* * * * - Mid height plot

——— - Bottom plot

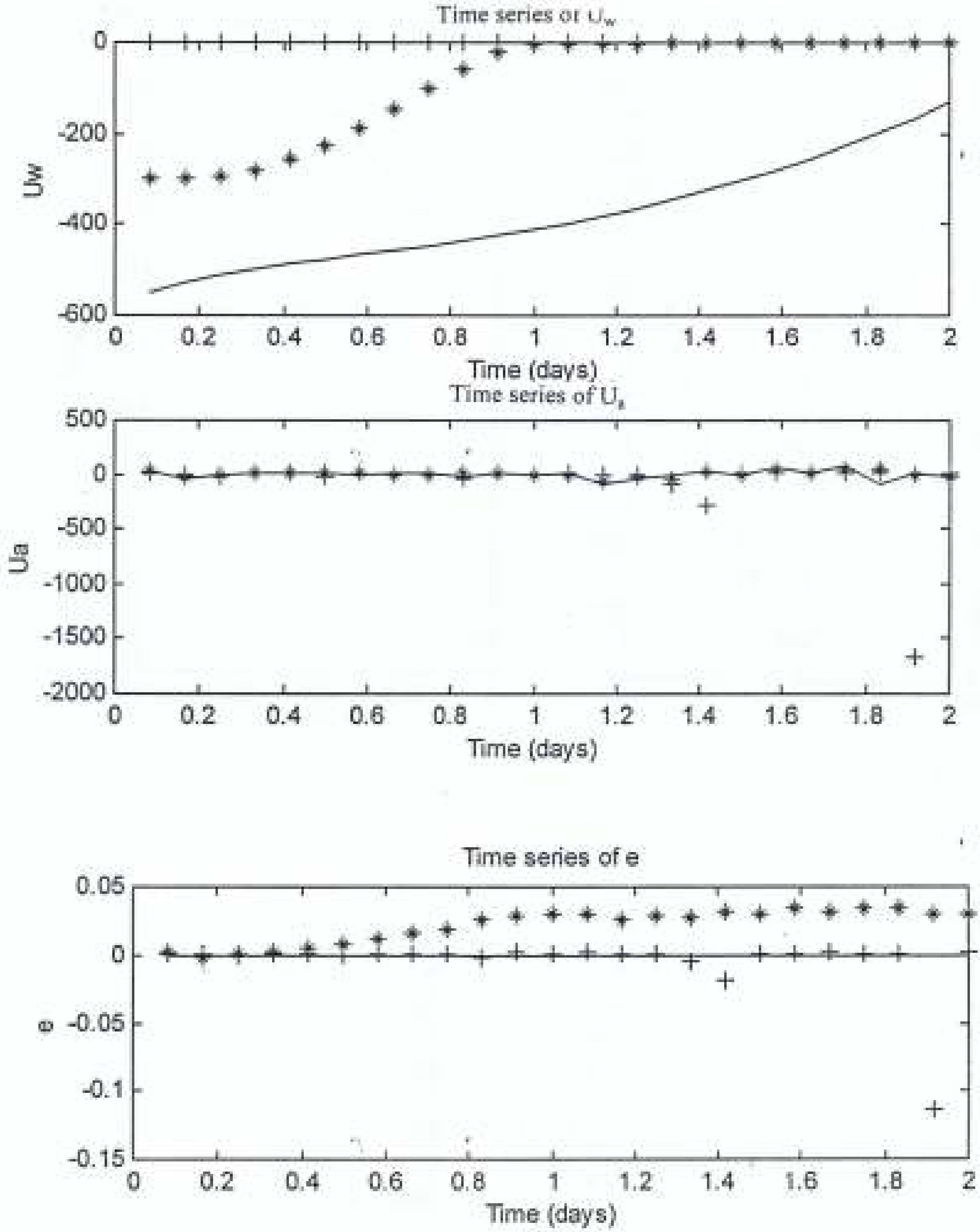

Fig. 3.8b: Time series of U_w, U_a and e for: $S_r = 60\%$, $C = 4.3 \times 10^{-3}$ cm^2/sec, $a_v = 1.72 \times 10^{-4} kN^{-1}$ ftime, simulation period = 172800secs

Case 4

Key: o o o o - Initial plot

+ + + + - Plot during consolidation

* * * * - Final plot

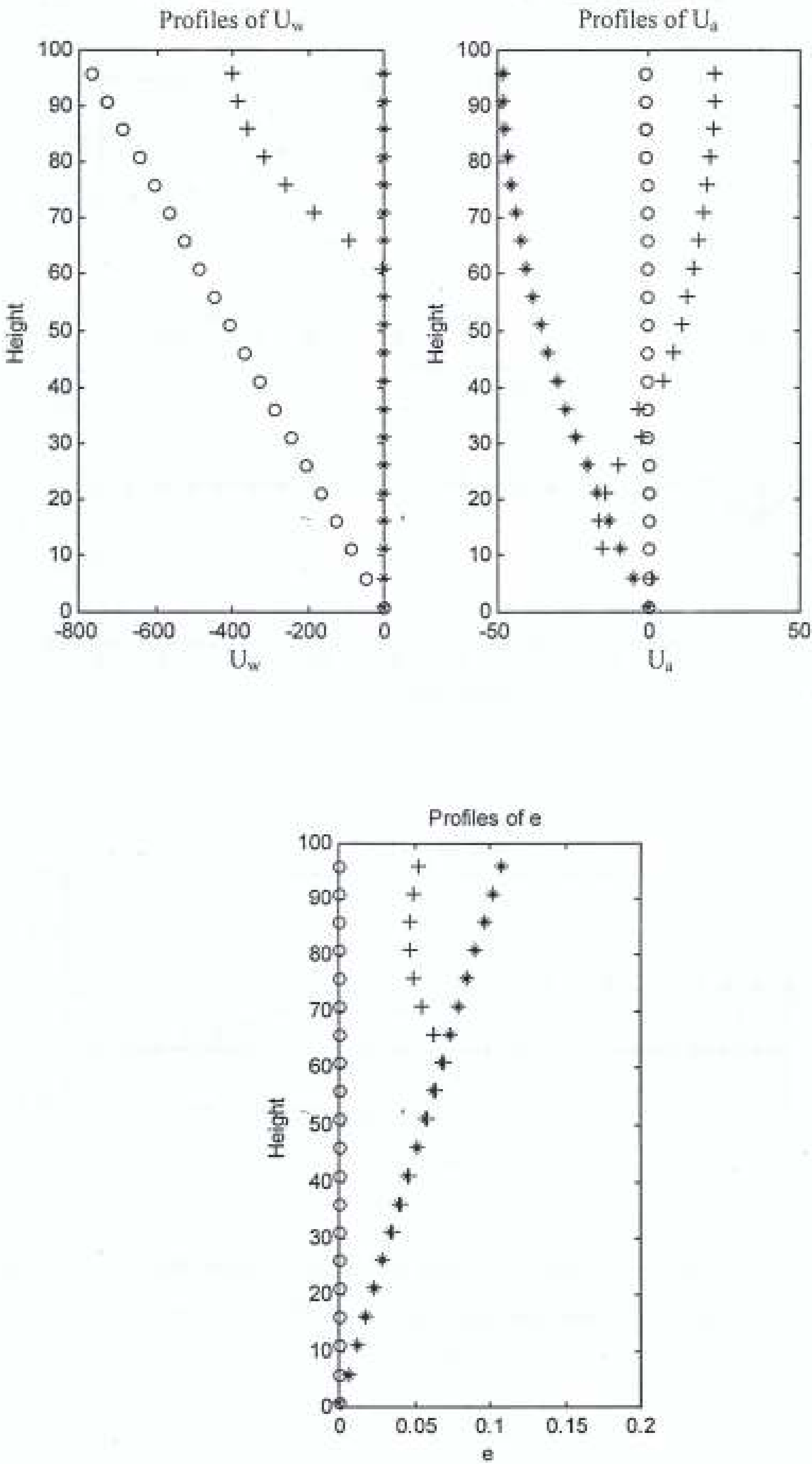

Fig. 3.9a: Profiles of U_w, U_a and e for: S_r = 80%, C = 9.98x 10^{-3} cm^2/sec, a_v = 1.76 x $10^{-4}kN^{-1}$ ftime, simulation period = 172800secs

Case 4

Key: + + + + - Surface plot

* * * * - Mid height plot

_____ - Bottom plot

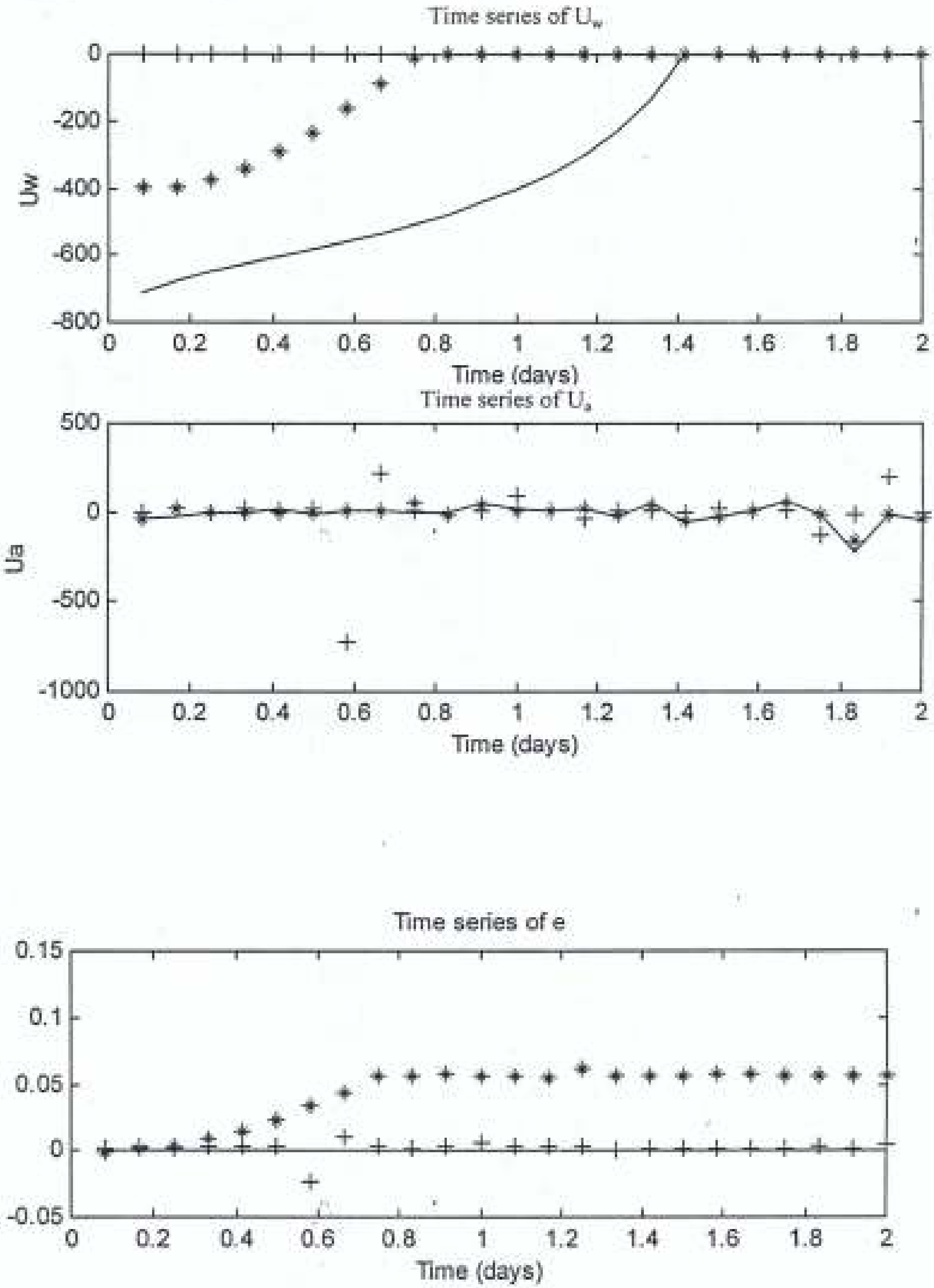

Fig. 3.9b: Time series of U_w, U_a and e for: $S_r = 80\%$, $C = 9.98 \times 10^{-3}\ cm^2/sec$, $a_v = 1.76 \times 10^{-4} kN^{-1}$ ftime, simulation period = 172800secs

Case 5

Key: o o o o - Initial plot

\+ + + + - Plot during consolidation

* * * * - Final plot

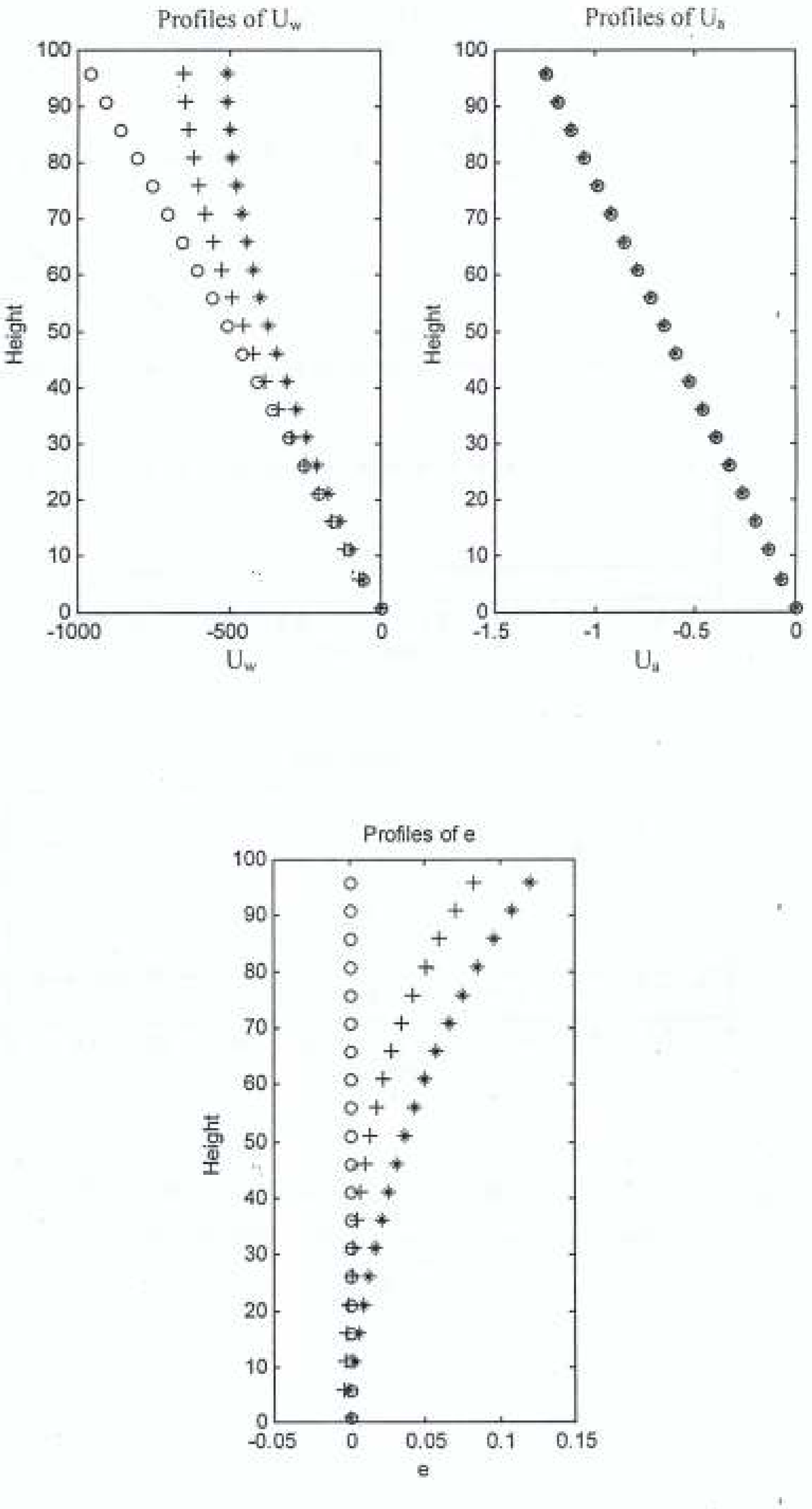

Fig. 3.10a: Profiles of U_w, U_a and e for: $S_r = 100\%$, $C = 1.07 \times 10^{-2}$ cm^2/sec, $a_v = 2.70 \times 10^{-4}$ kN^{-1} ftime, simulation period = 172800secs

Case 5

Key: + + + + - Surface plot

* * * * - Mid height plot

______ - Bottom plot

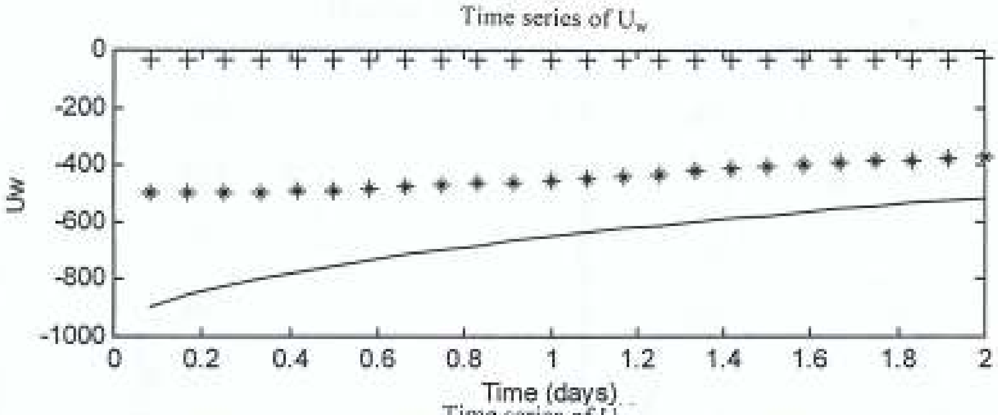

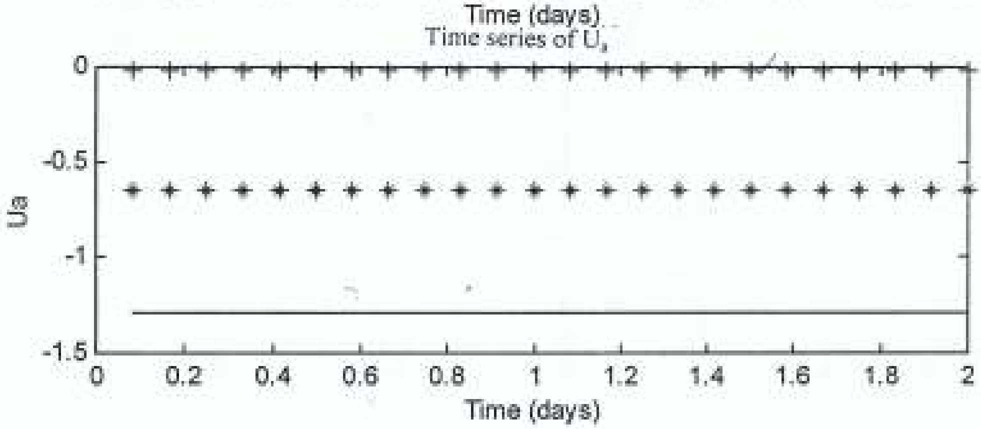

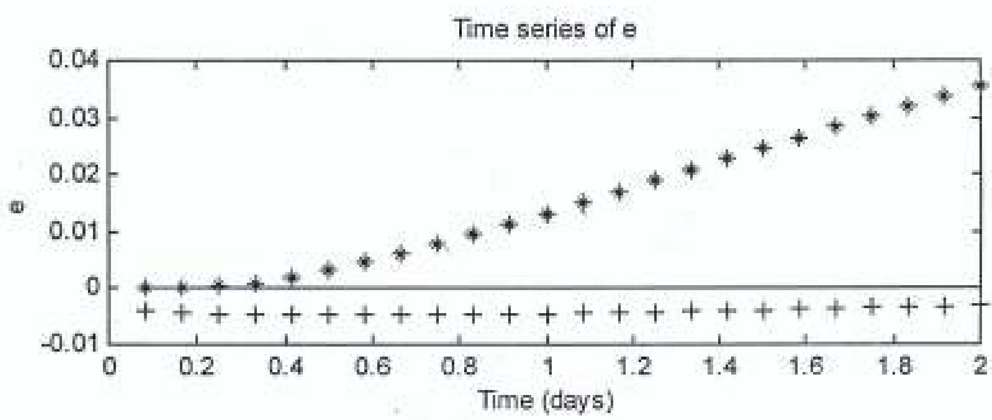

Fig. 3.10b: Time series of U_w, U_a and e for: $S_r = 100\%$, $C = 1.07 \times 10^{-2}$ cm^2/sec, $a_v = 2.70 \times 10^{-4}$kN^{-1} ftime, simulation period = 172800secs

Case5s

Key: o o o o - Initial plot
\+ + + + - Plot during consolidation
* * * * - Final plot

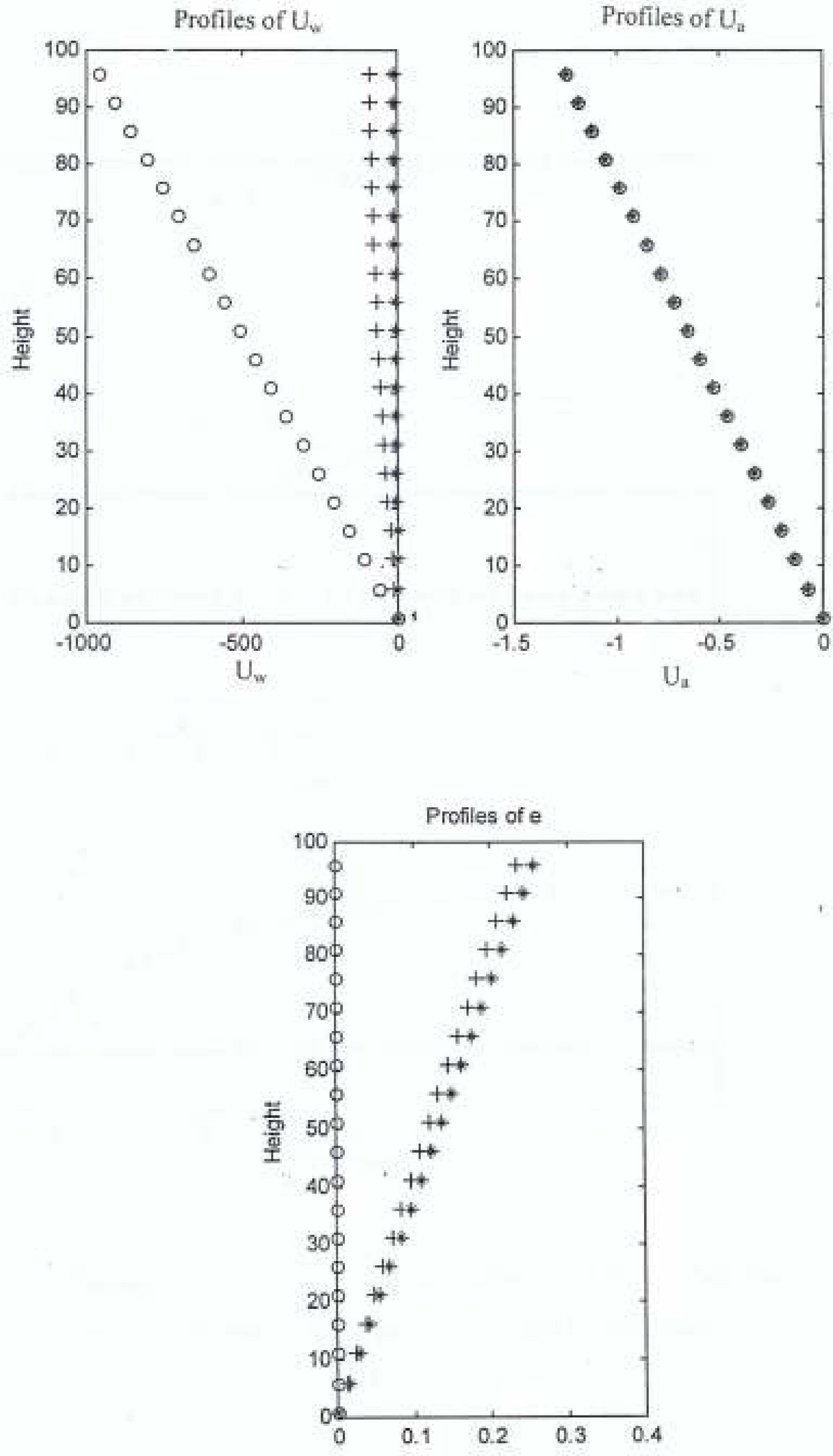

Fig. 3.11a: Profiles of U_w, U_a and e for: $S_r = 100\%$, $C = 1.07 \times 10^{-2}$ cm^2/sec, $a_v = 2.70 \times 10^{-4}$kN^{-1} ftime, simulation period = 1728000secs

Case 5s

Key: + + + + - Surface plot

* * * * - Mid height plot

_____ - Bottom plot

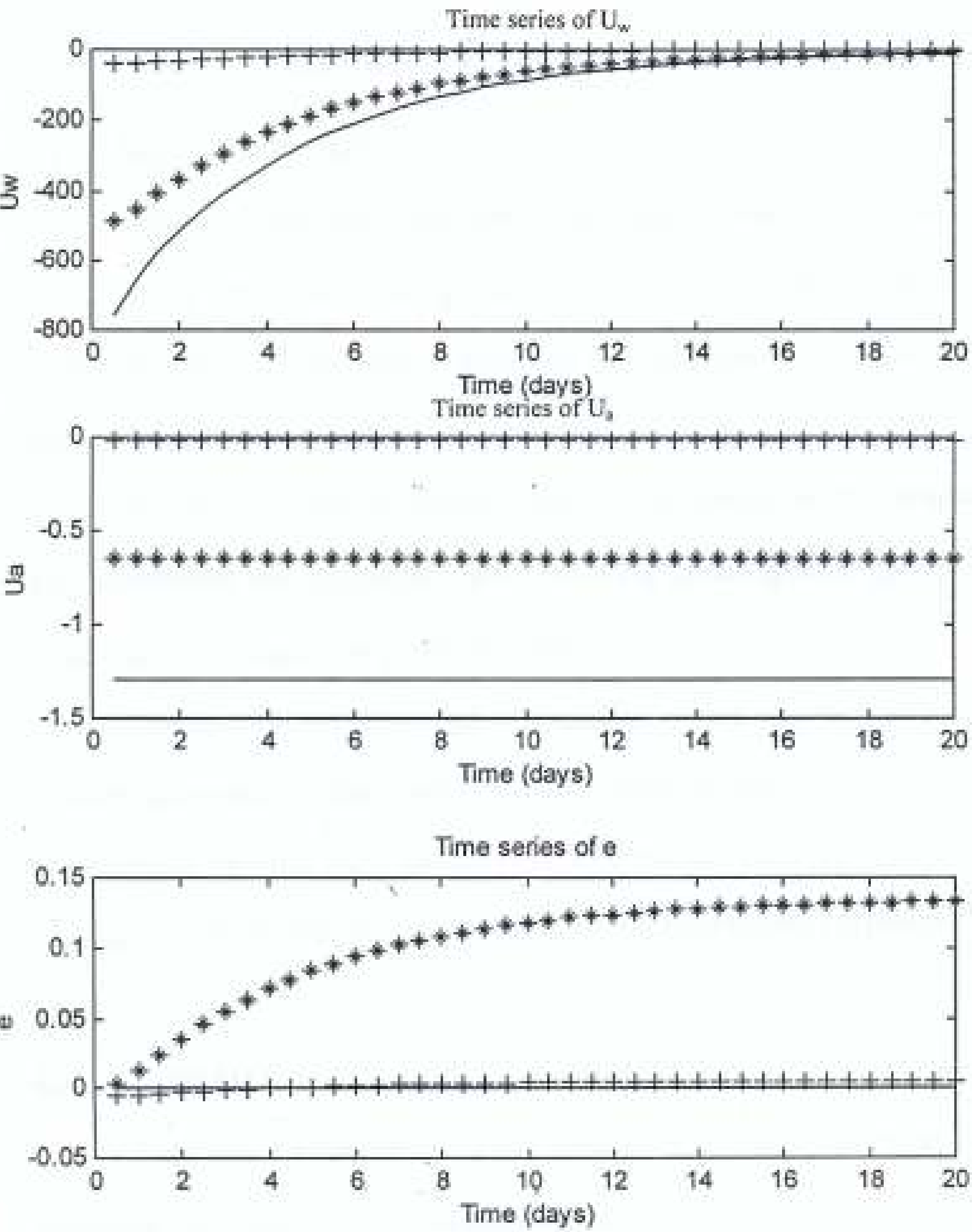

Fig. 3.11b: Time series of U_w, U_a and e for: S_r = 100%, C = 1.07×10^{-2} cm^2/sec, $a_v = 2.70 \times 10^{-4} kN^{-1}$ ftime, simulation period = 1728000secs

CHAPTER FOUR

EXPERIMENTAL PROGRAMME

4.1 METHODOLOGY

Relatively disturbed Black cotton soil samples were obtained at a depth of about 1.5m, from a section of existing road with black cotton soil subgrade from Numan to Guyuk off Yola – Gombe road in Adamawa State of Nigeria. The exact location of the site was at Banjiram along the Numan-Guyuk road.

Identification and classification tests were performed on the samples, notably; grain size distribution and hydrometer tests, Atterberg limits, specific gravity and compaction tests. These constituted the preliminary tests.

Compressibility and strength characteristics were determined using Oedometer and Triaxial compression tests, while suction measurements were conducted on samples compacted to specific water contents and degrees of saturation. The test procedure is in accordance with the BS1377:1975 (Soils for Civil Engineering Purposes).

4.2 IDENTIFICATION AND CLASSIFICATION

The characteristics of the Black cotton soil used are shown on Table 4.1 and the corresponding classification using the Textural classification, American Association of State Highway Officials method (AASHO), and the Unified Soil Classification System (USCS). The results of the grain size distribution and compaction test are presented in Figures 4.1 and 4.2. The details of the identification and classification tests are available in the appendix.

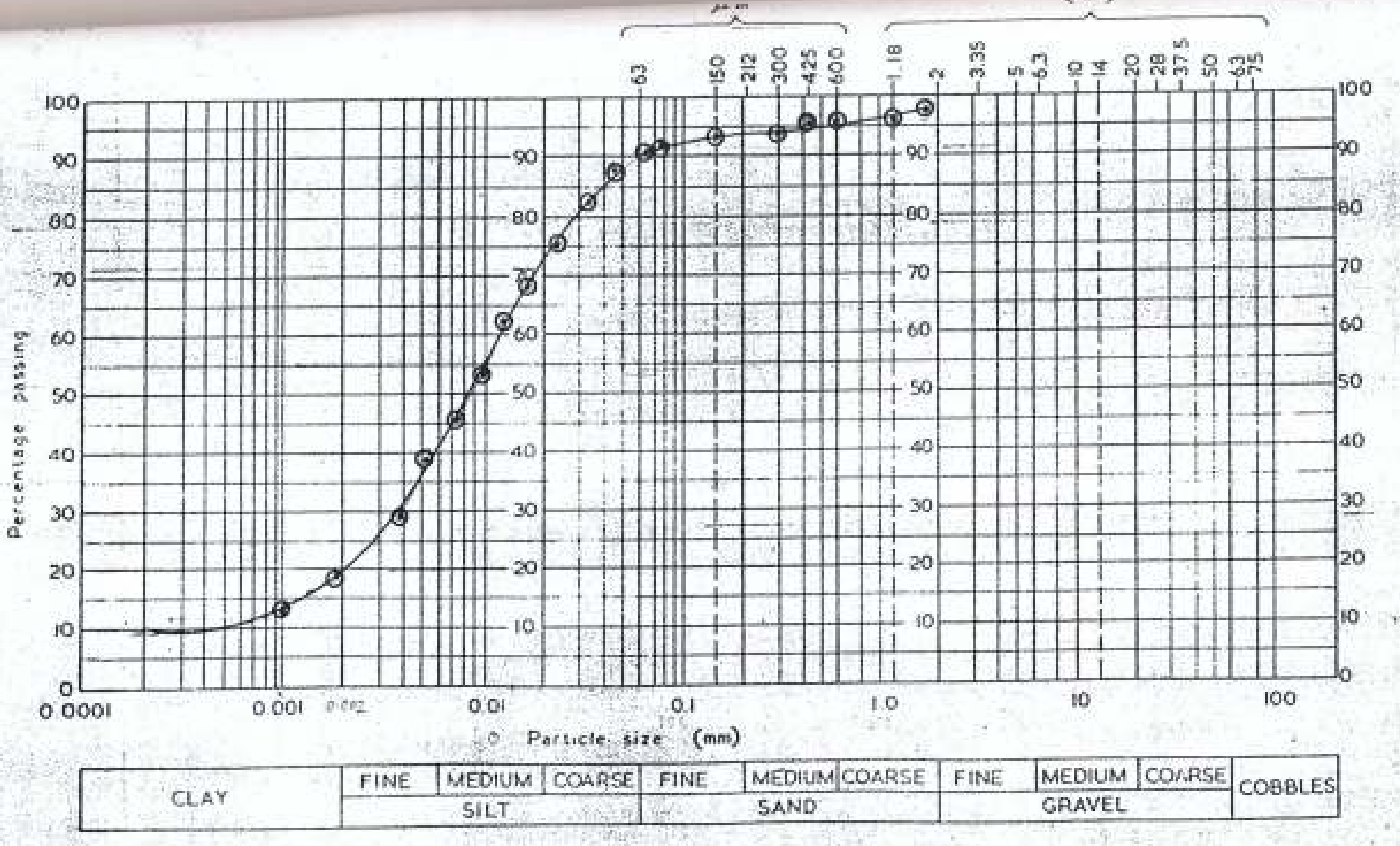

Figure 4.1 Particle size distribution for the Black Cotton Soil

Water Content Determination

Sample no.	1		2		3		4		5		6	
Moisture can no.												
Mass of cup + wet soil	63.9	57.0	49.6	50.2	58.3	58.4	51.9	49.3	47.0	47.7		
Mass of cup + dry soil	57.2	51.2	44.4	45.1	51.3	51.1	45.3	43.3	41.1	41.6		
Mass of water	6.7	5.8	5.2	5.1	7.0	7.3	6.6	6.0	5.9	6.1		
Mass of cup, g	16.3	16.3	16.3	16.3	16.3	16.3	16.3	16.3	16.3	16.3		
Mass of dry soil, g	40.9	34.9	28.1	28.8	35.0	34.8	29.0	27.0	24.8	25.3		
Water content, w%	16.4	16.6	18.5	17.7	02.0	21.0	22.8	22.2	23.8	24.2		

Density and Unit Weight [illegible]

Assumed water content						
Water content, w%	16.5	18.1	20.5	22.5	24.0	
Mass of soil + mold, g	10247	10573	10743	10789	10560	
Mass of mold, g	5472	5472	5472	5472	5472	
Mass of soil in mold, M_m	4775	5101	5271	5317	5088	
Wet unit weight, kN/m^3	20.55	21.95	22.68	22.88	21.89	
Dry unit weight γ, kN/m^3	17.64	18.59	18.82	18.68	17.65	

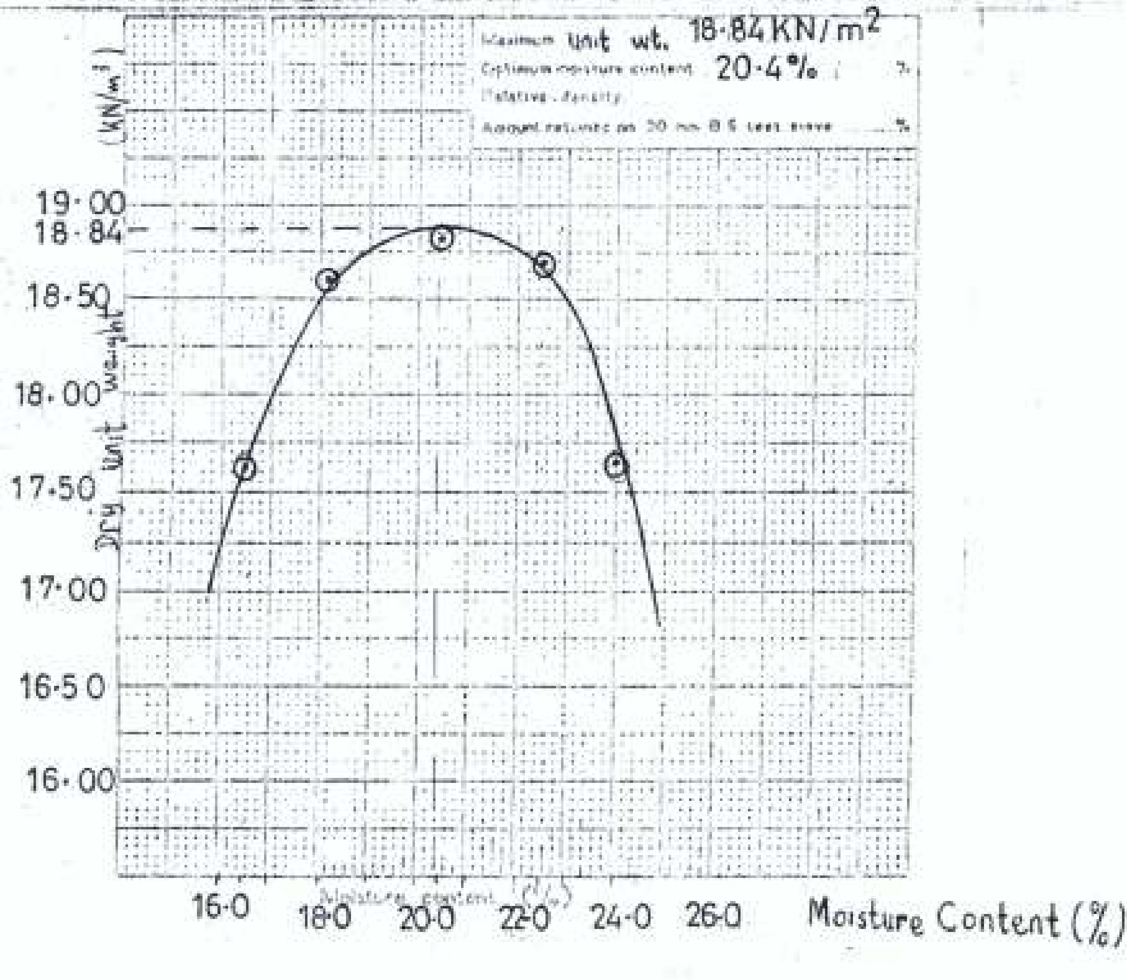

Figure 4.2: Dry unit weight versus moisture content

Table 4.1: Summarized Characteristics of Soil used

Property	**Black Cotton Soil**
Sampling location	BANJIRAM; Numan – Guyuk road off Yola – Gombe road, Adamawa State
Sampling depth (m)	1.5
Mechanical analysis (%):	
Sand (2 – 0.063mm)	9.9
Silt (74 - 5 μ)	51.1
Clay (< 5 μ)	39.0
Clay (< 2 μ)	18.0
Physical:	
Liquid Limit (%)	54.0
Plastic Limit (%)	23.0
Linear shrinkage (%)	11.0
Plasticity index	31.0
Max. dry density (kg/m^3)	1920.0
Opt. Moist. Content (%)	20.4
Spec. gravity	2.29
Chemical:	
Skempton's Activity	1.73
Predom. Clay mineral	Montmorillonite
Classification	
Textural	Silty Clay
AASHO	A-7-6
USCS	CH

4.3 PREPARATION OF SPECIMENS

Test specimens were prepared by mixing air dried Black Cotton soil with a predetermined amount of water (Equation 4.1) that will be required to achieve the specific degree of saturation after establishing the initial moisture content of the soil using the speedy moisture tester and statically compacting the mixture to an arbitrary density. The density used was the maximum dry density obtained from the preliminary compaction test ($1920 kg/m^3$). Based on the relationship between the degree of saturation 'S_r' and water content 'm' as in equation 4.1 (Rosenak, 1963)

$$S_r = \frac{m}{\frac{\gamma_w}{\gamma_d} - \frac{1}{G_s}} \qquad (4.1)$$

Where

S_r = Degree of saturation

G_S = Specific gravity

γ_d = Dry unit weight

γ_w = Unit weight of water

m = water content

From (4.1) making "m" the subject, we have

$$m = S_r\left[\frac{\gamma_w}{\gamma_d} - \frac{1}{G_s}\right] \qquad (4.2)$$

Using eqn (4.2) and the degree of saturation, 20%, 40%, 60%, 80% and 100%, the required percentage of water for compacting the samples to the required degree of saturation was determined.

Following compaction and trimming, all samples for both suction tests and stress-strain tests were coated with grease and stored in a desiccators for seven days before testing, to minimize changes due to thixotropic effects or increases in suction.

4.4 COMPRESSIBILITY CHARACTERISTICS (OEDOMETER TEST)

4.4.1 ONE-DIMENSIONAL CONSOLIDATION TEST FOR PARTIALLY SATURATED SOIL

Initially, the soil is quite compressible initially, since the pore fluid (air plus water) offers little resistance to compression until the degree of saturation exceeds 85%. During this initial phase, the effective stress increases while the pore pressure changes but little. Very little water will be squeezed out from the soil during this phase of a drained loading: thus it matters little whether drainage is permitted or prevented.

If the load increase is sufficient to compress, and dissolve all of the air in the pores, the soil will become fully saturated and now any further increase in load will be carried entirely by the pore fluid. If drainage is permitted, water will flow from the specimen as in a consolidation test upon an initially saturated soil. Once the applied load reaches its maximum value and becomes constant, a drained soil may again become only partially saturated.

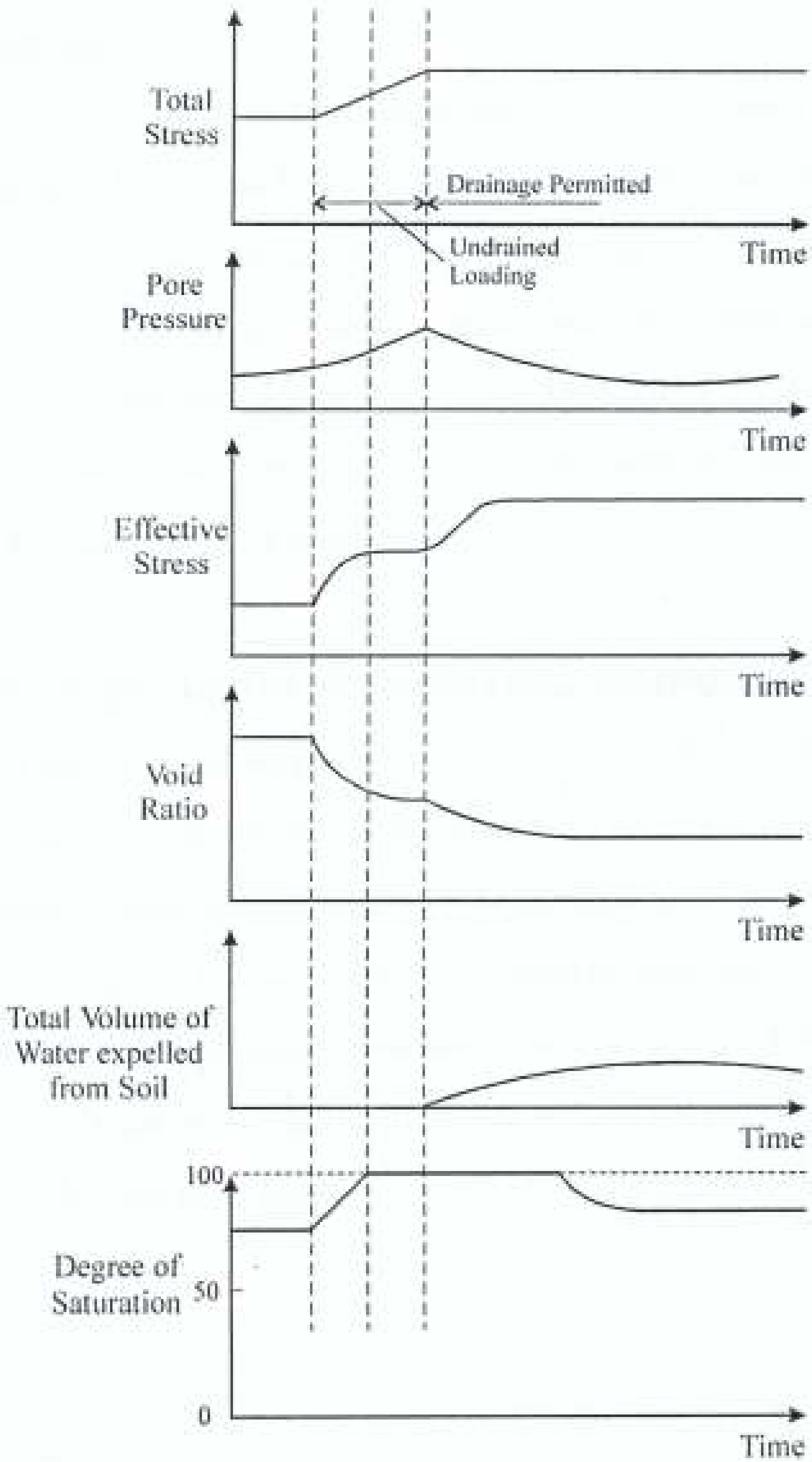

Figure 4.3: The events that occur during one-dimensional compression of a partially saturated soil in an Oedometer.

4.4.2 PROCEDURE

The procedure for testing the prepared partially saturated black cotton soil samples was according to the British Standard BS1377, 1975: Soils for Civil Engineering Purposes: loading and unloading the specimen was carried out in two cycles.

The Oedometer test was performed for black cotton soil samples compacted to; 20%, 40%, 60%, 80% and 100% degrees of saturation. The assembly of apparatus for the Oedometer test is shown in the picture in Photo 4.21. The results for this experiment is presented and discussed in chapter 5 of this report.

4.5 STRENGTH CHARACTERISTICS (TRIAXIAL COMPRESSION TEST)

With the normal triaxial equipment used for laboratory testing, it is not feasible to accurately determine the effective stresses in unsaturated soil samples. So the common practice is to conduct undrained triaxial tests on unsaturated soil samples and measure only the total stresses. Figure 4.30 shows a total stress failure envelope that will be obtained from a number of undrained triaxial tests conducted with a given initial degree of saturation. Failure envelopes were obtained for varying initial degree of saturation viz: 20%, 40%, 60%, 80% and 100% respectively.

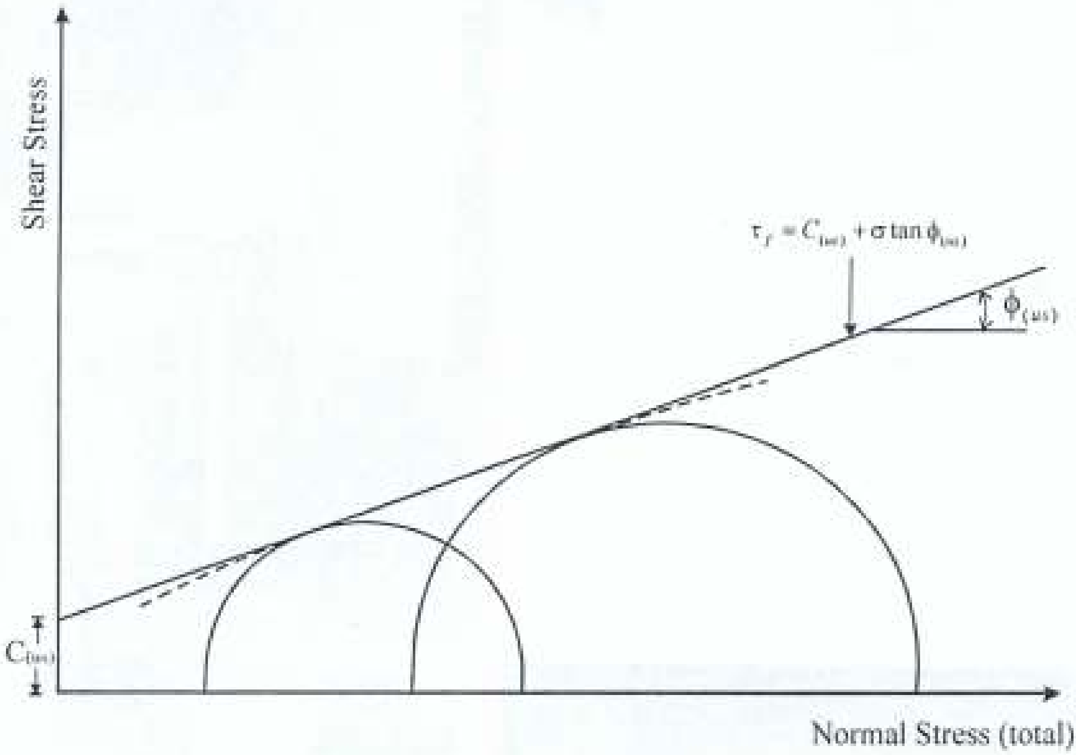

Figure 4.30: Total stress failure envelope for an unsaturated soil sample.

4.5.1 TRIAXIAL COMPRESSION TEST

This test covers the determination of the compressive strength of a specimen of prepared partially saturated Black Cotton soil in the triaxial compression apparatus. The test is limited to specimens in the form of right cylinders of nominal diameter 38mm and of height 76mm. The arrangement of the triaxial compression test apparatus for the experiment is shown in Photo 4.31.

The procedure for the experiment was in accordance with British Standard BS1377:1975. For each initial degree of saturation, three specimens of the black cotton soil was tested, to facilitate obtaining the failure envelope. The results for this test are presented and discussed in chapter 5 of this report.

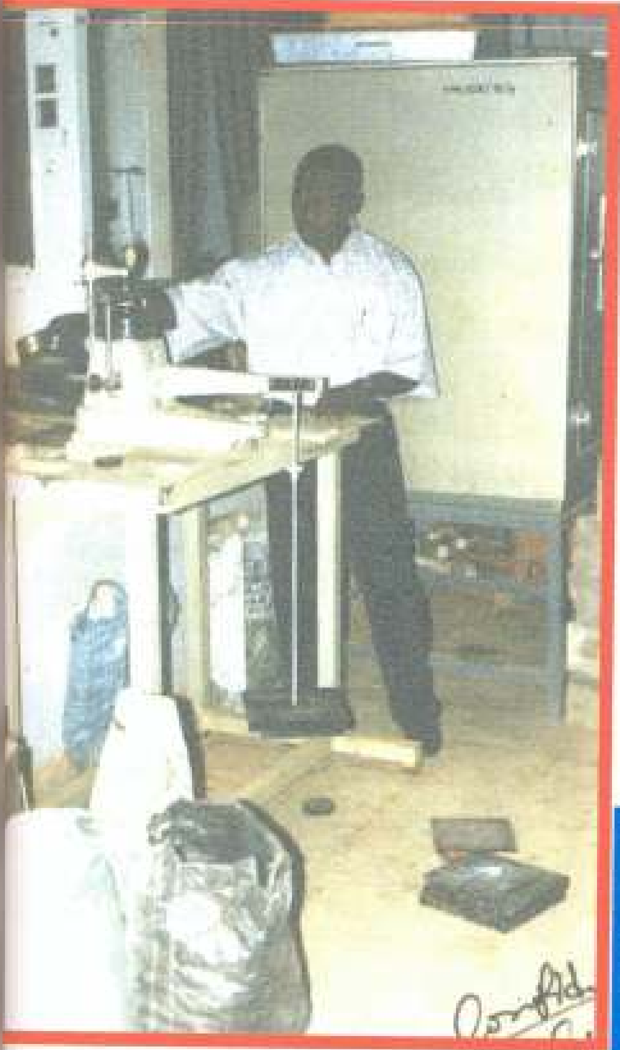

Photo 4.21: Set up of the Oedometer during the testing programme

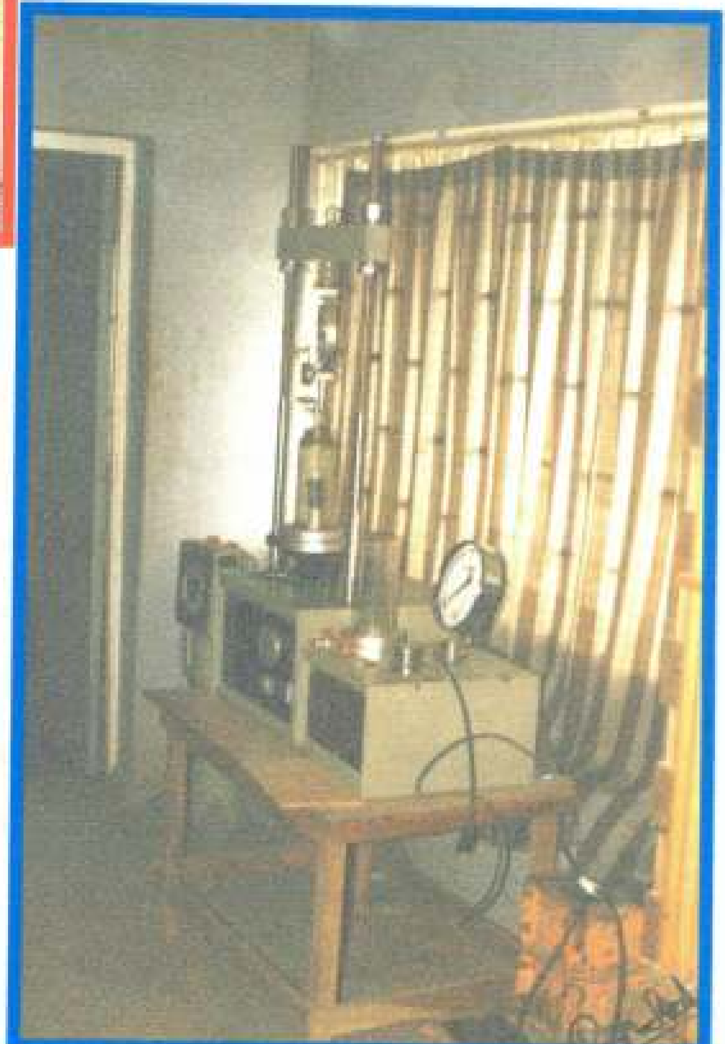

4.31: Arrangement of the triaxial compression test apparatus

4.6 SUCTION MEASUREMENTS

The filter paper method was used in the measurement of soil suction for the experiments performed. This involves the placement of a filter paper in direct contact with the soil specimen.

Moisture equalization between the filter paper and the soil should take place in a relatively constant temperature environment. The filter paper is allowed to equilibrate for at least one week prior to measuring their water contents. The water content is then used along with a calibration curve for filter paper water content versus suction to determine the suction of the soil.

4.6.1 MEASUREMENTS FOR THE BLACK COTTON SOIL SAMPLES

Black cotton soil samples, compacted with various moulding water contents to different degrees of saturation (i.e 20%, 40%, 60%, 80% and 100%) were coated with grease and stored for seven days in a desiccator before testing to minimize changes due to thixotropic effects or increases in suction.

Contact filter paper suction measurements were made on the samples in the laboratory. The filter paper was placed against the soil sample, double wrapped with kitchen foil and taped for contact measurements. The trimmed compacted cylindrical samples were about 40mm in height and 75mm in diameter. The samples were then stored in a cooled incubator, maintained at a constant temperature of 26^0C for one week.

The mettler balance: Type BD601, was used in weighing both the soil samples and the filter papers before and after the test. Photo 4.41 shows pictures of the apparatus used and the weighing process.

Photo 4.41 (a): Cooled incubator for maintaining constant temperature for one week

Photo 4.41 (b): Mettler balance for weighing both soil samples and filter papers

CHAPTER FIVE

RESULTS/DISCUSSION OF RESULTS

5.1 SUCTION TEST:

The result for the suction tests are as shown in Table 5.1;

Table 5.1: Suction test results

Molding water content(%)	Degree of saturation (%)	Sample wt. Before testing (g)	Sample wt. After 7 days (g)	Filter paper water content (%)	Corresponding suction value (Kpa)	Suction pressure (pF)
1.85	20	571.1	569.1	10	30,000	5.2
3.69	40	565.1	562.1	20	6,000	4.6
5.54	60	571.6	566.5	30	1,000	4.0
7.38	80	400.6	391.5	60	20	2.1
9.23	100	477.6	464.7	86	8	1.8

The calibration curve (Figure 5.0) for filter paper water content versus suction by McQUEEN and MILLER (1968), was used to convert the filter paper water content values to suction values.

The suction pressure can be expressed as negative pressure in Kpa or in other more convenient units. It has been shown that the most common units for soil suction are those which express it in terms of "cm" of water. The term pF, which has also been employed, is the $\log_{10}$ (cm of water) and is used for ease in plotting.

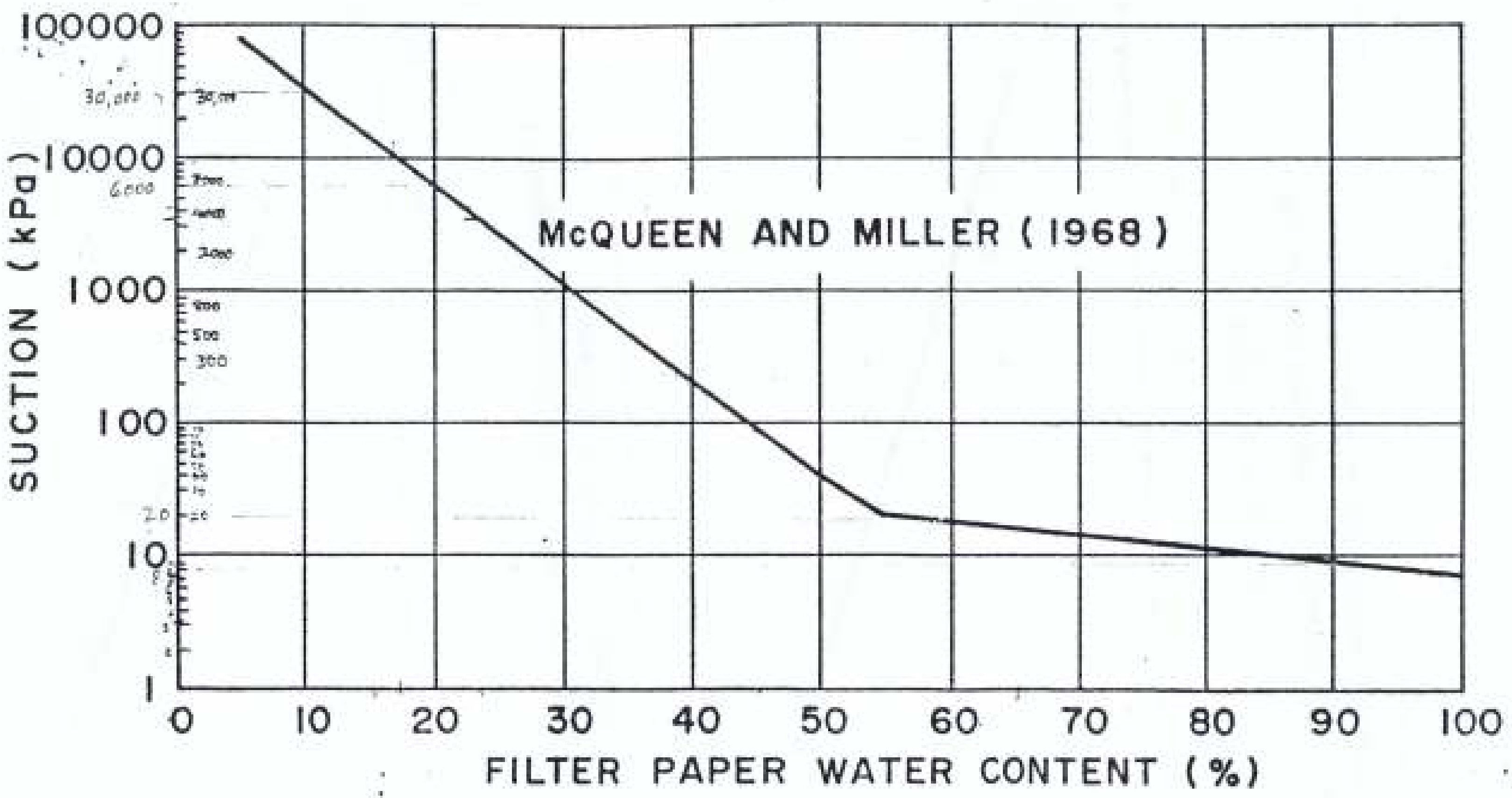

Figure 5.0: Calibration curve for filter paper versus suction

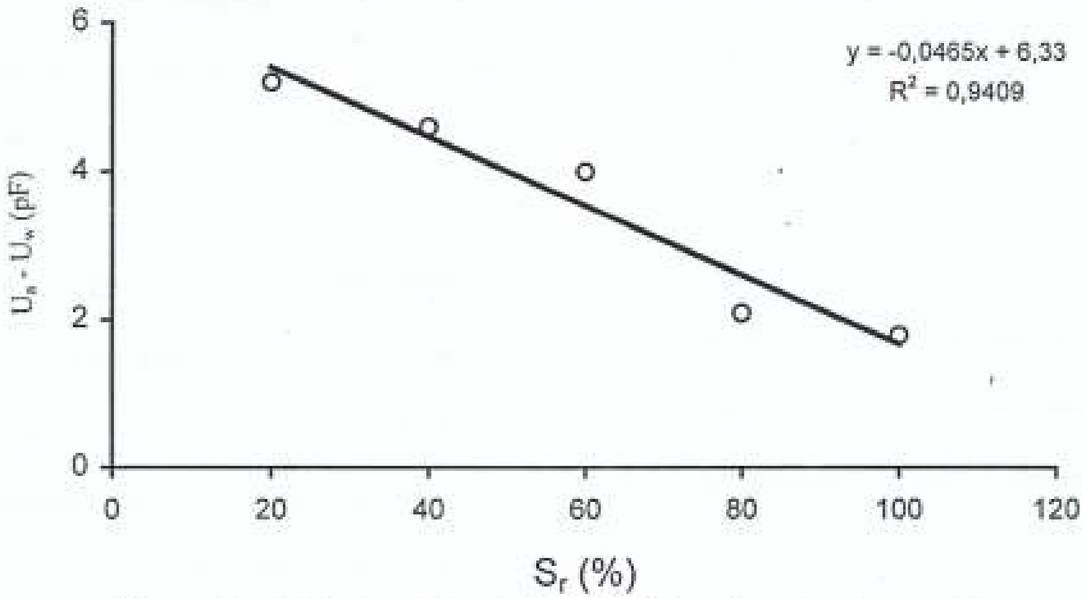

Figure 5.1a:Relationship between Soil Suction and degree of saturation for Black Cotton Soil

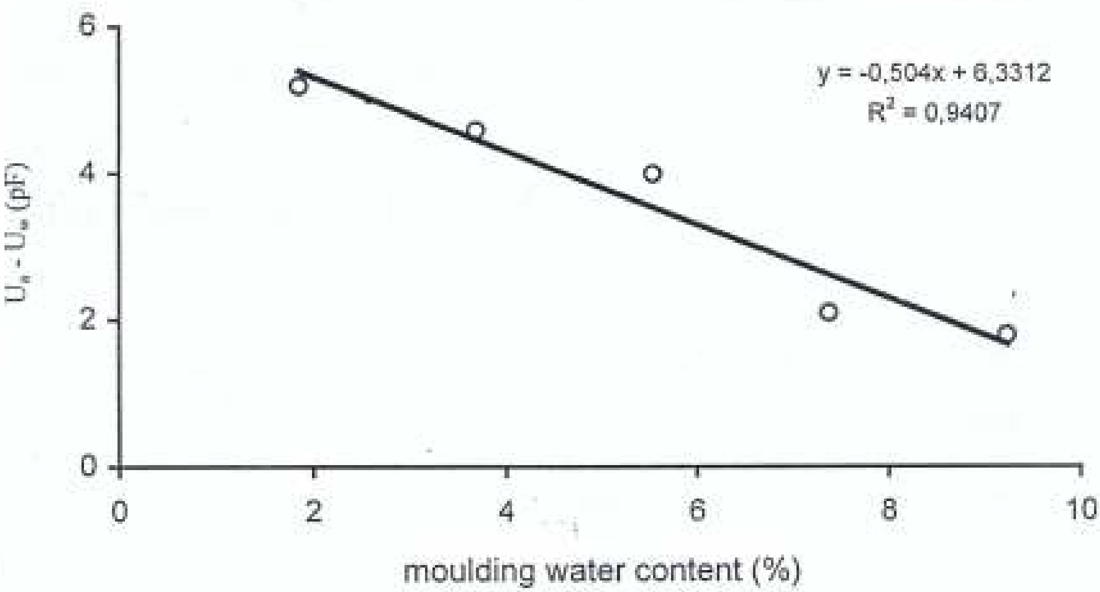

Figure 5.1b: Relationship between Soil Suction and moulding water content for Black Cotton Soil

The relationship between soil suction, moulding water content and degree of saturation for the Black cotton soil samples is illustrated graphically in Figures 5.1a and 5.1b.

5.2 TRIAXIAL COMPRESSION TEST

The results of the triaxial compression test on the Black cotton soil samples are presented in graphical form as Mohr circles with the Mohr-Coulomb envelope drawn to determine the cohesion intercept and the angle of shearing resistance. Figure 5.2 shows the Morh circles for the various degree of saturation.

The cohesion intercept "C" and the angle of shearing resistance ϕ obtained from the graphs are shown in Table 5.2

Table 5.2: Cohesion and angle of internal friction values for the Black cotton soil samples

Degree of Saturation S %	**C (kN/m^2)**	$\phi(^0)$
20	70	31.5
40	130	26.0
60	180	16.0
80	140	13.0
100	130	11.0

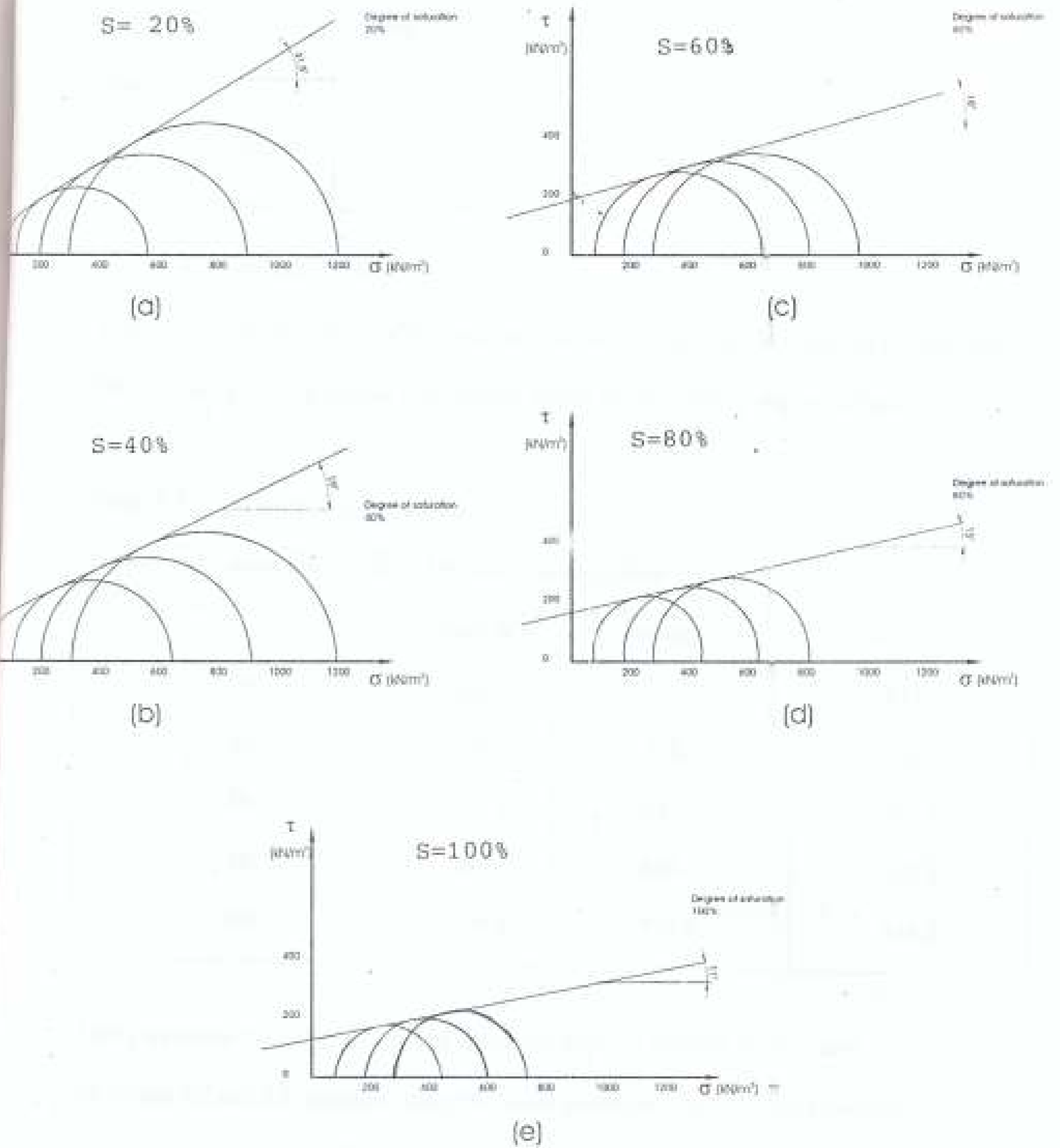

Figure 5.2: Mohr Circles for the black cotton soil

The shear strength values were then computed using the equation

$$\tau = c + \sigma_D \tan \phi \qquad 5.1$$

where

c = cohesion

ϕ = angle of internal friction

σ_D = deviator stress

Table 5.3 shows the values of the maximum deviator stress that was applied to load each of the three samples of prepared specimen to failure for the various degrees of saturation.

Table 5.3: Deviator stress values

Degree of saturation 'Sr' (%)	**Deviator Stress (kN/m^2)**		
	Sample I	**Sample II**	**Sample III**
20	426.2	717.4	919.3
40	555.6	720.5	912.5
60	561.4	643.7	701.8
80	356.2	469.5	522.2
100	356.0	421.4	446.2

Using equation 5.1and the values of cohesion, angle of internal friction, and deviator stress in Tables 5.2 and 5.3, the shear strength values shown in Table 5.4, were obtained.

Table 5.4: Shear strength value for the Black cotton soil for various degrees of Saturation

Degree of saturation 'Sr' (%)	Shear strength (kN/m^2)			Average shear strength(kN/m^2)
	Sample I	Sample II	Sample III	
20	331.2	509.6	633.3	491.4
40	401.0	481.4	575.1	485.8
60	341.0	364.6	381.2	362.3
80	222.2	248.4	260.6	243.7
100	199.2	211.9	216.7	209.3

The variation of shear strength with deviator stress for the various degrees of saturation is illustrated graphically in Figure 5.3. The strain values for deviator stresses are tabulated in Table 5.5

Table 5.5: Strain values for the Black cotton soil for increasing deviator stress at various degrees of saturation.

Degree of Saturation 'Sr' (%)	Strain $\frac{\Delta L}{L}$(%)			Average strain (%)
	Sample I	Sample II	Sample III	
20	5.59	6.9	6.60	6.36
40	4.60	6.25	5.92	5.59
50	6.90	5.92	6.58	6.00
80	3.95	5.92	6.25	5.37
100	4.60	5.92	6.25	5.59

Values of strain with deviator stress is shown in Figure 5.4 for varying degrees of saturation. The data sheets for the triaxial compression tests, containing details of stress and strain measurement are available in the appendix.

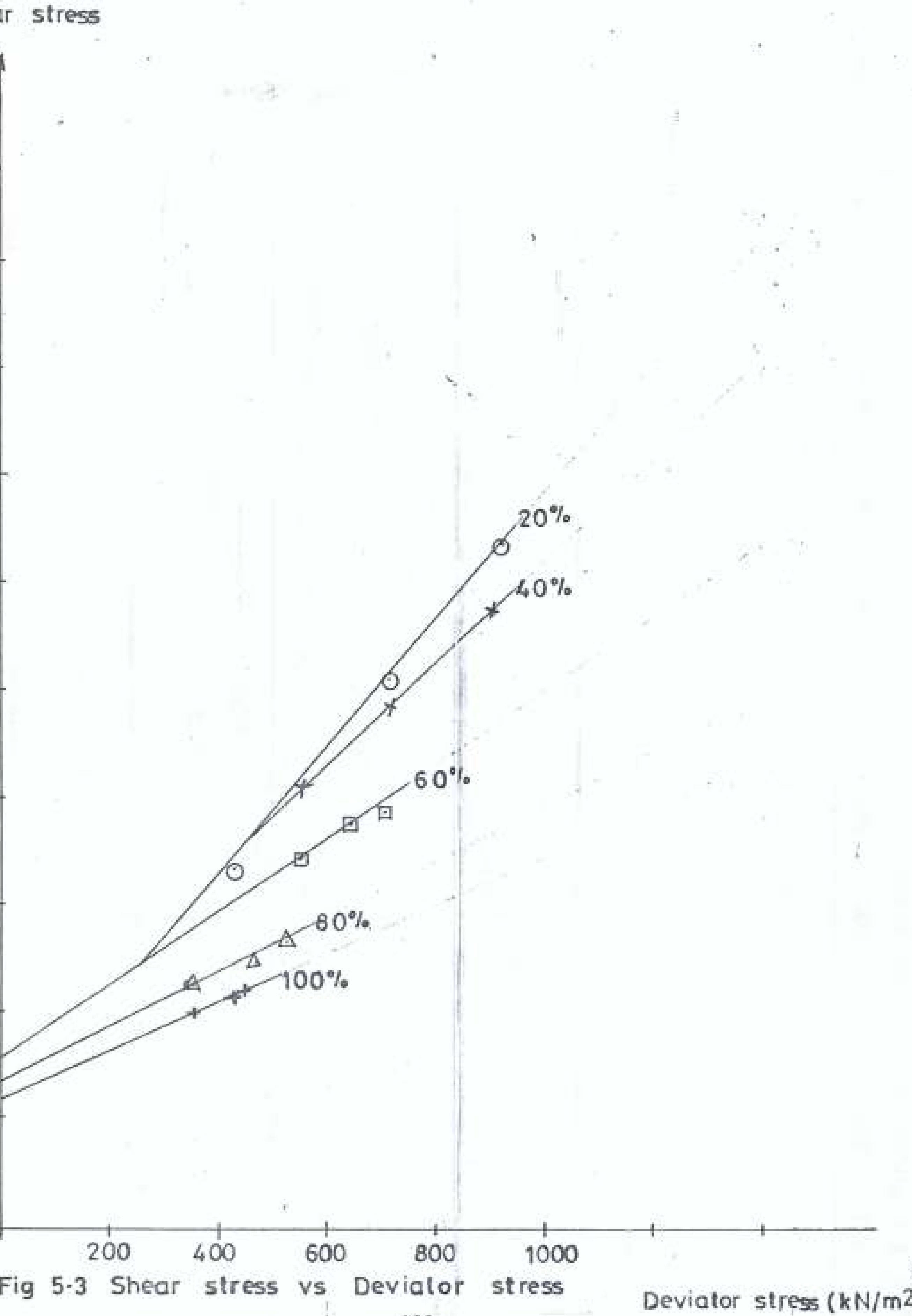

Fig 5·3 Shear stress vs Deviator stress

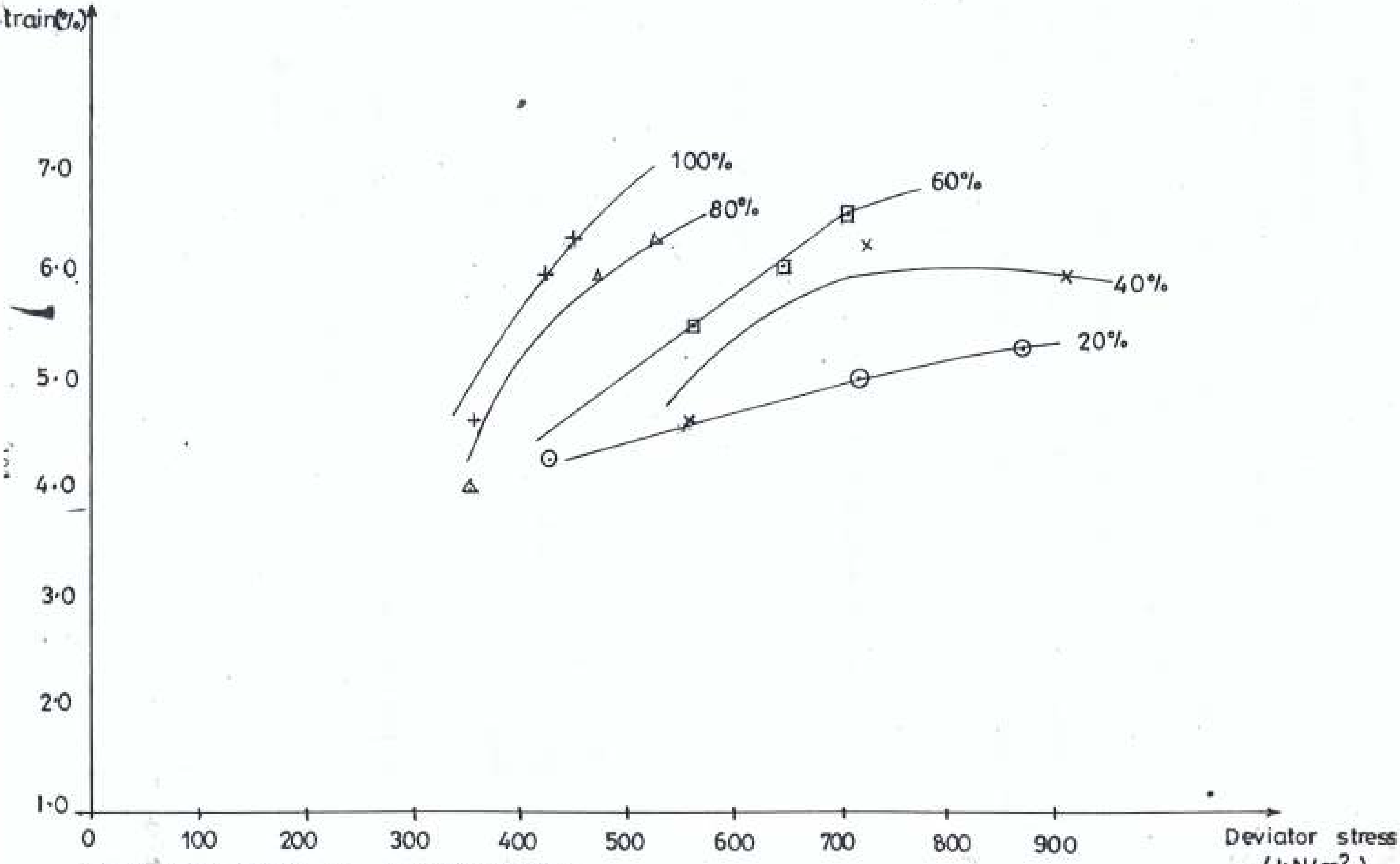

Figure 5·4 Strain vs Deviator Stress·

5.3 OEDOMETER TESTS

5.3.1 COMPRESSIBILITY CHARACTERISTICS

The compressibility characteristics have been suitably illustrated by plotting the compression of the specimen as ordinate on a linear scale and the corresponding applied pressure, P in kN/m^2 as abscissa on a logarithmic scale. The compression index "Cc" and the swell index "Cs" were computed for each of the plots, from the slope of the virgin compression curve and the rebound curve respectively. The results of the Oedometer test are presented in Figures 5.5a, 5.5b, 5.5c, 5.5d and 5.5e. A summary of the compression and swell indices are shown in Table 5.6

Table 5.6: Compression and swell indices for Black cotton soil at various degrees of saturation.

Degree of saturation 'Sr' (%)	**Compression index "Cc"**	**Swell index "Cs"**
20	0.0880	0.022
40	0.1570	0.056
60	0.1927	0.053
80	0.2181	0.024
100	0.3238	0.068

Also the values of the coefficient of compressibility 'a_v' determined from the slope of the graphs of voids ratio 'e' versus applied pressure "P" plotted on a linear scale can be seen in Table 5.7.

Figure 5.5a: Void Ratio 'e' vs. LogP plot (S=20%)

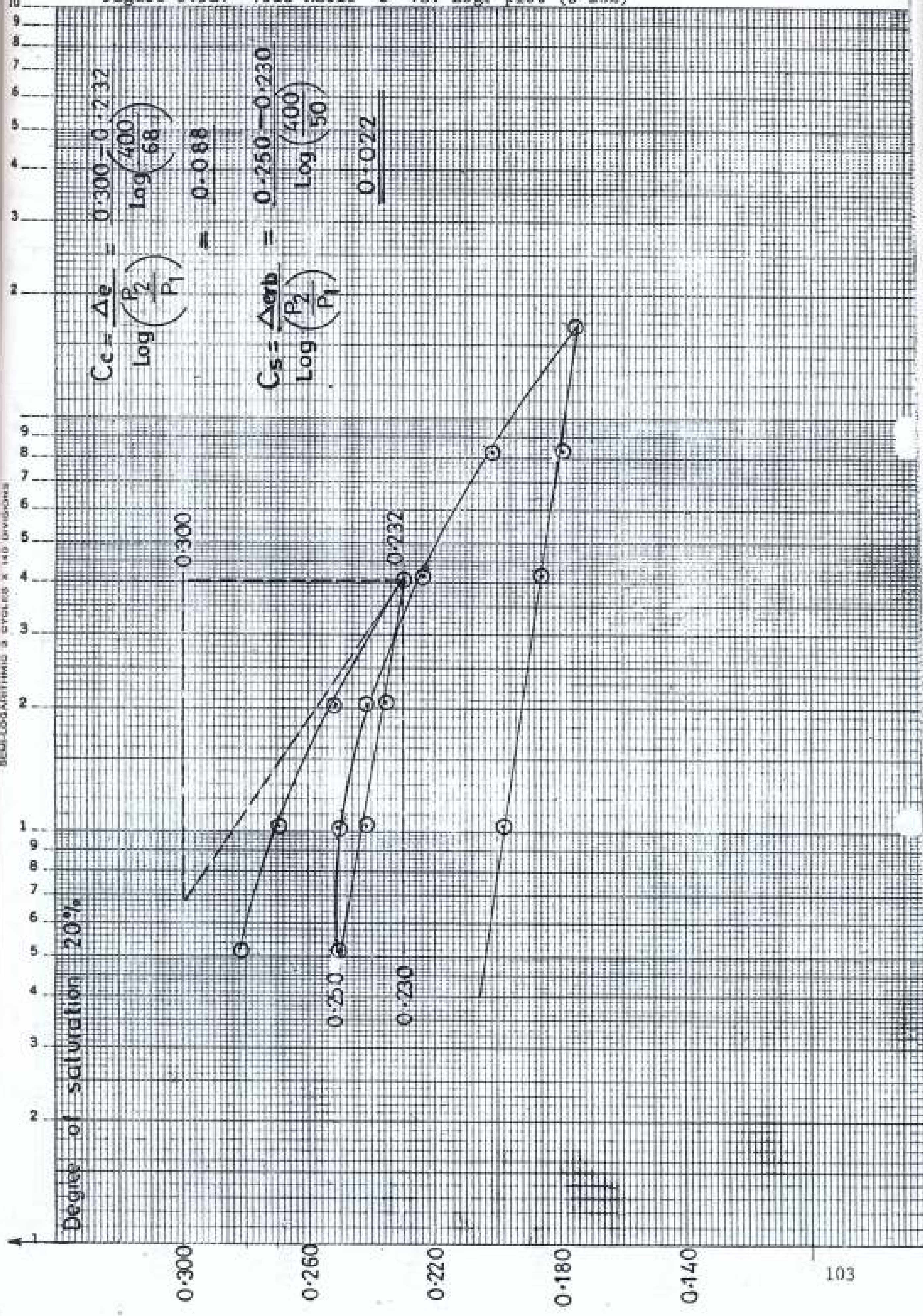

Figure 5.5b: Void Ratio 'e' vs. LogP plot (S=40%)

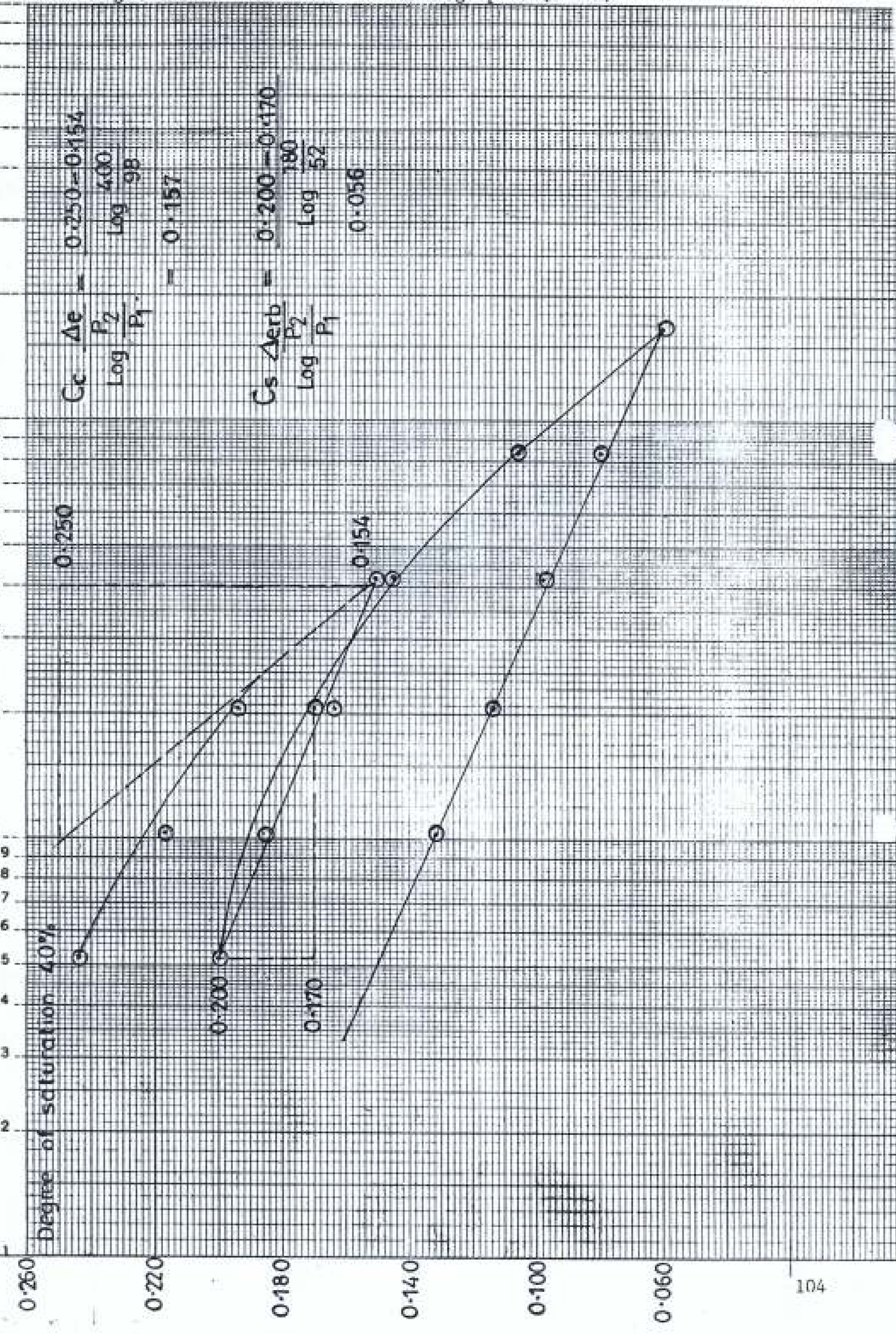

Figure 5.5c: Void Ratio 'e' vs. LogP plot (S=60%)

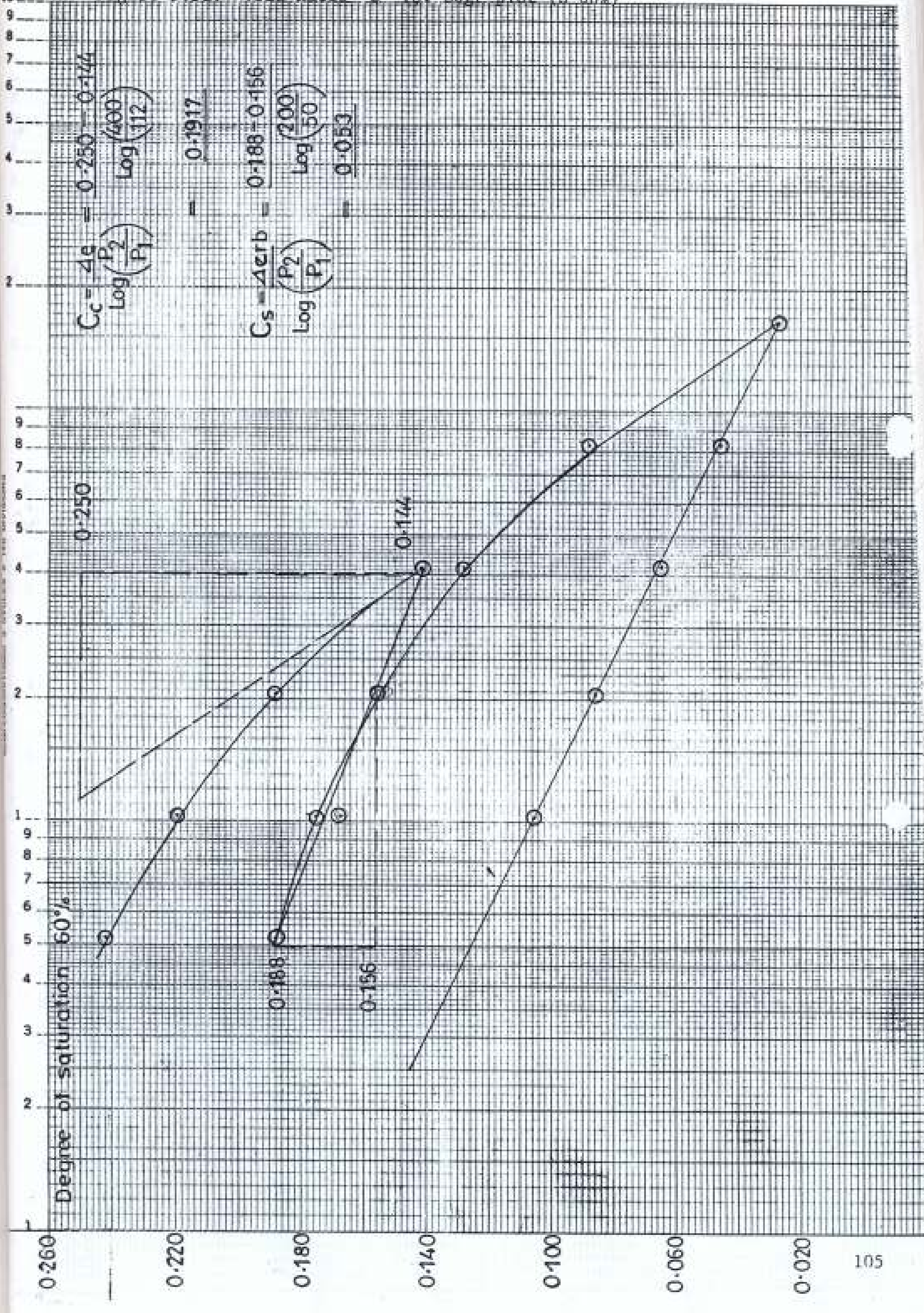

Figure 5.5d: Void Ratio 'e' vs. LogP plot (S=80%)

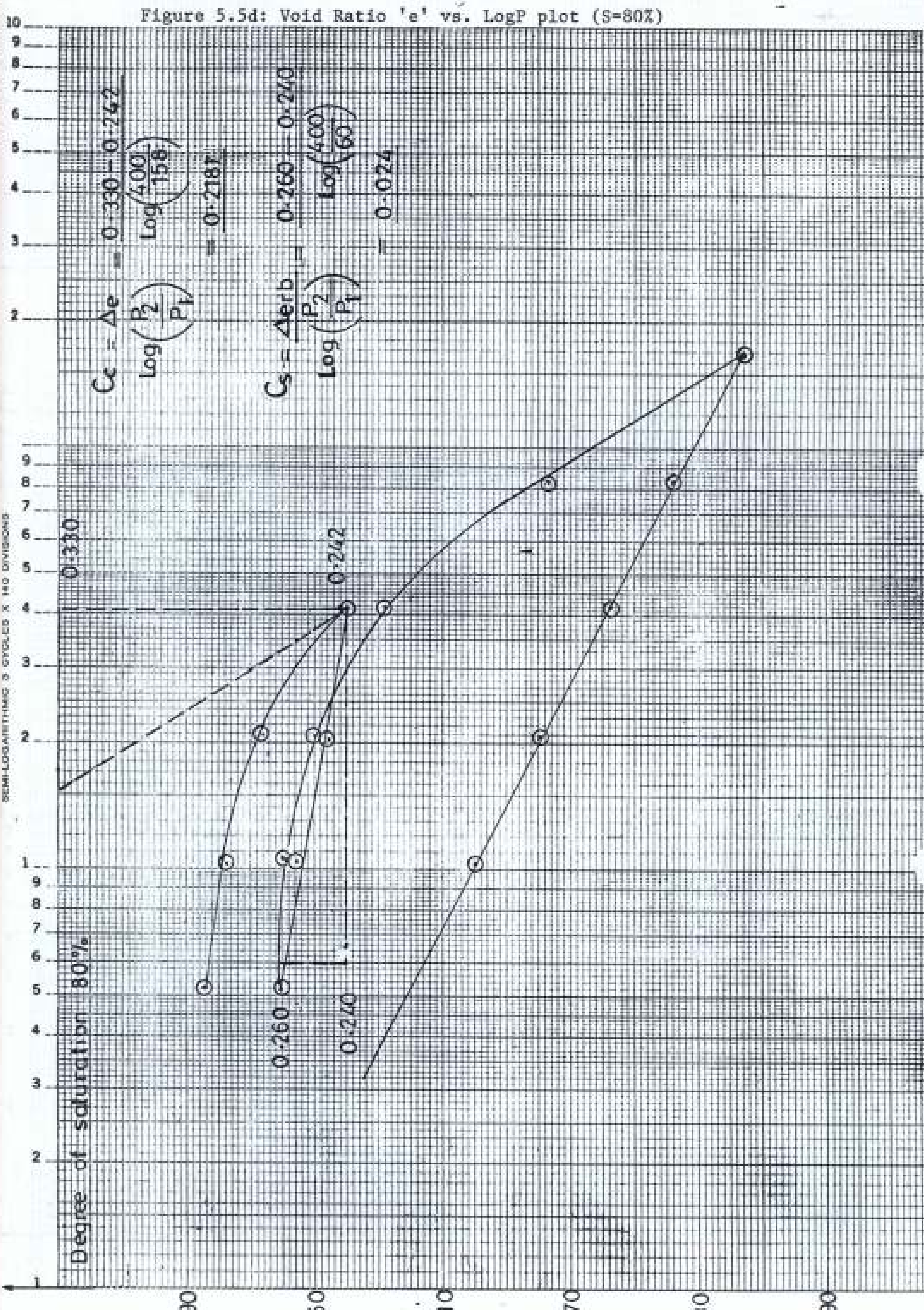

Figure 5.5e: Void Ratio 'e' Vs. LogP plot (S=100%)

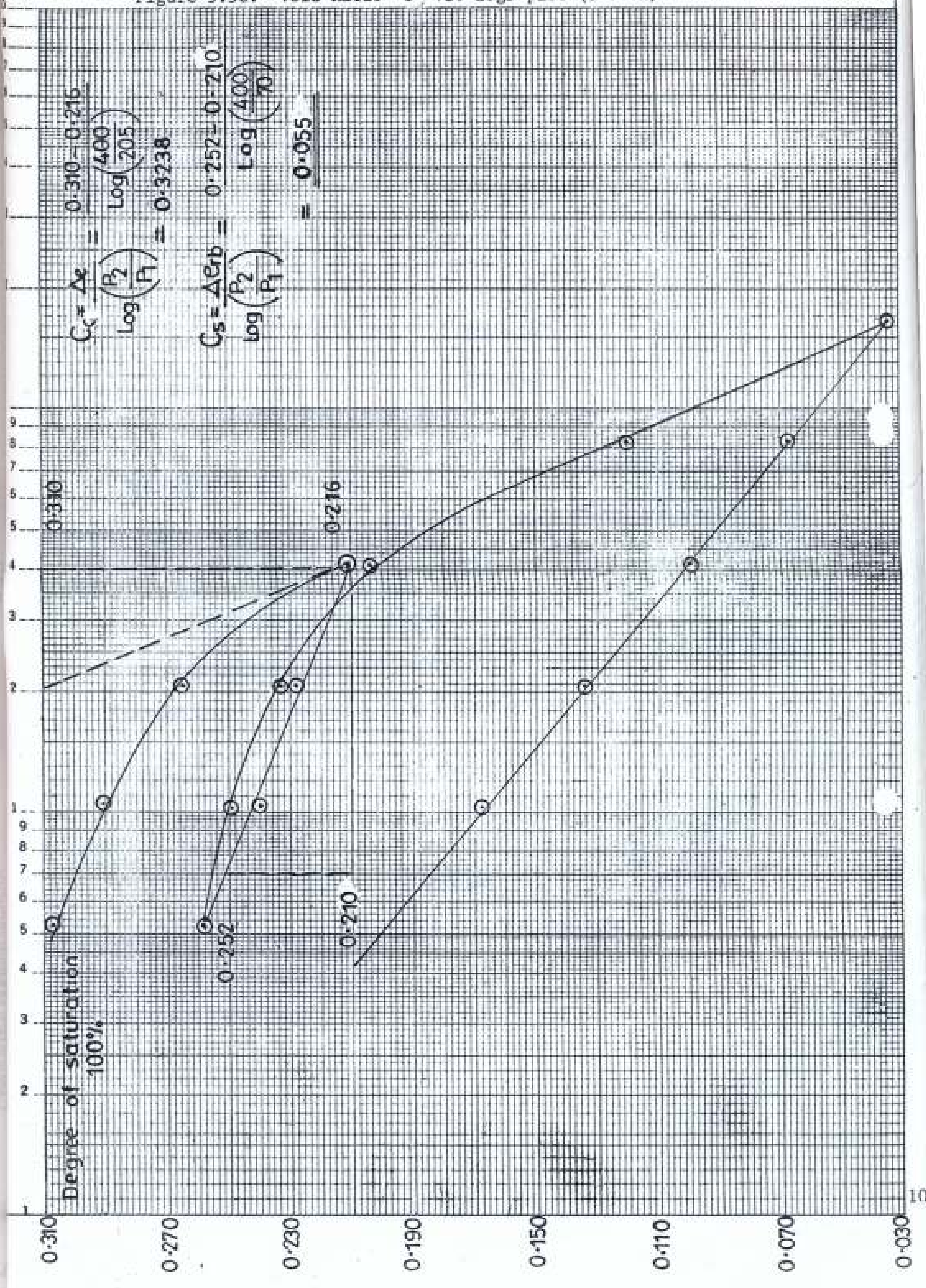

Table 5.7: Coefficient of compressibility for the Black cotton soil samples.

Degree of saturation 'Sr' (%)	Coefficient of compressibility 'a_v' (kN^{-1})
20	0.7×10^{-4}
40	1.29×10^{-4}
60	1.72×10^{-4}
80	1.76×10^{-4}
100	2.70×10^{-4}

The coefficient of consolidation 'C_v' for the black cotton soil samples at the various load increment values for the different degrees of saturation were also computed. The square root of time fitting method was used. The values of 't_{90}' obtained for each of the load increments at different degrees of saturation are shown in Table 5.8. The values of the coefficient of consolidation computed based on the 't_{90}' values are summarized in Table 5.9. The coefficient of consolidation 'C_v' in cm^2/min was computed using the equation

$$C_v = \frac{0.848\overline{H}^2}{t_{90}} \qquad \text{..................(5.2)}$$

where

$\overline{H}$ = Average thickness of the specimen

Details of the Time-Compression data are available in the appendix.

Table 5.8: Summary of "t_{90}" values for the Black cotton soil at various degrees of saturation. (t_{90} = Time for 90% Consolidation)

			Load increment (kN/m^2)				
			52	104	208	416	832
			t_{90} (MINS)				
Degree of saturation	20%	1st CYCLE	9.00	15.21	7.29	7.29	
		2nd CYCLE		9.00	16.00	9.00	12.25
	40%	1st CYCLE	16.00	9.00	11.56	12.25	
		2nd CYCLE		9.00	10.89	10.89	10.24
	60%	1st CYCLE	10.89	16.00	12.25	11.56	
		2nd CYCLE		6.76	9.00	13.69	16.00
	80%	1st CYCLE	2.89	2.25	9.00	11.56	7.84
		2nd CYCLE		6.76	10.89	7.84	
	100%	1st CYCLE	4.41	5.29	6.25	6.76	
		2nd CYCLE		2.25	6.25	4.84	7.84

Table 5.9: Coefficient of consolidation "C_v" for the Black cotton soil at various degrees of saturation.

			Load increment (kN/m^2)						
			52	104	208	416	832		
			C_v (cm^2/min)					**Average C_v value**	
Degree	20%	1st CYCLE	0.3705	0.2133	0.4342	0.4204		0.2739	0.3168
		2nd CYCLE		0.3439	0.1897	0.3286	0.2332	0.2692	
	40%	1st CYCLE	0.2093	0.3594	0.2685	0.2396		0.2852	0.2772
of		2nd CYCLE		0.3385	0.2729	0.2631	0.2664	0.2469	
	60%	1st CYCLE	0.3025	0.1963	0.2453	0.2435		0.2469	0.2603
		2nd CYCLE		0.4275	0.3111	0.1967	0.1592	0.2736	
	80%	1st CYCLE	1.160	1.464	0.3612	0.2728		0.8145	0.5990
Saturation		2nd CYCLE		0.4714	0.2898	0.3942	0.3784	0.3835	
	100%	1st CYCLE	0.7523	0.6052	0.4958	0.4305		0.5710	0.6401
		2nd CYCLE		1.394	0.4770	0.6039	0.3614	0.7091	

5.4 DISCUSSION OF RESULTS

The summary of the suction test results is presented in Table 5.1 and Figures 5.1a and 5.1b. The results show an increase in soil suction (negative pore water pressure) as the molding water content and degree of saturation, for the compacted black cotton soil decreases. These agrees with the results obtained by Fredlund and Rahardjo, 1987, for compacted glacial till. Sauer and Monismith, 1968 also obtained a similar result.

5.4.1 STRENGTH CHARACTERISTICS

As expected, the computed shear strength values from the triaxial compression test results show an increase in shear strength with decreasing degree of saturation, as presented in Table 5.4. From the plot of shear stress against deviator stress, a linear increase of the shear stress with deviator stress for the different degrees of saturation was obtained (Figures 5.2 and 5.3).

However, the rate of increase in shear stress and the angle of shearing resistance with deviator stress can be seen to be increasing with decreasing degree of saturation, especially for the 20%, 40% and 60% degrees of saturation. The values obtained for the angle of friction or angle of shearing resistance for the partially saturated black cotton soil samples, (between11^0 and 31.5^0), corroborates the findings of Yoder and Witczak, 1975, that for partially saturated clays, the angle of friction will vary between 0 and about 30 degrees. The rates of increase in shear stress with deviator stress for the 80% and 100% saturation can be seen to be almost the same (Figure 5.3). From this, it can be inferred that when the degree of saturation of the black cotton soil reaches 80% and above, saturated soil mechanics principles can be applied to analyse the soil without expecting serious errors.

The shear strength for the 20%, 40% and 60% saturation converged to an initial value of about 250kN/m^2, while for 80% and 100% saturation, the shear strength converged to about 125kN/m^2 at a lower deviator stress. (Ola, 1983) obtained an unconfined compressive strength and vane shear strength of about 120.0 kN/m^2 for unstabilised black cotton soil at optimum moisture content. The degree of saturation is expected to be between 80% and 100% at this moisture content.

Change in strain with deviator stress for the different degrees of saturation presented in Figure 5.4, shows an increase in strain values with increase in deviator stress for the black cotton soil samples. Similar results were reported by (Holtz and Kovacs, 1981), for normally consolidated and over consolidated clays. The failure mode of the triaxial compression test, cylindrical specimens, which was that of cracking and bulging of the specimen rather than sliding of a portion of the specimen relative to the other, has resulted in the increasing deviator stress at a fairly constant strain value during failure of the specimen as can be seen on the curves. Higher degrees of saturation i.e (80% and 100%) produced higher strain values while lower degrees of saturation (i.e 20%, 40%,and 60%) produced lower strain values with higher deviator stress.

5.4.2 COMPRESSIBILITY CHARACTERISTICS

From the Oedometer test results presented in section 5.3, the compression indices for the black cotton soil samples, decrease as the degree of saturation decreases (Table 5.6). The highest compression index for Cc = 0.3238, obtained from the slope of the virgin compression curve of the e vs logP plot for the case of 100% saturation, agrees with Skempton's approximation for compression index which for remolded sample, is

$$Cc = 0.007(LL - 10) \quad \ldots\ldots\ldots\ldots\ldots\ldots \quad 5.2$$

where,

LL = Liquid limit

$\therefore \quad Cc = 0.007\,(54\text{-}10)$

$= 0.308$

The swell indices, however do not show a regular pattern, but it can still be observed that the value of the swell index decreases with decreasing, degree of saturation as expected. The coefficient of compressibility 'a_v' summarized in Table 5.7 show an increase in coefficient of compressibility with increasing degree of saturation as expected.

Using the square root of time fitting method, the time for 90% consolidation "t_{90}" was computed at various load increment values and hence the coefficient of consolidation "Cv" using equation 5.2. The average values of the coefficient of consolidation for the 1st and 2nd cycles at different degrees of saturation are summarized in Table 5.9. As can be observed, higher values of average coefficient of consolidation were obtained for 80% and 100% saturation. Also the average values of Cv for the 20%, 40% and 60% saturation can be seen to be within a close range. This confirms that the behaviour of partially saturated black cotton soil during consolidation differ by a wide margin from the behaviour of saturated or almost saturated layer of the same soil.

5.4.3 RELATIONSHIP BETWEEN SOIL SUCTION (NEGATIVE PORE-WATER PRESSURE) AND SOIL BEHAVIOUR IN PARTIALLY SATURATED SOIL

In the previous section, it has been shown that soil suction is related to degree of saturation and moulding water content (Figure 5.1a, 5.1b). It is now possible to establish approximate relationships between soil suction and compression index (Cc), coefficient of compressibility (a_v), Swelling index (Cs), Coefficient of consolidation (Cv) and shear strength (T_f).

A summary of the various soil parameters at different degrees of saturation moulding water content and suction values is presented in Table 5.10. The plots of the compression index "Cc" against degree of saturation and soil suction on a linear and semi-log scale are shown in Figures 5.6a and 5.6b. Figures 5.7 to 5.10 shows the relationship between other soil parameters and soil suction, plotted on a linear and semi-log scale. The statistical trend line of best fit for the plots and the corresponding equations can be seen on the plots.

Table 5.10: Black cotton soil parameters at different degrees of saturation.

S_r (100%)	W (%)	Ua – Uw (pF)	C_c	a_v (KN^{-1})	C_s	C_v (cm^2/min)	τ_f(KN/m^2)
20	1.85	5.2	0.0880	0.70×10^{-4}	0.022	0.3168	491.4
40	3.69	4.6	0.1570	1.29×10^{-4}	0.056	0.2772	485.8
60	5.54	4.0	0.2917	1.72×10^{-4}	0.053	0.2603	362.3
80	7.38	2.1	0.2181	1.76×10^{-4}	0.024	0.5990	243.7
100	9.23	1.8	0.3238	2.70×10^{-4}	0.068	0.6401	209.3

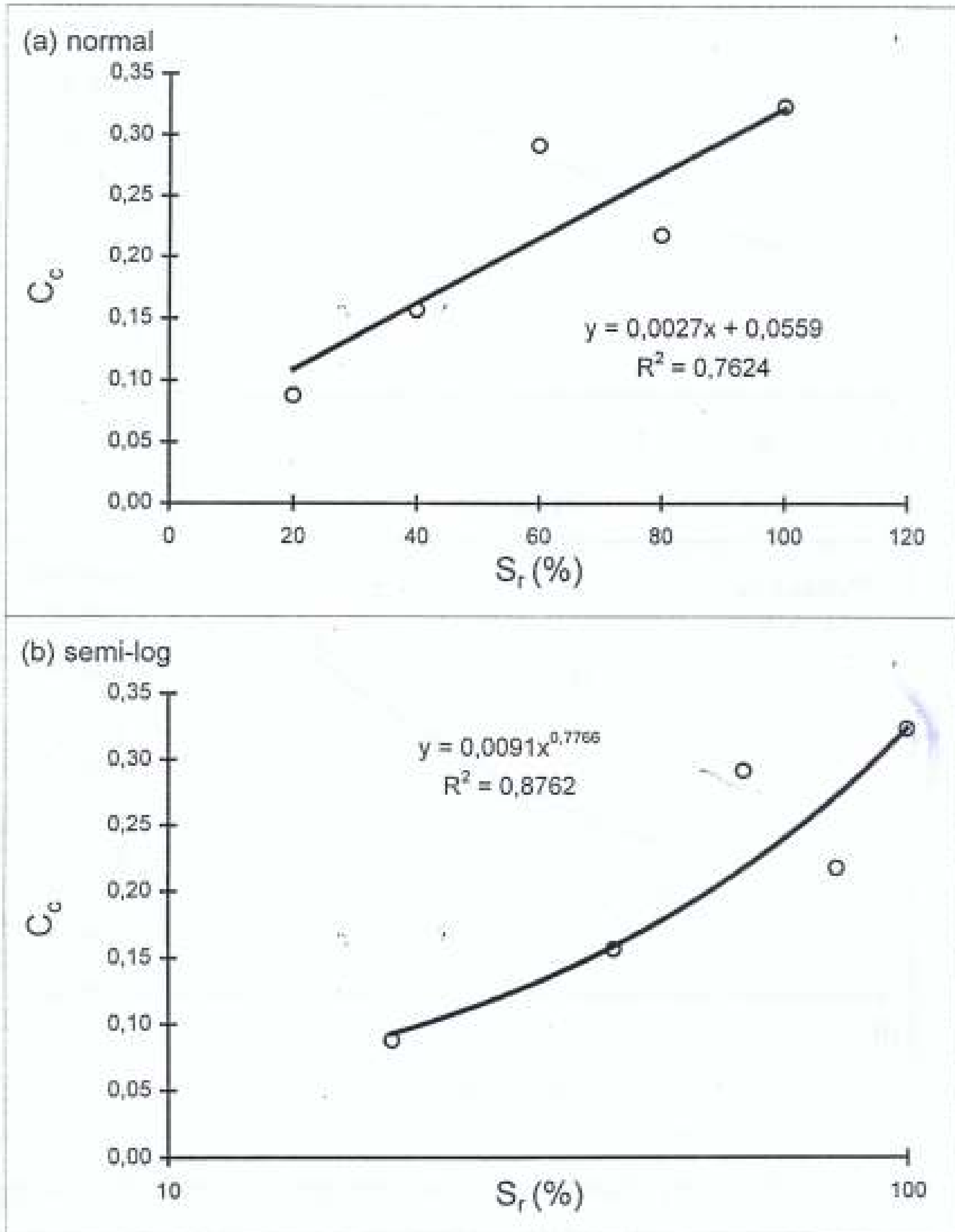

Figure 5.6a: Relationship between Compression index (C_c) and degree of saturation (S_r)

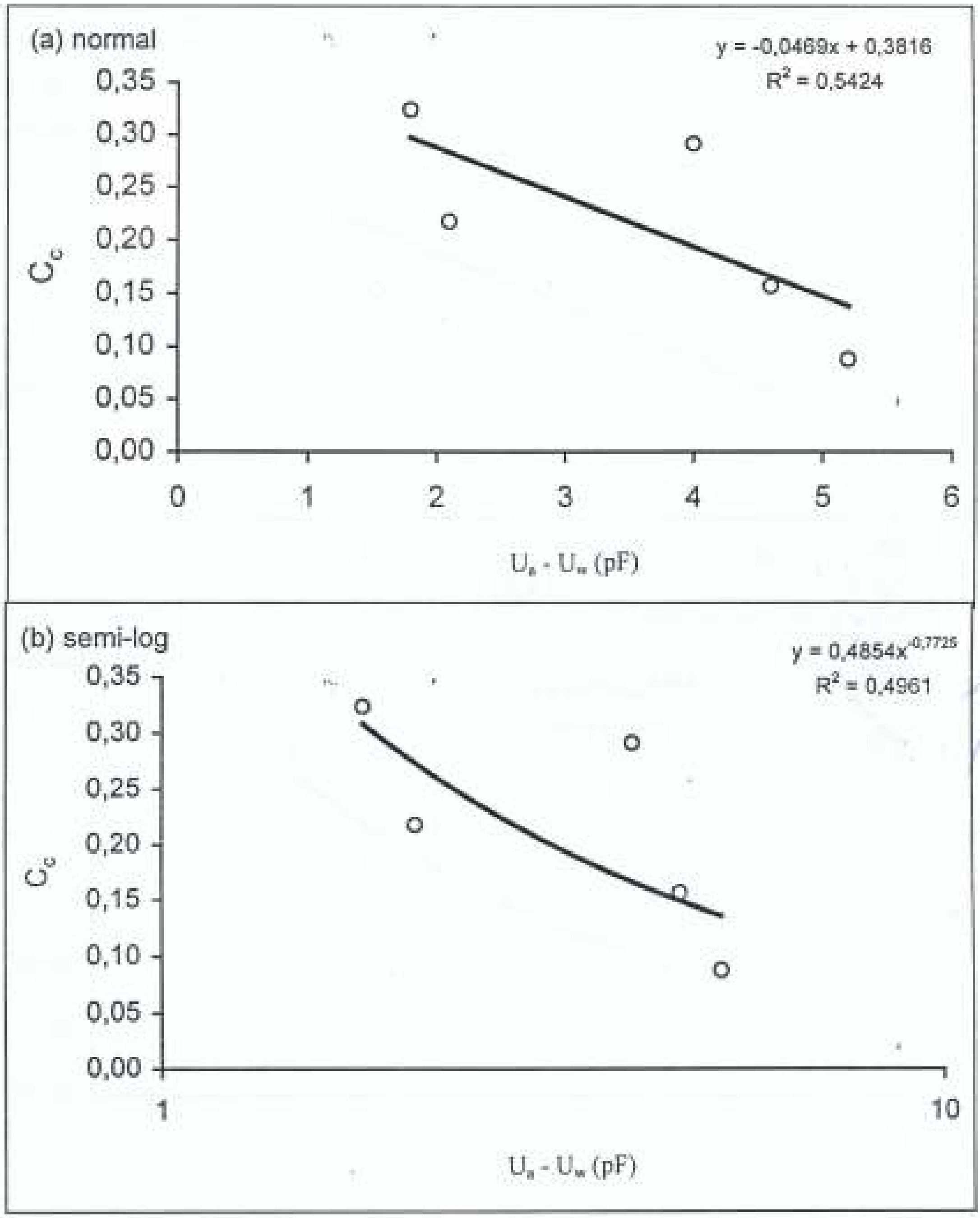

Figure 5.6b: Relationship between Compression index (C_c) and soil suction(u_a-u_w)

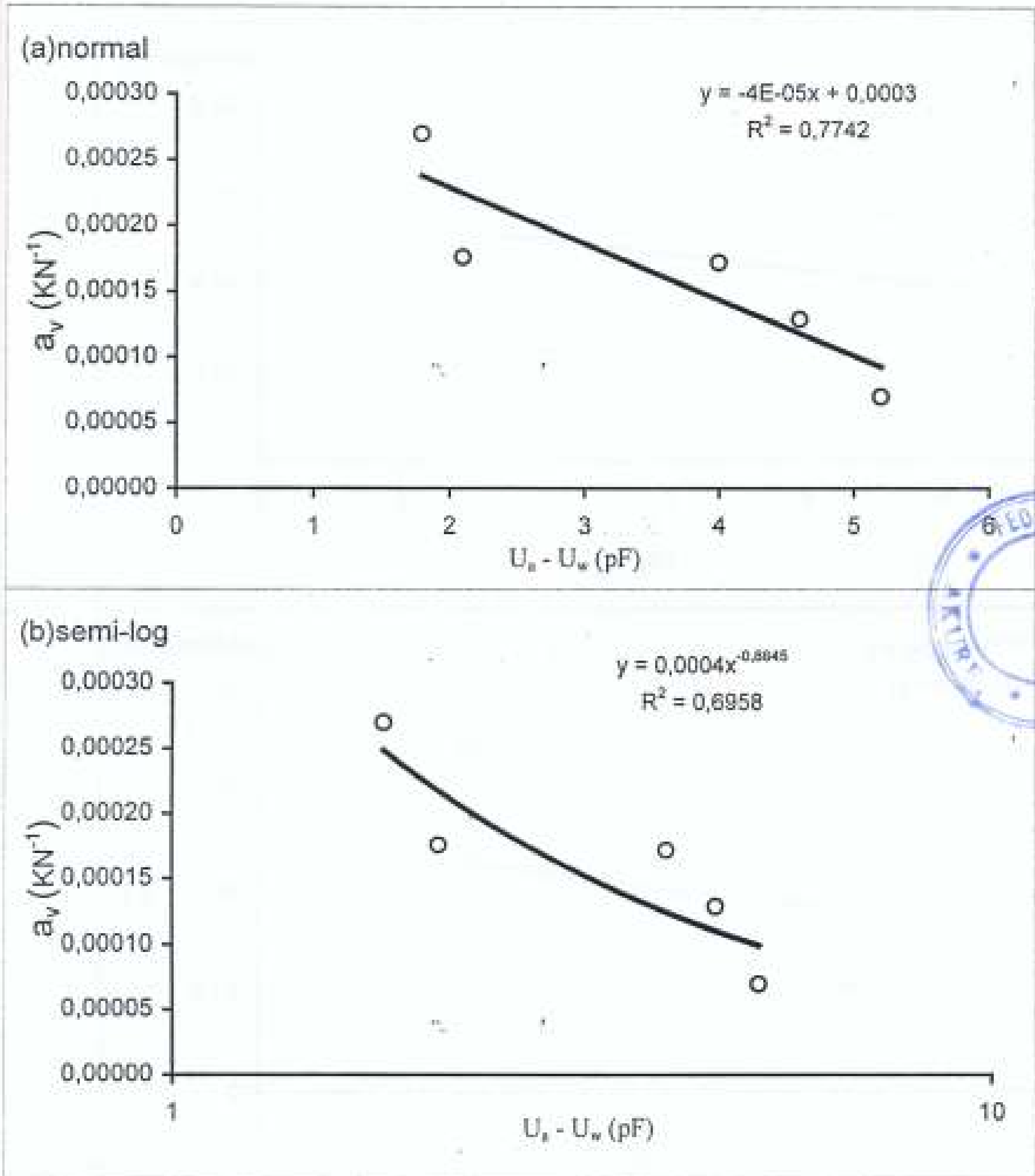

Figure 5.7 : Relationship between Coefficient of Compressibility(a_v) and soil suction (u_a-u_w)

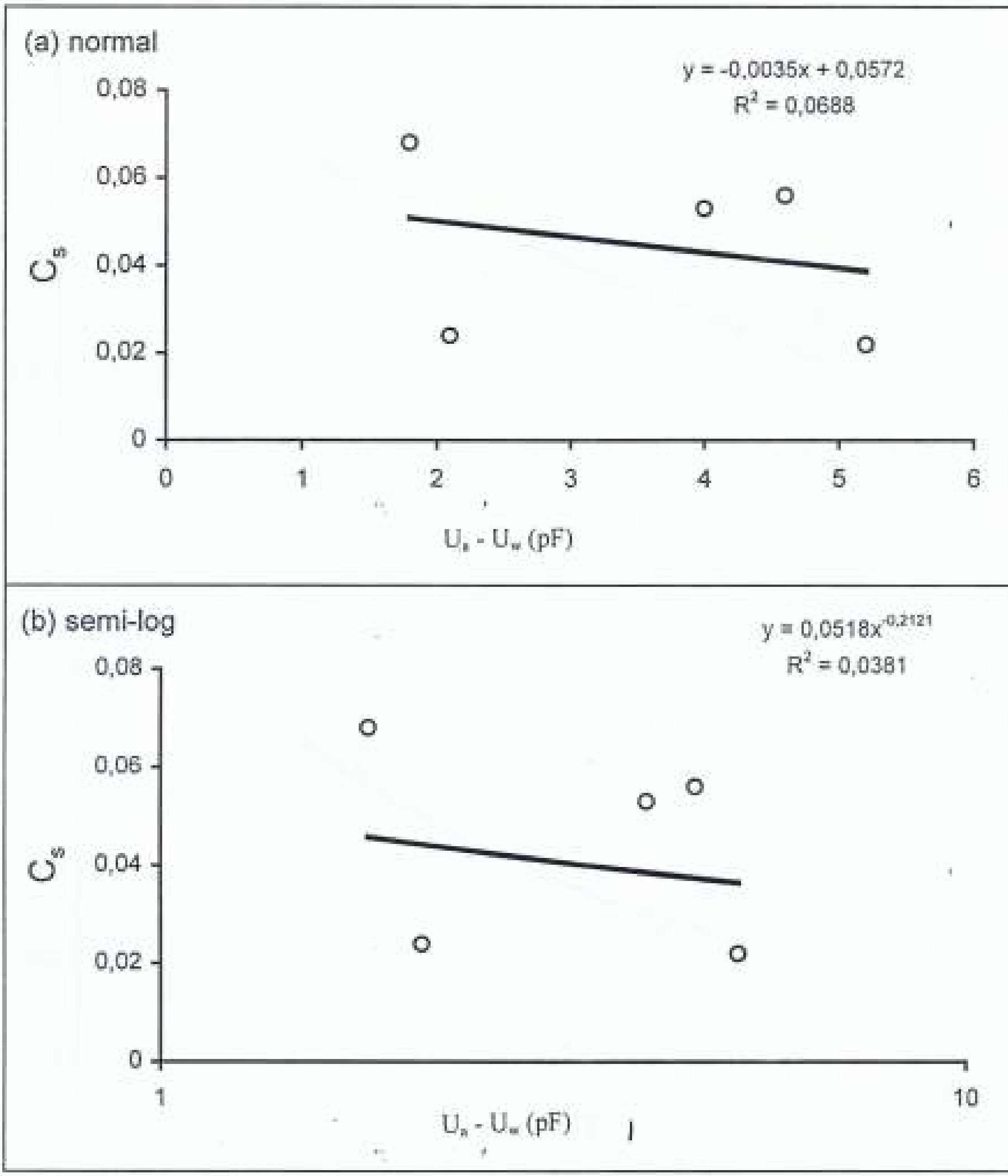

Figure 5.8 : Relationship between Swell index(C_s) and soil suction (u_a-u_w)

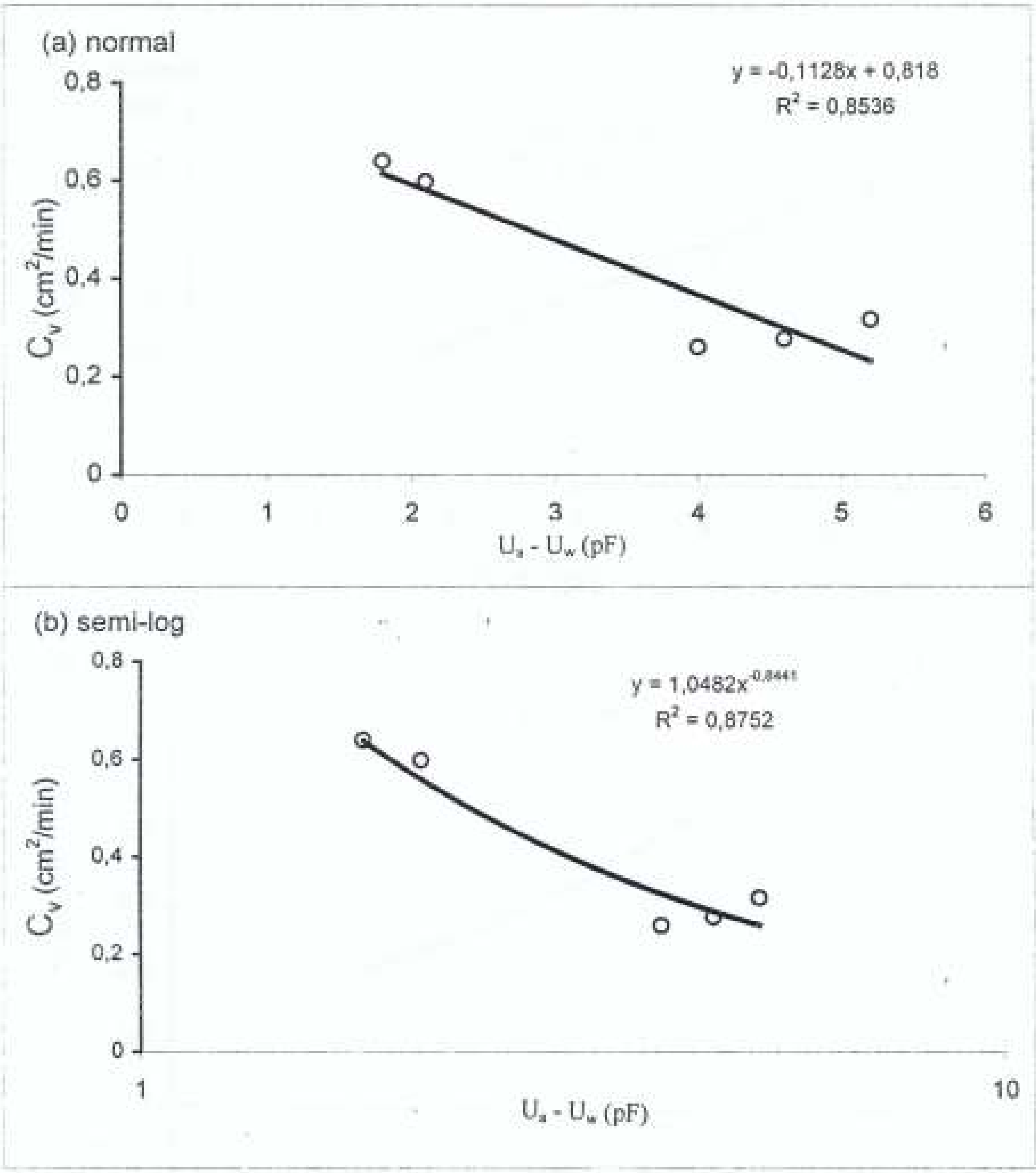

Figure 5,9 : Relationship between Coefficient of Consolidation(C_v) and soil suction (u_a-u_w)

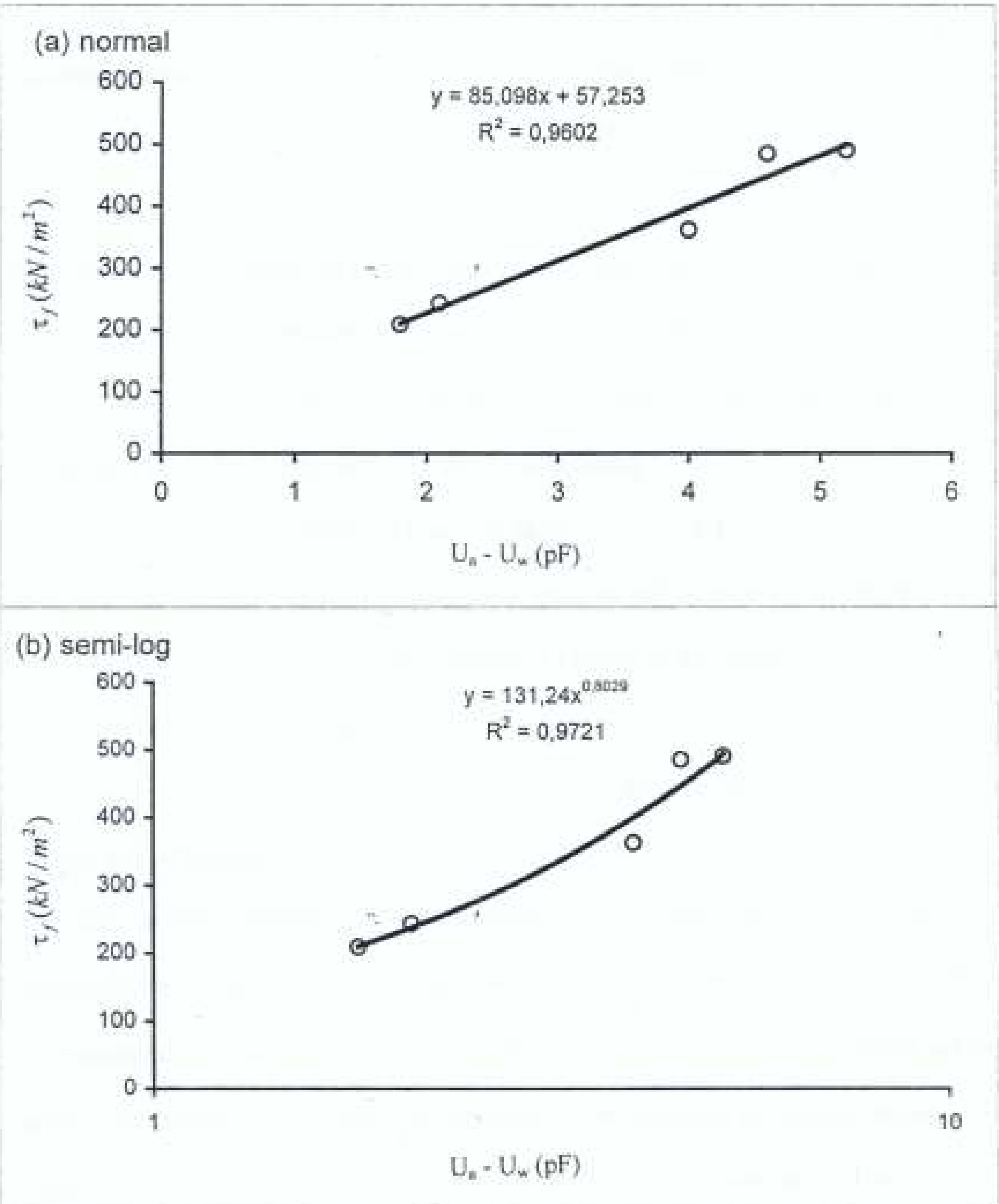

Figure 5.10: Relationship between Shear Strength (τ_f) and soil suction (u_a-u_w)

The relationship between compression index "Cc" and degree of saturation "S_r" (Figure 5.71), has given the best trend line on a semi-log plot with a higher coefficient of determination of $R^2 = 0.8762$ and a corresponding power series equation;

$$Cc = 0.0091 S_r^{0.7766} \qquad 5.3$$

The quantity "R^2" called coefficient of determination is an index of correlation between the two variables and varies between zero and one. It is always non-negative and it is the square of the coefficient of correlation "R" which lies between –1 and +1.

From the coefficient of determination for the plot of compression index "Cc" versus soil suction (Ua – Uw), (figure 5.72), the linear relation;

$$Cc = -0.0469 (Ua - Uw) + 0.3816 \qquad 5.4$$

gives the best equation relating compression index to soil suction for the black cotton soil. From the plots, it is obvious that the pattern of change in the compression index "Cc" and coefficient of compressibility "a_v" with soil suction are similar. Generally, the compression index and coefficient of compressibility decrease with increase in soil suction. The pattern of change in the swell index "C_s" with soil suction in Figure 5.8 has given a low value of the coefficient of determination $R^2 = 0.0688$, which does not give a good relationship between swell index Cs and soil suction. This can be explained by referring to the procedure for the Oedometer test in the laboratory. For this test, black cotton soil samples at various initial degrees of saturation were subjected to loading during which all of the air in the pores was dissolved and the soil became fully saturated. The swell index is obtained from the unloading branch of the e vs logP plot, and since the initial degree of saturation and therefore the soil suction is not maintained at this stage of the experiment, it has not given a significant effect on the swell index.

The coefficient of consolidation "C_v" generally decreases with increasing soil suction value (Figure 5.9). The semi-log, plot Figure 5.9 (b) has given the best relationship with coefficient of determination $R^2 = 0.8752$ and the power series relation;

$$C_v = 1.0482\,(U_a - U_w)^{-0.8441} \qquad 5.5$$

The trend for the shear strength shown in Figure 5.10 is that of increase with increasing soil suction values. The highest coefficient of determination $R^2 = 0.9721$ is given by the semi-log plot Figure 5.10 with the corresponding power series equation;

$$\tau_f = 131.24\,(Ua - Uw)^{0.8029} \qquad 5.6$$

This implies that the greatest influence of soil suction on the black cotton soil parameters is on shear strength. In the light of the foregoing discussion it has been established that soil suction (negative pore water pressure) plays a significant role in controlling the change in various soil parameters especially in partially saturated soils.

Generally, compression index "C_c", coefficient of compressibility "a_v", coefficient of consolidation "C_v" and moulding water content "w" all increase with degree of saturation, but soil suction "$U_a - U_w$" and shear strength "τ_f" decrease with degree of saturation.

5.4.4 THEORETICAL RESULTS

The proposed basic differential equations for the theory of one-dimensional consolidation for partially saturated soils, was solved using an implicit method of numerical analysis, imposing the assumed initial and boundary conditions. The results were presented in chapter 3. The model was tested using the experimental values of the degree of saturation and various soil parameters obtained.

The results for the change in pore water pressure 'U_w' and pore air pressure 'U_a with height from the bottom of the clay layer, which is closest to the water table shown in figures 3.6 –3-10(a), shows that the farther away form the water table the slower the rate of dissipation of excess pore pressure. The profile for the void ratio 'e' can be seen to follow a similar pattern. The profiles for the different degrees of saturation in figures 3.6 – 3.10(a) are for a simulation period of two days. The profile for 'Uw' and 'Ua' at 100% saturation shown in figure 3.11(a) and the corresponding time series in figure3.11(b) is for a simulation period of twenty days. This is the result for the case 5s which has essentially the same input data as the case 5 at 100% saturation except that it was allowed a longer simulation period. It was observed that all the excess pore water pressure dissipated after a simulation period of 20 days. This confirms that the hydrodynamic period of consolidation for a saturated soil is much greater than that of the partially saturated soil.

The time series for pore water pressure 'Uw' and pore air pressure 'Ua' at different points along the height of the clay layer for a simulation period of 2 days are shown in Figures 3.6-3.10(b). It is interesting to note that the rate of change in pore water pressure increases with decreasing degree of saturation. It should be noted however that in as much as this project is not aimed at establishing exact values of soil parameters for the partially saturated soil nor seeking to predicts the exact number of days it would take for the consolidation in the field. It has been sufficient to show, the rate of change of these soil parameters with degree of saturation and soil suction.

Experimental and theoretical trends for the variation in pore water and pore air pressures with degree of saturation are in reasonably good qualitative agreement for the partially saturated black cotton soil, but exhibit some quantities variance which may reasonably be attributed to experimental error. In general, soil suction (negative pore water pressure decreases and tends to zero as the consolidation period expires for the partially saturated soil.

CHAPTER SIX

CONCLUSION AND RECOMMENDATION

6.1 CONCLUSION

This work has demonstrated the significant effect of the presence of the air/gaseous phase in the compressibility of partially saturated soils. The theoretical studies have led to the derivation of basic differential equations for the one-dimensional consolidation in a partially saturated clay soil. Equations (3.14) (3.16) and (3.17) has been used to predict the rate of dissipation of pore pressures and change in voids ratio for compacted partially saturated black cotton soil samples. The results show that the farther away form the water table the slower the rate of dissipation of excess pore pressure. It is also interesting to note that the rate of change in pore water pressure increases with decreasing degree of saturation or increasing soil suction.

The experimental results show a trend of increase in compressibility with increasing degree of saturation, for the partially saturated black cotton soil samples. Equations 5.3 and 5.4 has established a relationship between compression index 'Cc' and degree of saturation/soil suction for the Black Cotton Soil; These are;

$$Cc = 0.0091S_r^{0.7766} \text{.....................................} (5.3)$$

$$Cc = -0.0469(Ua\text{-}Uw) + 0.3816 \text{........................} (5.4)$$

Soil suction has been identified as a major factor controlling the expansive nature of black cotton soil i.e swelling- shrinkage properties. The use of index properties such as liquid limit, plasticity index and activity of clay mineral can therefore be misleading.

The results also show that the strength of a partially saturated soil can be expressed as a function of two independent components, applied stress and soil suction. Equation (5.6) gives the established relation between shear strength and soil suction with a very high coefficient at determination (i.e $R^2 = 0.9721$), and is expressed as:

$$\tau_f = 131.24\,(U_a - U_w)^{0.8029} \qquad \text{.............................(5.6)}$$

Thus the behaviour of a partially saturated soil subjected to different stress paths cannot be explained or predicted in terms of any one single equation without reference to the changing state of the soil. The rates of increase in shear stress with deviator stress for the 80% and 100% saturation can be seen to be almost the same (Figure 5.3). From this it can be inferred that when the degree of saturation of the black cotton soil reaches 80% and above, saturated soil, mechanics principles can be applied to analyze the soil without expecting serious errors. It should be noted however, that there were certain aspects of the experimental testing procedures, which created some uncertainty regarding the absolute values of the measurements taken. The measurement of soil suction using the filter paper method, involved maintaining a constant temperature for one week in a cooled incubator, and weighing of filter papers on a Metler balance, immediately the filter paper is removed from contact with the soil sample. Fluctuations in supply of power to the cooled incubator and the losses in moisture form the filter paper before weighing are likely areas of uncertainly. It is nonetheless felt that results are of sufficient accuracy to represent, at least to good design approximation, the range and magnitude of values that can be expected in this particular region with this particular kind of material. Thus these data demonstrate the significance of evaluating the fundamental properties of soils in relationship to their environment under simulated groundwater table and degree of saturation conditions. In this way procedures for more meaningful evaluations of pavement performance and more realistic pavement analysis and designs may be possible. The theoretical and experimental studies confirm that the period for complete consolidation increases as the degree of saturation increases as expected, with the 100% degree of saturation giving the longest hydrodynamic period.

6.2 RECOMMENDATIONS

1. The prediction of the magnitude and rate of consolidation settlement for a layer partially saturated clay in arid or semi-arid region can now be done for a specific state of the soil i.e degree of saturation. Equations (5.3), (3.14), (3.16), and (3.17), have degree of saturation 'Sr' as an independent variable.
2. It is not meaningful to evaluate the engineering properties of any soil unless its environment, or soil moisture properties, are specified. For unsaturated soils, there is a considerable variation in properties corresponding to changes in soil moisture. Consequently for the designs of highway or airport pavement, two sets of boundary conditions are required materials changes and significant changes in soil suction. This implies that just as material testing is essential prior to construction of pavements, soil suction measurements under existing subgrade would be required to determine the appropriate construction method for the highway or airport pavement, especially in a semi-arid/arid region.

3. The theory of consolidation for partially saturated soils should be further studied especially in the more realistic three dimensions, in order to improve on the proposed one-dimensional theory for consolidation of a partially saturated soil.
4. Devices for measuring negative pore water pressures or soil suction should be further developed and studies are required to ascertain their reliability and accuracy
5. During construction of road on Black Cotton soils, all precaution should be taken to minimize the variations in soil moisture, and equilibrium moisture conditions should be maintained as far as possible. Delays between excavation, spreading and compaction should be minimized and the sub-grade should be covered with a granular layer to prevent evaporation.

REFERENCES

1. **Adeyeri, J.B.** (1988) Engineering Characteristics of Some Nigeria Residual Soil for Highway Construction Transportation Research Record No 1192 Washington D.C.
2. **Adeyeri, J.B.** (1998) Unpublished Lecture Notes on 'Advanced Soil Mechanics' for M. Eng. Department of Civil Engineering Federal University Technology Akure.
3. **Adeyeri, J.B.** and **Mawadi, G.W.** (1995) Some Engineering Properties of the Numan Black Cotton Soil of Northern Nigeria. Geotechnical Lab. Report GLR03, Dept of Civil Engineering Ondo State University Ado Ekiti.
4. **Barden, L** (1965) Consolidation of compacted and unsaturated Clay, Geotechnique. Vol. 15, No 2.
5. **Bishop, A.W. et al** (1960) Factors controlling the strength of partly saturated cohesive soils. Proc. of Research Conference on shear strength of Cohesive soils. Published by A.S.C.E.
6. **Bowles, J.E.** (1984) 'Physical and Geotechnical Properties of soils' 2nd edition, McGraw-Hill, Book Company. New York.
7. **Bowles, J.E.** (1992) Engineering Properties of Soil and their Measurements , McGraw-Hill, Inc.
8. **B.S.I** (1975) Soils for Civil Engineering Purposes, BS1377 British Standards Institute, London.
9. **Croney, D** and **Coleman J.D** (1961). 'Pore pressure and Suction in Soil' paper 5, Conference on Pore Pressure and suction in soils, Butterworths, London.
10. **Das, M. Braja** (1990) 'Principles of Geotechnical Engineering' 2nd edition PWS - KENT, England.
11. **Du., Y, et al** (1999) 'Swelling – Shrinkage properties and soil improvement of compacted expansive soil', Ning – Liang highway China. Engineering Geology. Vol 53 No. 3 – 4, ELSEVIER Publishing Company, Netherlands.

12. **Fredlund, D.G.** (1985) 'Soil Mechanics Principles That Embrace Unsaturated Soils'. Proc, 11th International Conference on soil Mechanics and Foundation Engineering, San Francisco. Vol 1.

13. **Fredlund, D.G** and **Rahardjo H.** (1987) 'Soil Mechanics Principles for Highway Engineering in Arid Regions'. Transportation Research Board, A2L06 Session.

14. **Holtz, R.D** and **Kovacs W.D.** (1981) 'An Introduction to Geotechnical Engineering' Prentice – Hall Inc.

15. **Ibrahim, A.** (1983) Black Cotton Soil in road pavement design, construction and performance. In S.A. Ola (Editor). Tropical Soils of Nigeria in Engineering Practice. A.A. Balkerma/Rotterdam.

16. **Lambe, T.W & Whitman R.V** (1969). 'Soil Mechanics' John Wiley & Sons Inc, New York

17 **Matyas, E.L** and **Radhakrishna** (1968): 'Volume Change Characteristics of Partially Saturated Soils'. Geotechnique, Vol. 18.

18. **Meigs, P.** (1953): World Distribution of Arid and Semi-arid Homo Climates In UNESCO Reviews of Research on Arid Zone Hydrology. Arid Zone Res., I.

19. **Mesinger, F.& Arakawa A.** (1976): Numerical Methods used in Atmospheric Models vol I. Global Atmospheric Research Programme (GARP) Publication series No 17

20 **NBRRI** (1983): 'Engineering Properties of Black Cotton Soils of Nigeria and related Pavement Design'. Research Paper No 1, NBRRI, Lagos

21 **Nelkon, M.** (1982); "Principles of Physics" 4th edition, Heinemann.

22. **Ola, S A** (1983): 'Geotechnical Properties of Nigerian Black Cotton Soils'. In S.A. Ola (Editor), Tropical soils of Nigeria in engineering practice A.A. Balkerma / Rotterdam.

23. **Richards, B.G.** (1974): 'Behaviour of Unsaturated Soils'. In soil mechanics New Horizon, Edited by I.K Lee American Elsevier Publishing Company Inc. New York.

24. **Sauer, E K& Monismith, C.L** (1968) 'Influence of soil sunction on behaviour of a Glacial till subjected to repeated Loading' Highway Research Record No 215

25. **Schiffmann, R.L.** (1959) 'Flow of visco plastic fluids through porous media' Office of Naval Research Project NR-081-244 Contract Nour-591(11). Department of Civil Engineering Division of Soil Mechanics Rensselae Polytechnic Institute, Troy, New York.

26. **Schrivastava, S.P.** (1969); 'Consolidation of partially saturated soil' Journal of the I.N.S. of S.M and F. Engineering.

27 **Sidney, Rosenak** (1963); 'Soil Mechanics' B.T Batsford Ltd, London

28 **Simons, N.E. & Menzies, B.K** (1977) A short course in Foundation Engineering Butterworths

29. **Smith, G.D.** (1978) Numerical Solutions of Partial Differential Equations. Finite Difference Methods, 2nd Edition Oxford: Clarendon Press.

30. **Smith, G.N.** (1982) Elements of soil mechanics for civil and mining Engineers 5th edition, GRANADA.

31. **Smith, M.J.** (1970) 'Soil Mechanics' 2nd edition ELBS.

32. **Sutton, B.H.C.** (1975) Solutions of problem in soil mechanics Pitman.

33. **Terzaghi, K.** (1943) Theoretical Soil Mechanics. John Wiley & Sons, New York.

34. **Van der Raadt, P.** (1984); Soils Suction Measurement At Several Sites in Western Canada.Transportation Research Board Committee A2L06TRB. Washington D.C.

35 **Yoder, E.J.** and **Witczak, M.W.** (1975); 'Principles of pavement Design' 2nd Edition. John Wiley &Sons Inc., New York

APPENDICES

APPENDIX 1

FLOW CHART FOR THE COMPUTER PROGRAM TO SOLVE 1-D CONSOLIDATION MODEL FOR A PARTIALLY SATURATED SOIL

a. SUBROUTINE DIFFUSION

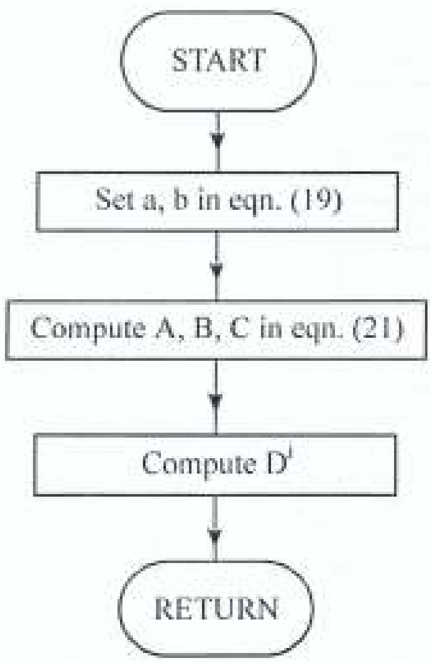

b. SUBROUTINE FORECAST

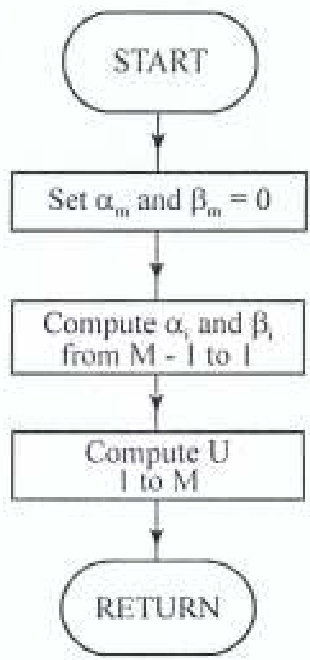

MAIN PROGRAM

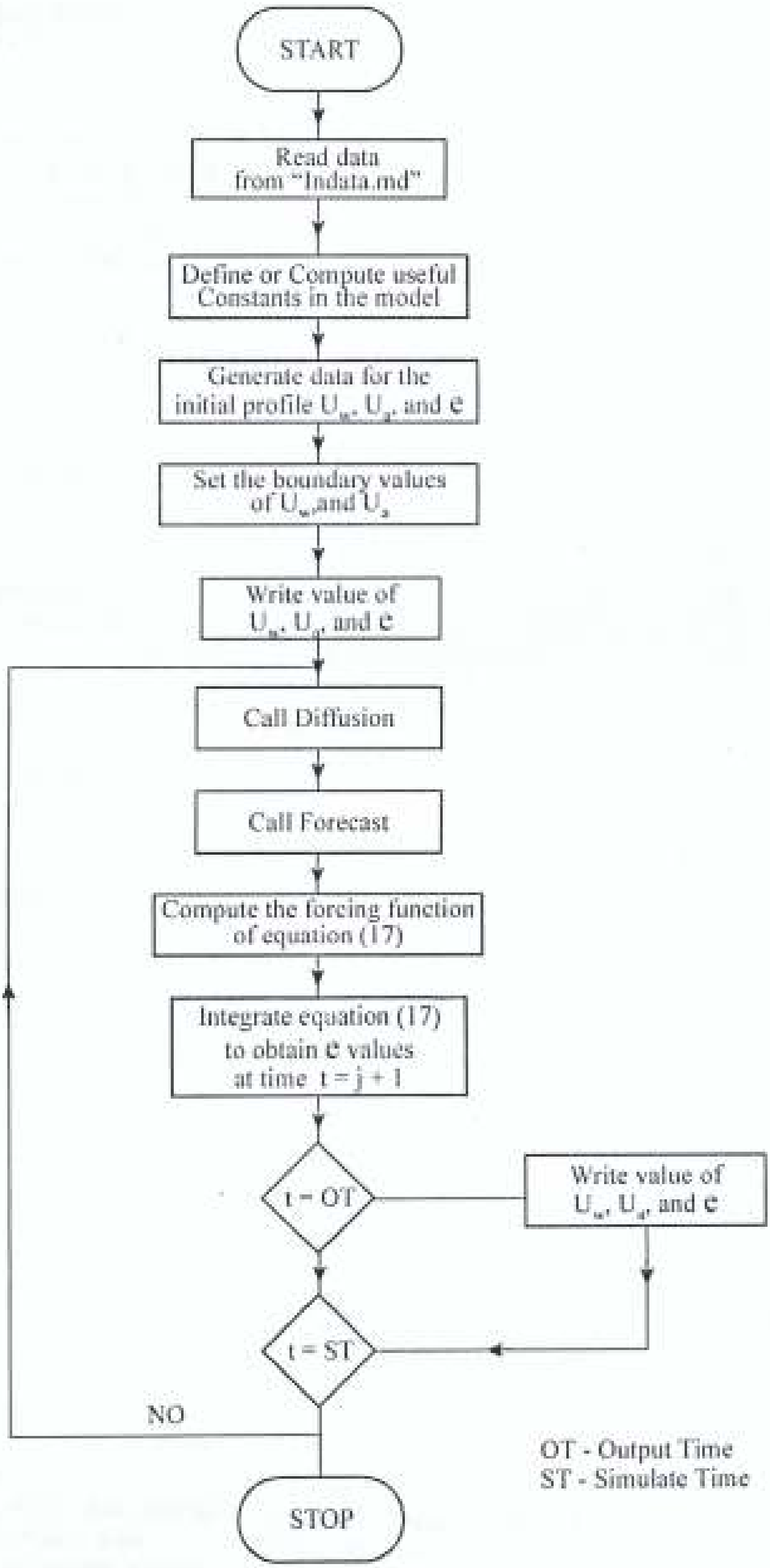

APPENDIX 2: COMPUTER PROGRAM LISTING

```
USE PORTLIB

! ***********************************************************************
!
! This is a model  for
! one dimensional consolidation for partially a saturated soil
!
! Program Language: Fortran 90
!***********************************************************************

include 'commonblk'
open(unit = 1,file='indata.md')
open(unit = 2,file='oudata.md')
open(unit = 3,file='time.md')
open(unit = 4,file='forst.md')
open(unit = 5,file='mforst.md')


!Read in some variables
read(1,*)
read(1,*) ni,nj,nk
read(1,*) dx,dy,dz
read(1,*) dt,stime,rtime
read(1,*) ck
read(1,*) srk
read(1,*) alphak
read(1,*) gammaW, gammaA
read(1,*) uwA,uwB, uaA,uaB
read(1,*) av

close(1)

! Calculate some constants
if (srk .ge. 0.9) then
gammak = 0
else
gammak = gammaW/gammaA
endif
pi = 22.d0/7.d0

r = dt/(dz**2)

Ltime = stime/dt
rtime = rtime*60
Duw = 0
Dua = 0
Dew = 0
Dea = 0
Dewp = 0
Deap = 0



if (ni .ge. imax.or. &
   nj .ge. jmax .or. &
   nk .ge. kmax) then
write (*,*)"Nx Ny Nz must not exceed ",imax-1,jmax-1,kmax-1
write (*,*)"Presently they are       ",ni, nj, nk
write(*,*)"Hence the program aborts..."
stop
endif


! Compute the heights
z(0) = 0
```

```
 k = 1,nk
k) = z(k-1) + dz
ddo


Compute initia data for uw and ua
 i=1,ni
 j=1,nj
 k =1,nk
(i,j,k)= - srk*gammaW*z(k)
(i,j,k)= - srk*gammaA*z(k)
i,j,k) = 0
ddo
ddo
ddo

et the boundary condition
 i=1,ni
 j=1,nj
(i,j,1)  = uwB
(i,j,nk) = uwA
(i,j,1)  = uaB
(i,j,nk) = uaA
ddo
ddo

ite(2,10) (((z(k),uw(i,j,k),ua(i,j,k), &
                    e(i,j,k),i=1,ni),j=1,nj),k=1,nk,5)




 itim = 1,sLtime
eTime = itim*dt

ompute the Coefficients for Uw and Ua

i = 1,ni
j = 1,nj
k = 2,nk-1
 = 0.5*(uw(i,j,k+1) + uw(i,j,k))
= ck * uwm**2 + ck*gammak*alphak
= srk * uwm**2 + alphak*(1-srk)
(i,j,k) = KA/KB

 = 0.5*(ua(i,j,k+1) + ua(i,j,k))
= alphak*ck + ck*gammak*uam**2
= (1-srk)*uam**2-alphak*srk
(i,j,k) = KA/KB


p(i,j,k) = av*(srk)
(i,j,k)  = uw(i,j,k)

p(i,j,k) = av*(1-srk)
(i,j,k)  = ua(i,j,k)

do
do
do

ntegrate to obtain the values of
w and Ua for the next time step

l diffs_uw
```

```
all forcst_uw

f (srk .lt. 0.9) then
all diffs_ua
all forcst_ua
ndif


Compute the Coefficients for e
o i = 1,ni
o j = 1,nj
o k = 2,nk-2
ew(i,j,k) = av*(srk)
ea(i,j,k) = av*(1-srk)
nddo
nddo
nddo

 Integrate to obtain the values of
 e for the next time step

all Tendency_e



Set the boundary condition
o i=1,ni
o j=1,nj
w(i,j,1)  = uwB
w(i,j,nk) = uwA
a(i,j,1)  = uaB
a(i,j,nk) = uaA
nddo
nddo



 Check if it is the middle of the simulation period to write out
 the profile results

(itim .eq. sLtime/2) then
ite(5,10) (((z(k),uw(i,j,k),ua(i,j,k), &
                  e(i,j,k),i=1,ni),j=1,nj),k=1,nk,5)
dif


 Check if it is the right time
 to write out the time series results

t = mod(theTime,rtime)
(rst .eq. 0) then
ite(*,*) itim,'  of  ', sLtime
eTimeM = theTime/(3600.0*24.0)

ite(3,12) ((theTimeM,uw(i,j,2),ua(i,j,2), &
                     e(i,j,2),&
                     uw(i,j,nk/2),ua(i,j,nk/2), &
                     e(i,j,nk/2),&
                     uw(i,j,nk-1),ua(i,j,nk-1), &
                     e(i,j,nk-1),&
                     i=1,ni),j=1,nj)
dif


ddo
```

```
! Write the profile result for the end of simulation time
write(4,10) (((z(k),uw(i,j,k),ua(i,j,k), &
                    e(i,j,k),i=1,ni),j=1,nj),k=1,nk,5)



10 format(4(e20.6,2x))
12 format(10(e20.6,2x))


close(2)
close(3)
close(4)
close(6)

stop
end
```

```
ubroutine forcst_uw
nclude 'commonblk'
eal*8 dum(-1:imax,-1:jmax,-1:kmax)
quivalence (uw(-1,-1,-1),dum(-1,-1,-1))

o i = 1,ni
o j = 1,nj

lfa(i,j,nk) = 0;
eta(i,j,nk) = 0;


o k = nk-1,2,-1
  alfa(i,j,k) = C1(i,j,k)/(B1(i,j,k)-A1(i,j,k)*alfa(i,j,k+1))
  beta(i,j,k) = (dkuw(i,j,k)+ A1(i,j,k)*beta(i,j,k+1)) / &
                (B1(i,j,k)-A1(i,j,k)*alfa(i,j,k+1))
nddo

nddo
nddo

o i = 1,ni
o j = 1,nj
um(i,j,1) = beta(i,j,2)/(1-alfa(i,j,2))

o k = 2,nk
  dum(i,j,k) = alfa(i,j,k)*dum(i,j,k-1) + beta(i,j,k)
nddo

nddo
nddo

eturn
nd

ubroutine forcst_ua
nclude 'commonblk'
eal*8 dum(-1:imax,-1:jmax,-1:kmax)
quivalence (ua(-1,-1,-1),dum(-1,-1,-1))

o i = 1,ni
o j = 1,nj

lfa(i,j,nk) = 0;
eta(i,j,nk) = 0;


o k = nk-1,2,-1
  alfa(i,j,k) = C1(i,j,k)/(B1(i,j,k)-A1(i,j,k)*alfa(i,j,k+1))
  beta(i,j,k) = (dkua(i,j,k)+ A1(i,j,k)*beta(i,j,k+1)) / &
                (B1(i,j,k)-A1(i,j,k)*alfa(i,j,k+1))
nddo

nddo
nddo

o i = 1,ni
o j = 1,nj
um(i,j,1) = beta(i,j,2)/(1-alfa(i,j,2))

o k = 2,nk
  dum(i,j,k) = alfa(i,j,k)*dum(i,j,k-1) + beta(i,j,k)
nddo

nddo
```

```
euddo

return
end
```

```
broutine diffs_uw ! Diffussion for uw
clude 'commonblk'
al*8 dum(-1:imax,-1:jmax,-1:kmax),KK(-1:imax,-1:jmax,-1:kmax)
uivalence (uw(-1,-1,-1),dum(-1,-1,-1)) , &
          (Kuw(-1,-1,-1),KK(-1,-1,-1))

 =  0.75d0
 = 1-bb

 i=1,ni
o j = 1,nj
do k = 2,nk-1

 A1(i,j,k) = bb*r(i,j,k)*KK(i,j,k+1)
 B1(i,j,k) = 1 + bb*r(i,j,k)*(KK(i,j,k+1)+KK(i,j,k))
 C1(i,j,k) = bb*r(i,j,k)*KK(i,j,k)
enddo
enddo
enddo


o i = 1,ni
do j = 1,nj
 do k = 2,nk-1
Kuw(i,j,k) = dum(i,j,k) &
         + &
         aa*r(i,j,k)*( KK(i,j,k+1)*dum(i,j,k+1) - &
        (KK(i,j,k+1)+ KK(i,j,k))*dum(i,j,k) + &
                       KK(i,j,k)*dum(i,j,k-1) )

ddo
ddo
ddo

return
end


broutine diffs_ua ! Diffussion for ua
clude 'commonblk'
al*8 dum(-1:imax,-1:jmax,-1:kmax),KK(-1:imax,-1:jmax,-1:kmax)
uivalence (ua(-1,-1,-1),dum(-1,-1,-1)), &
          (Kua(-1,-1,-1),KK(-1,-1,-1))

 =  0.75d0
 = 1-bb

 i=1,ni
o j = 1,nj
do k = 2,nk-1

 A1(i,j,k) = bb*r(i,j,k)*KK(i,j,k+1)
 B1(i,j,k) = 1 + bb*r(i,j,k)*(KK(i,j,k+1)+KK(i,j,k))
 C1(i,j,k) = bb*r(i,j,k)*KK(i,j,k)
enddo
enddo
enddo


o i = 1,ni
do j = 1,nj
 do k = 2,nk-1
kua(i,j,k) = dum(i,j,k) &
         + &
         aa*r(i,j,k)*( KK(i,j,k+1)*dum(i,j,k+1) - &
```

```
          (KK(i,j,k+1)+ KK(i,j,k))*dum(i,j,k) + &
                           KK(i,j,k)*dum(i,j,k-1) )

enddo
enddo
enddo

 return
 end

subroutine Tendency_e ! Tedency of uw
include 'commonblk'

 do i = 1,ni
  do j = 1,nj
   do k = 1,nk
    e(i,j,k) = e(i,j,k) + &
                 ( (Kea(i,j,k) *(ua(i,j,k) - uap(i,j,k)))+ &
                   (Kew(i,j,k) *(uw(i,j,k) - uwp(i,j,k)))  )
enddo
enddo
enddo
return
end
```

APPENDIX 3

a. DATA SHEET FOR TRIAXIAL COMPRESSION

Sr = 20%

INITIAL WT.: 162 gms — **DIA. OF SAMPLE: 38mm**

FINAL WT. — **LENGTH OF SAMPLE: 76mm**

1	2	3	4	Cell Pressures								
				$\sigma 3_1$			$\sigma 3_2$			$\sigma 3_3$		
Disp. Dial Rdg Div.	Change in length L Col. X gauge const.	Strain $\frac{\Delta L}{L_0} \times 10^{-4}$	Corr. Area A_c $\frac{A_0}{1-\varepsilon} \times 10^{-4} m^2$	Load dial Rdg. LRD (Div)	Devia-tor load L_D LRD x LRF KN	Deviator stress $\sigma_D = \frac{L_D}{A_c}$ KN/m²	Load dial Rdg. LDR (Div)	Devia-tor load L_D LRD x LRF KN	Deviator stress $\sigma_D = \frac{L_D}{A_c}$ KN/m²	Load dial Rdg. LRD (Div)	Devia-tor load L_D LRD x LRF KN	Deviator st $\sigma_D = \frac{L_D}{A_c}$ K N/ m²
25	0.25	32.9	11.379	18	0.036	31.64	30	0.060	52.7	42	0.084	73.8
50	0.50	65.79	11.416	30	0.060	52.56	64	0.128	112.1	56	0.112	98.1
75	0.75	98.68	11.454	46	0.092	80.3	94	0.188	164.1	71	0.142	124.0
100	1.0	131.58	11.494	62	0.124	107.9	122	0.244	212.3	142	0.284	2384
125	1.25	164.47	11.531	82	0.164	142.2	148	0.296	256.7	166	0.312	270.6
150	1.5	197.37	11.573	100	0.200	172.8	178	0.356	307.6	182	0.364	314.5
175	1.75	230.26	11.614	133	0.266	229.0	212	0.424	356.1	202	0.404	347.8
200	2.00	263.16	11.655	152	0.301	260.8	242	0.484	415.3	228	0.456	391.3
225	2.25	296.05	11.697	171	4	292.4	270	0.540	461.7	254	0.502	429.2
250	2.5	328.95	11.739	186	0.342	333.9	292	0.584	491.5	290	0.580	494.1
275	2.75	361.84	11.783	208	0.392	353.1	316	0.632	536.4	342	0.884	580.5
300	3.00	394.74	11.807	224	0.416	379.4	338	0.676	572.5	394	0.788	667.4
325	3.25	427.65	11.870	236	0.448	397.6	359	0.718	604.9	420	0.840	707.7
350	3.50	460.53	11.916	243	0.472	407.9	380	0.760	637.8	458	0.916	768.7
375	3.75	493.42	11.961	250	0.486	418.0	400	0.800	668.8	482	0.964	806.0
400	4.00	526.32	11.971	254	0.500	424.4	414	0.828	691.7	504	1.008	842.0
425	4.25	559.21	12.031	256	0.508	426.2	426	0.852	709.2	510	1.020	849.1
450	4.5	592.11	12.055	245	0.512	406.5	431	0.862	715.1	522	1.044	866.0
475	4.75	625.00	12.102		0.490		433	0.866	715.6	556	1.112	918.9
500	5.0	657.90	12.140				435	0.870	716.6	558	1.116	919.3
525	5.25	690.79	12.183				437	0.874	717.4	510	1.020	857.2
550	5.5	723.68	12.226				438	0.876	716.5			

b. DATA SHEET FOR TRIAXIAL COMPRESSION

Sr = 40%

INITIAL WT.: 162 gms   **DIA. OF SAMPLE: 38mm**

FINAL WT.   **LENGTH OF SAMPLE: 76mm.**

1	2	3	4	Cell Pressures								
				$\sigma 3_1$			$\sigma 3_2$			$\sigma 3_3$		
Disp. Dial Rdg Div.	Change in length L Col. X gauge const.	Strain $\frac{\Delta L}{L_0} \times 10^{-4}$	Corr. Area A_c $\frac{A_0}{1} \times 10^{-4} m^2$	Load dial Rdg. LRD (Div)	Deviator load L_D LRD x LRF KN	Deviat or stress $\sigma_D = \frac{L_D}{A_c}$	Load dial Rdg. LDR (Div)	Deviator load L_D LRD x LRF KN	Deviat or stress $\sigma_D = \frac{L_D}{A_c}$	Load dial Rdg. LRD (Div)	Deviat or load L_D LRD x LRF KN	De… str… σ…
25	0.25	32.9	11.379	35	0.070	61.5	46	0.092	80.9	50	0.100	
50	0.50	65.79	11.416	65	0.130	113.9	82	0.164	143.7	92	0.184	[illegible]
75	0.75	98.68	11.454	92	0.184	160.6	112	0.224	195.6	140	0.280	[illegible]
100	1.0	131.58	11.494	118	0.236	205.32	160	0.320	278.4	202	0.404	[illegible]
125	1.25	164.47	11.531	140	0.280	242.8	210	0.420	364.2	270	0.540	[illegible]
150	1.5	197.37	11.573	152	0.304	262.7	245	0.490	423.4	350	0.700	[illegible]
175	1.75	230.26	11.614	194	0.388	334.1	270	0.540	465.0	300	0.780	[illegible]
200	2.00	263.16	11.655	214	0.428	367.2	300	0.600	514.8	340	0.844	[illegible]
225	2.25	296.05	11.697	240	0.480	410.4	325	0.650	555.7	422	0.900	[illegible]
250	2.5	328.95	11.739	264	0.528	449.8	349	0.698	594.6	450	0.940	[illegible]
275	2.75	361.84	11.783	286	0.572	485.5	370	0.740	628.0	470	0.980	[illegible]
300	3.00	394.74	11.807	308	0.616	521.7	388	0.716	657.2	490	1.012	[illegible]
325	3.25	427.65	11.870	342	0.648	545.9	400	0.800	674.0	506	1.036	[illegible]
350	3.50	460.53	11.916	331	0.662	555.6	408	0.816	684.8	518	1.048	[illegible]
375	3.75	493.42	11.961	331	0.662	553.5	415	0.830	693.9	524	1.076	[illegible]
400	4.00	526.32	11.971	331		424.4	422	0.844	701.7	538	1.086	[illegible]
425	4.25	559.21	12.031			426.2	429	0.858	714.2	543	1.092	[illegible]
450	4.5	592.11	12.055			406.5	433	0.866	718.4	546	1.100	[illegible]
475	4.75	625.00	12.102				436	0.872	720.5	550	1.104	[illegible]
500	5.0	657.90	12.140				436	0.872	718.3	552	1.106	[illegible]
525	5.25	690.79	12.183				436			553	1.122	[illegible]
550	5.5	723.68	12.226				438			556		
										557		

c. DATA SHEET FOR TRIAXIAL COMPRESSION

Sr = 60%

INITIAL WT.: 161 gms | **DIA. OF SAMPLE: 38mm**

FINAL WT. | **LENGTH OF SAMPLE: 76mm.**

1	2	3	4	Cell Pressure								
				$\sigma 3_1$			$\sigma 3_2$			$\sigma 3_3$		
Disp. Dial Rdg Div.	Change in length L Col. X gauge const.	Strain $\frac{\Delta L}{L_0} \times 10^{-4}$	Corr. Area $\frac{A_0}{1} \times 10^{-4} m^2$	Load dial Rdg. LRD (Div)	Deviator load L_D LRD x LRF KN	Deviator stress $\sigma_D = \frac{L_D}{A_c}$	Load dial Rdg. LDR (Div)	Deviator load L_D LRD x LRF KN	Deviator stress $\sigma_D = \frac{L_D}{A_c}$	Load dial Rdg. LRD (Div)	Deviator load L_D LRD x LRF KN	D st σ
25	0.25	32.9	11.379	32	0.064	56.2	35	0.070	61.5	48	0.096	8
50	0.50	65.79	11.416	54	0.108	94.6	66	0.132	115.6	81	0.162	1
75	0.75	98.68	11.454	80	0.160	139.7	94	0.188	164.1	119	0.238	2
100	1.0	131.58	11.494	104	0.208	180	122	0.244	212.3	144	0.288	2
125	1.25	164.47	11.531	126	0.252	218.5	148	0.296	256.7	196	0.392	3
150	1.5	197.37	11.573	152	0.304	262.7	172	0.344	297.2	234	0.468	4
175	1.75	230.26	11.614	176	0.352	303.1	206	0.412	354.7	263	0.526	4
200	2.00	263.16	11.655	255	0.410	351.8	243	0.488	417.0	285	0.570	4
225	2.25	296.05	11.697	226	0.452	386.4	274	0.548	468.5	308	0.616	5
250	2.5	328.95	11.739	250	0.500	425.9	284	0.568	483.9	326	0.652	5
275	2.75	361.84	11.783	266	0.532	451.5	310	0.620	526.2	338	0.672	5
300	3.00	394.74	11.807	280	0.560	474.3	328	0.656	555.6	356	0.712	6
325	3.25	427.65	11.870	295	0.590	497.1	340	0.680	572.9	370	0.740	6
350	3.50	460.53	11.916	310	0.620	520.3	362	0.724	607.6	386	0.772	6
375	3.75	493.42	11.961	324	0.648	541.8	374	0.748	625.4	396	0.792	6
400	4.00	526.32	11.971	330	0.660	551.3	380	0.760	634.9	408	0.816	6
425	4.25	559.21	12.031	332	0.664	552.7	386	0.772	642.6	415	0.830	6
450	4.5	592.11	12.055	334	0.668	534.1	388	0.776	643.7	419	0.838	6
475	4.75	625.00	12.102	338	0.676	558.6	388	0.766	641.2	424	0.848	7
500	5.0	657.90	12.140	340	0.680	560.1				426	0.852	7
525	5.25	690.79	12.183	342	0.684	561.44				427	0.854	7
550	5.5	723.68	12.226	342	0.684	559.5				427	0.854	

d. DATA SHEET FOR TRIAXIAL COMPRESSION

Sr = 80%

INITIAL WT.: 161gms

DIA. OF SAMPLE: 38mm

FINAL WT.

LENGTH OF SAMPLE:

1	2	3	4	Cell Pressure									
				$\sigma 3_1$			$\sigma 3_2$			$\sigma 3_3$			
Disp. Dial Rdg Div.	Change in length L Col. X gauge const.	Strain $\frac{\Delta L}{L_0} \times 10^{-4}$	Corr. Area A_c $\frac{A_0}{1} \times 10^{-4} m^2$	Load dial Rdg. LRD (Div)	Deviator load L_D LRD x LRF KN	Deviator stress $\sigma_D = \frac{L_D}{A_c}$	Load dial Rdg. LDR (Div)	Deviator load $\sigma_u = LRD \times LR$	Deviator stress L_q	Load dial Rdg. LRD (Div)	Deviator load L_D LRD x LRF KN	De St σ_D
25	0.25	32.9	11.379	10	0.020	17.6	20	0.040	35.2	53	0.106	93.
50	0.50	65.79	11.416	20	0.040	35.0	35	0.070	61.3	93	0.186	16.
75	0.75	98.68	11.454	33	0.066	57.6	62	0.124	108.3	127	0.254	22
100	1.0	131.58	11.494	48	0.096	83.5	95	0.190	165.3	156	0.312	27
125	1.25	164.47	11.531	62	0.124	107.5	120	0.240	208.1	185	0.370	32
150	1.5	197.37	11.573	85	0.170	146.9	142	0.284	245.4	207	0.414	35
175	1.75	230.26	11.614	116	0.232	199.8	164	0.328	282.4	225	0.450	38
200	2.00	263.16	11.655	140	0.280	240.2	172	0.344	295.2	242	0.484	46.
225	2.25	296.05	11.697	164	0.328	280.4	184	0.368	314.6	258	0.516	44
250	2.5	328.95	11.739	181	0.362	308.2	200	0.400	340.7	270	0.540	46
275	2.75	361.84	11.783	195	0.390	331.0	214	0.428	363.2	281	0.562	47
300	3.00	394.74	11.807	203	0.406	343.9	226	0.452	382.8	290	0.580	49
325	3.25	427.65	11.870	208	0.416	350.5	238	0.476	401.0	297	0.544	50
350	3.50	460.53	11.916	211	0.422	354.1	250	0.500	419.6	306	0.612	51
375	3.75	493.42	11.961	213	0.426	356.2	258	0.516	431.4	308	0.616	51
400	4.00	526.32	11.971	213	0.426	355.9	260	0.520	434.4	310	0.620	51
425	4.25	559.21	12.031			552.7	272	0.544	452.8	312	0.624	51
450	4.5	592.11	12.055			534.1	278	0.556	461.2	314	0.628	52
475	4.75	625.00	12.102			558.6	282	0.564	466.0	316	0.632	52
500	5.0	657.90	12.140			560.1	284.	0.568	467.9	317	0.634	52
525	5.25	690.79	12.183			561.44	286	0.572	469.5	317	0.634	52
550	5.5	723.68	12.226			559.5	286	0.572	467.9			

e. DATA SHEET FOR TRIAXIAL COMPRESSION

Sr = 100%

INITIAL WT.: 158gms | **DIA. OF SAMPLE:**

FINAL WT. | **LENGTH OF SAMPLE:**

1	2	3	4	Cell Pressure								
				$\sigma 3_1$			$\sigma 3_2$			$\sigma 3_3$		
Disp. Dial Rdg Div.	Change in length L Col. X gauge const.	Strain $\frac{\Delta L}{L_0}\times 10^{-}$	Corr. Area A_c $\frac{A_c}{1}\times 10^{-4}m$	Load dial Rdg. LRD (Div)	Deviator load L_D LRD x LRF KN	Deviator stress $\sigma_D = \frac{L_D}{A_c}$	Load dial Rdg. LDR (Div)	Deviator load L_D LRD x LRF KN	Deviator stress $\sigma_D = \frac{L_D}{A_c}$	Load dial Rdg. LRD (Div)	Deviator load L_D LRD x LRF KN	Devi stre $\sigma_D =$
25	0.25	32.9	11.379	18	0.036	31.6	32	0.064	56.2	47	0.094	82.6
50	0.50	65.79	11.416	28	0.056	49.1	56	0.112	98.1	77	0.154	134.
75	0.75	98.68	11.454	42	0.054	73.3	64	0.128	111.8	112	0.224	195.
100	1.0	131.58	11.494	55	0.110	95.7	112	0.224	194.9	138	0.276	240.
125	1.25	164.47	11.531	74	0.148	128.4	130	0.260	225.5	162	0.324	281.
150	1.5	197.37	11.573	94	0.188	162.5	144	0.288	248.9	183	0.366	316.
175	1.75	230.26	11.614	114	0.228	196.3	158	0.316	272.1	197	0.394	339.
200	2.00	263.16	11.655	134	0.268	229.9	170	0.340	291.7	212	0.424	339.
225	2.25	296.05	11.697	150	0.300	256.5	182	0.364	311.2	223	0.446	363.
250	2.5	328.95	11.739	168	0.336	308.9	194	0.388	330.5	232	0.464	381.
275	2.75	361.84	11.783	182	0.364	328.6	208	0.416	353.1	242	0.484	325.
300	3.00	394.74	11.807	194	0.388	343.7	218	0.436	369.3	250	0.500	410.
325	3.25	427.65	11.870	204	0.408	355.8	222	0.444	374.1	255	0.516	424.
350	3.50	460.53	11.916	212	0.424	351.1	234	0.468	397.8	258	0.522	429.
375	3.75	493.42	11.961	210	0.420	357.5	244	0.488	408.0	261	0.528	433.
400	4.00	526.32	11.971	208	0.416		249	0.498	416.0	264	0.534	436.
425	4.25	559.21	12.031				253	0.506	421.2	267	0.536	441.
450	4.5	592.11	12.055				254	0.508	421.4	268	0.540	444.
475	4.75	625.00	12.102				254	0.508	419.8	270	0.540	444.
500	5.0	657.90	12.140							270		446.
525	5.25	690.79	12.183									444.
550	5.5	723.68	12.226									

f. DATA SHEET FOR SPECIFIC GRAVITY TEST.

PROJECT: Experiment on Black cotton soil **BOREHOLE No.**

LOCATION: BANJIRAM, Adamawa State **SAMPLE No.**

DESCRIPTION: **DEPTH: 1.5m.**

Bottle No		**Sample No**			**Sample No**	
		1	2			
Weight of bottle + soil	W_2	140.6	134.8			
Weight of bottle	W_1	78.7	77.7			
Weight of soil $W_2 - W_1$	$= W_S$	61.9	57.1			
Weight of bottle + soil + water	W_3	238.2	233.2			
Weight of bottle + soil	W_2	140.6	134.8			
Weight added water $W_3 - W_2$	V_a	97.6	98.4			
Weight of bottle full of water	W_4	203.6	200.9			
Weight of bottle	W_1	78.7	77.7			
Weight of water $W_4 - W_1$	$= V_B$	124.9	123.2			
Weight of water	V_B	124.9	123.2			
Weight of added water	V_a	97.6	98.4			
Volume of soil = $V_B - V_a$	$=V_s$	27.3	24.8			
S.G. = W_s/V_s		2.27	2.30			

Average S.G. = 2.29 Average S.G.

g. **DATA SHEET FOR HYDROMETER ANALYSIS**

PROJECT:

DEPTH

LOCATION:

HYDROMETER CONSTANT

DESCRIPTION:

DRY MASS USED: 50gms

INITIAL WT. USED: WT. PASSING:

CORRECTIONS: $C_m = 0.5$ $C_w = 1.0$ M_t: 0.8 $X_d = +3.5$ $C_t = C_m + C_w + M_t + X_d = -1.2$

K = 0.00447 $D = k\sqrt{\frac{H}{t}}$ G_s = 2.29

Elapsed time t (min)	Hyd-Rdg. Rh	Actual Hyd. Rdg. $R_a = R_h + C_m$	Eff. Depth H (mm) 220-4.1Ra H	Corr.Hyd. Rdg. $Rc = R_h + Ct$	Particle size D (mm)	% tage finer N%	Cum. % tage Fine N
½	28.5	29.0	101.0	27.3	0.06356	96.90	90.12
1	28.0	28.5	103.15	26.8	0.04540	95.15	88.49
2	26.5	27.0	109.55	25.3	0.03304	89.82	83.53
4	24.0	24.5	119.55	22.8	0.02443	80.95	75.28
8	22.0	22.5	127.75	20.8	0.01786	73.85	68.68
15	20.0	20.5	135.95	18.8	0.01346	66.75	62.38
30	17.5	18.0	146.20	16.3	0.00987	57.87	53.82
60	15.6	15.5	156.45	13.8	0.00722	49.00	45.57
120	13.0	13.5	164.65	11.8	0.00524	41.89	38.96
240	10.0	10.5	176.95	8.8	0.00384	31.24	29.05
1080	6.0	6.45	193.35	5.3	0.00189	18.82	17.50

$$N\% = \frac{100Gs}{Wd(Gs-1)}R_c$$

h. DATA SHEET FOR SIEVE ANALYSIS

Project

Location

Description

Initial (Wt Used: 200gms.

Sieve size (mm)	Wt. Ret (gms).	% Ret.	% Passing
1.700	5	2.5	97.5
1.180	2	1.0	96.5
0.600	1	0.5	96.0
0.425	1	0.5	95.5
0.300	2	1.0	94.5
0.150	2	1.0	93.5
0.075	1	0.5	93.0

i. DATA SHEET FOR CONSOLIDATION TEST

(Calculation of coefficient of consolidation and compression ratios)

Equivalent height of the solid Hs = 1.532 Cm

Degree of saturated 'S' = 20%

1ST CYCLE

Pressure (KN/m^2)	52	104	208	416
In. ht. (H_I)	20.00	19.66	19.46	19.18
In. D.R.	1000	966	948	920
F. D. R	966	948	920	886
Δ D.R	34	18	28	34
Δ ht.	0.34	0.18	0.28	0.34
F. ht. (H_f)	19.66	19.46	19.18	18.84
Av. Ht. (mm) $[\frac{1}{2}(H_I + H_F)]$	19.83	19.56	19.32	19.01
Cv (Cm^2/min)	0.3705	0.2133	0.4342	0.4204
e_1	0.282	0.270	0.252	0.230
e_2	0.252	0.242	0.236	

2ND CYCLE

Pressure(KN/m^2)	104	208	416	832	1664
In. ht. (H_I)	19.18	19.15	19.03	18.75	18.41
In. D.R.	900	897	885	857	823
F. D. R	897	885	857	823	784
Δ D.R	3	12	28	34	39
Δ ht.	0.03	0.12	0.28	0.34	0.39
F. Ht.	19.15	19.03	18.75	18.41	18.02
Av. ht. (mm) $[\frac{1}{2}(H_I + H_F)]$	19.17	19.09	18.89	18.58	18.22
Cv (Cm^2/min)	0.3439	0.1892	0.3286	0.2332	0.2741
e_1	0.250	0.242	0.224	0.202	0.176
e_2	0.198		0.187	0.180	

j. DATA SHEET FOR CONSOLIDATION TEST

(Calculation of coefficient of consolidation and compression ratios)

Equivalent height of the solid Hs = 1.587 Cm

Degree of saturated 'S' = 40%

1ST CYCLE

Pressure(KN/m^2)	52	104	208	416
In. ht. (H_I)	20.00	19.74	19.32	18.95
In. D.R.	1000	974	932	894
F. D. R	974	932	894	827
Δ D.R	26	42	38	67
Δ ht.	0.26	0.42	0.38	0.67
F. ht. (H_f)	19.74	19.32	18.94	18.27
Av. ht. (mm) $[\frac{1}{2}(H_I + H_F)]$	19.87	19.53	19.13	18.61
Cv (Cm^2/min)	0.2093	0.3594	0.2685	0.2396
e_1	0.244	0.217	0.194	0.151
e_2	0.200	0.186	0.164	

2ND CYCLE

Pressure(KN/m^2)	104	208	416	832	1664
In. ht. (H_I)	19.04	18.87	18.57	18.19	17.68
In. D.R.	900	883	850	812	771
F. D. R	883	850	812	771	685
Δ D.R	17	30	38	51	86
Δ ht.	0.17	0.30	0.38	0.51	0.86
F. ht.(H_f)	18.87	18.57	18.19	17.68	16.82
Av. ht. (mm) $[\frac{1}{2}(H_I + H_F)]$	19.00	18.72	18.38	17.94	17.25
Cv (Cm^2/min)	0.3385	0.2729	0.2631	0.2664	0.2863
e_1	0.189	0.170	0.146	0.106	0.060
e_2	0.132	0.114	0.098	0.080	

k. DATA SHEET FOR CONSOLIDATION TEST

(Calculation of coefficient of consolidation and compression ratios)

Equivalent height of the solid Hs = 1.564 Cm

Degree of saturated 'S' = 60%

1ST CYCLE

Pressure(KN/m^2)	52	104	208	416
In. ht. (H_I)	20.00	19.42	19.07	18.58
In. D.R.	1000	942	907	858
F. D. R	942	907	858	786
Δ D.R	58	35	49	72
Δ ht.	0.58	0.35	0.49	0.72
F. ht. (H_F)	19.42	19.07	18.58	17.86
Av. ht. (mm) $[\frac{1}{2}(H_I + H_F)]$	19.71	19.25	18.83	18.22
Cv (Cm^2/min)	0.3025	0.1913	0.2453	0.2435
e_1	0.242	0.219	0.188	0.142
e_2	0.188	0.167	0.156	

2ND CYCLE

Pressure(KN/m^2)	104	208	416	832	1664
In. ht. (H_I)	18.58	18.34	18.00	17.64	17.02
In. D.R.	900	886	852	818	748
F. D. R	886	852	818	748	654
Δ D.R	14	34	34	62	94
Δ ht.	0.14	0.34	0.34	0.62	0.94
F. ht.(H_F)	18.34	18.00	17.64	17.02	16.08
Av. ht. (mm) $[\frac{1}{2}(H_I + H_F)]$	18.46	18.17	17.82	17.33	16.55
Cv (Cm^2/min)	0.4275	0.3111	0.1967	0.1592	0.2738
e_1	0.175	0.153	0.128	0.088	0.028
e_2	0.106	0.086	0.065	0.046	

I. DATA SHEET FOR CONSOLIDATION TEST

(Calculation of coefficient of consolidation and compression ratios)

Equivalent height of the solid Hs = 1.538 Cm

Degree of saturated 'S' = 80%

1ST CYCLE

Pressure(KN/m^2)	52	104	208	416
In. ht. (H_I)	20.00	19.76	19.66	19.50
In. D.R.	1000	976	966	950
F. D. R	976	966	950	907
Δ D.R	24	10	16	43
Δ ht.	0.24	0.10	0.16	0.43
F. ht. (H_f)	19.76	19.66	19.50	19.07
Av. ht. (mm) $[\frac{1}{2}(H_I + H_F)]$	19.88	19.71	19.58	19.29
Cv (Cm^2/min)	1.160	1.464	0.3612	0.2728
e_1	0.285	0.278	0.268	0.240
e_2	0.260	0.256	0.247	

2ND CYCLE

Pressure(KN/m^2)	104	208	416	832	1664
In. ht. (H_I)	19.42	19.35	19.23	18.95	18.46
In. D.R.	900	893	881	853	804
F. D. R	893	881	853	804	751
Δ D.R	7	12	28	49	53
Δ ht.	0.07	0.12	0.28	0.49	0.53
F. ht.(H_f)	19.35	19.23	18.95	18.46	17.93
Av. ht. (mm) $[\frac{1}{2}(H_I + H_F)]$	19.39	19.29	19.09	18.71	18.20
Cv (Cm^2/min)	0.4714	0.2898	0.3942	0.3784	0.3825
e_1	0.258	0.250	0.228	0.177	0.116
e_2	0.200	0.180	0.158	0.138	

m. DATA SHEET FOR CONSOLIDATION TEST

(Calculation of coefficient of consolidation and compression ratios)

Equivalent height of the solid Hs = 1.495 Cm

Degree of saturated 'S' = 100%

1ST CYCLE

Pressure(KN/m^2)	52	104	208	416
In. ht. (H_I)	20.00	19.56	19.30	18.93
In. D.R.	1000	956	930	893
F. D. R	956	930	893	812
Δ D.R	44	26	37	81
Δ ht.	0.44	0.26	0.56	0.62
F. ht. (H_f)	19.56	19.30	18.93	18.12
Av. ht. (mm) $[\frac{1}{2}(H_I + H_F)]$	19.78	19.43	19.12	18.53
Cv (Cm^2/min)	0.7523	0.6052	0.4958	0.4305
e_1	0.308	0.291	0.266	0.212
e_2	0.258	0.240	0.228	

2ND CYCLE

Pressure(KN/m^2)	104	208	416	832	1664
In. ht. (H_I)	18.96	18.67	18.45	18.00	16.74
In. D.R.	900	871	849	804	678
F. D. R	871	849	804	678	550
Δ D.R	29	22	45	126	128
Δ ht.	0.29	0.22	0.45	1.26	1.28
F. ht.(H_f)	18.67	18.45	18.00	16.74	15.46
Av. ht. (mm) $[\frac{1}{2}(H_I + H_F)]$	18.81	18.56	18.23	17.37	16.10
Cv (Cm^2/min)	1.3450	0.4770	0.6039	0.3614	0.7081
e_1	0.249	0.234	0.204	0.120	0.034
e_2	0.168	0.134	0.100	0.068	

APPENDIX 4

(a) Results of Liquid Limit Test.

Form 8

Liquid and plastic limits

Liquid limit using the cone penetrometer

Operator: Job: Site:

Date: Borehole No:

Description of soil: Black Cotton Soil Sample No:

Depth of sample: 1·5m

Test details: Proportion of sample on 425 μm BS test sieve 95·5 %.
Soil conditions natural moisture content, air dried, unknown*
*Delete as appropriate
Soil equilibrated with water for ...... h.

Test No.		1	2	3	4	5	6
Type of test† Liquid Limit (LL)							
Initial dial gauge reading	mm	6·5	7·0	6·5	6·4	6·3	
Final dial gauge reading	mm	19·8	28·5	27·1	30·8	32·0	
Cone penetration	mm	13·3	16·5	20·6	24·4	26·3	
Container No.							
Mass of wet soil + container	g	28·2	31·3	31·1	31·1	33·0	
Mass of dried soil + container	g	24·3	26·3	25·9	26·3	29·4	
Mass of container	g	16·3	16·3	16·3	16·3	16·3	
Mass of moisture	g	3·9	5·0	5·2	5·7	7·9	
Mass of dry soil	g	8·0	10·0	9·6	10·0	13·1	
Moisture content (w)	%	48·8	50·0	54·2	57·0	60·3	

†Type of test: Natural moisture content (N), Liquid limit (LL), Plastic limit (PL).

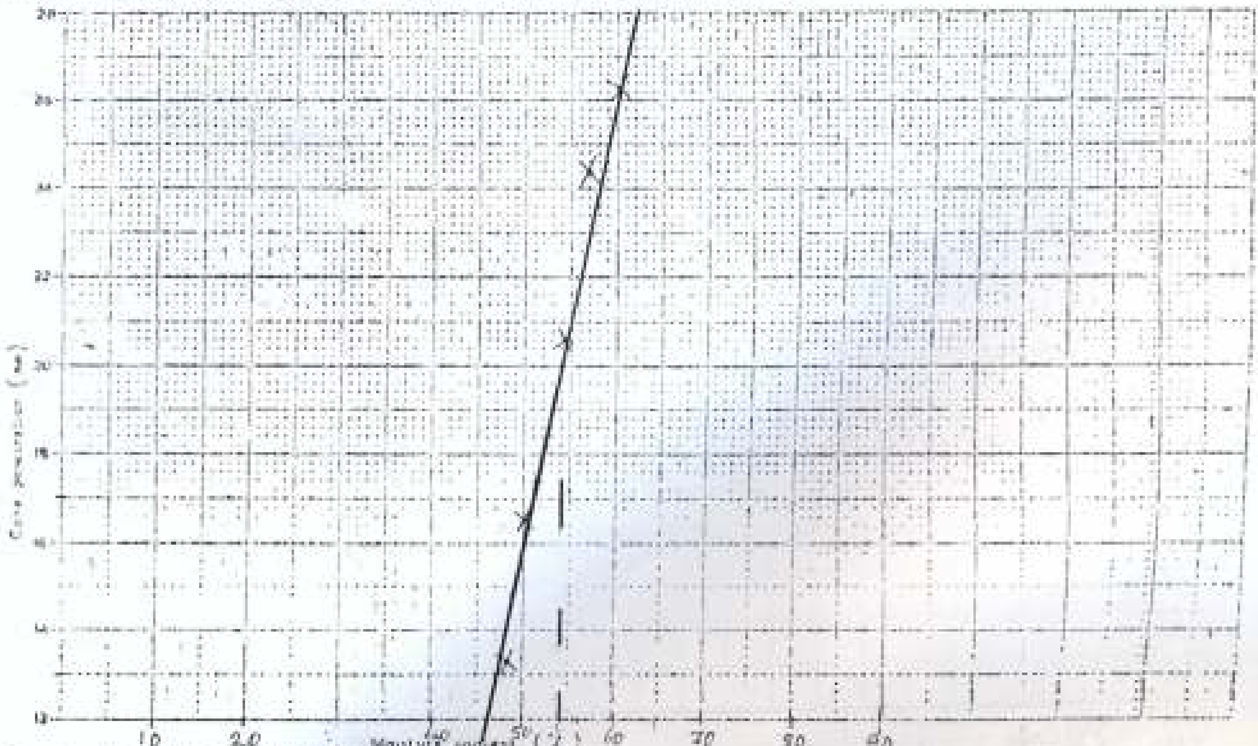

Results: Liquid limit (LL): 54%

Plastic limit (PL) 22·8%

Plasticity index (PI) 31·2%

54% Soil classification

(b) Results of Plastic Limit Test.

Form B

Liquid and plastic limits

Liquid limit using the cone penetrometer

Operator | Job: | Site:
Date: | | Borehole No:
Description of soil: Black Cotton Soil | | Sample No:
| | Depth of sample: 1·5 m

Test details: Proportion of sample on 425 μm BS test sieve, 95·5 %.
Soil conditions natural moisture content, air dried, unknown*
*Delete as appropriate
Soil equilibrated with water for ...... h.

L_o = 140mm
L_f = 125mm

Test No.		1	2	3	4	5	6
Type of test† Plastic Limit (PL)							
Initial dial gauge reading Final dial gauge reading Cone penetration	mm mm mm						
Container No. Mass of wet soil + container Mass of dried soil + container Mass of container	 g g g	 40·0 35·6 16·3	 33·0 30·0 16·3				
Mass of moisture Mass of dry soil Moisture content (w)	g g %	4·4 19·3 22·8	3·1 13·7 22·7				

† Type of test: Natural moisture content (N), Liquid limit (LL), Plastic limit (PL).

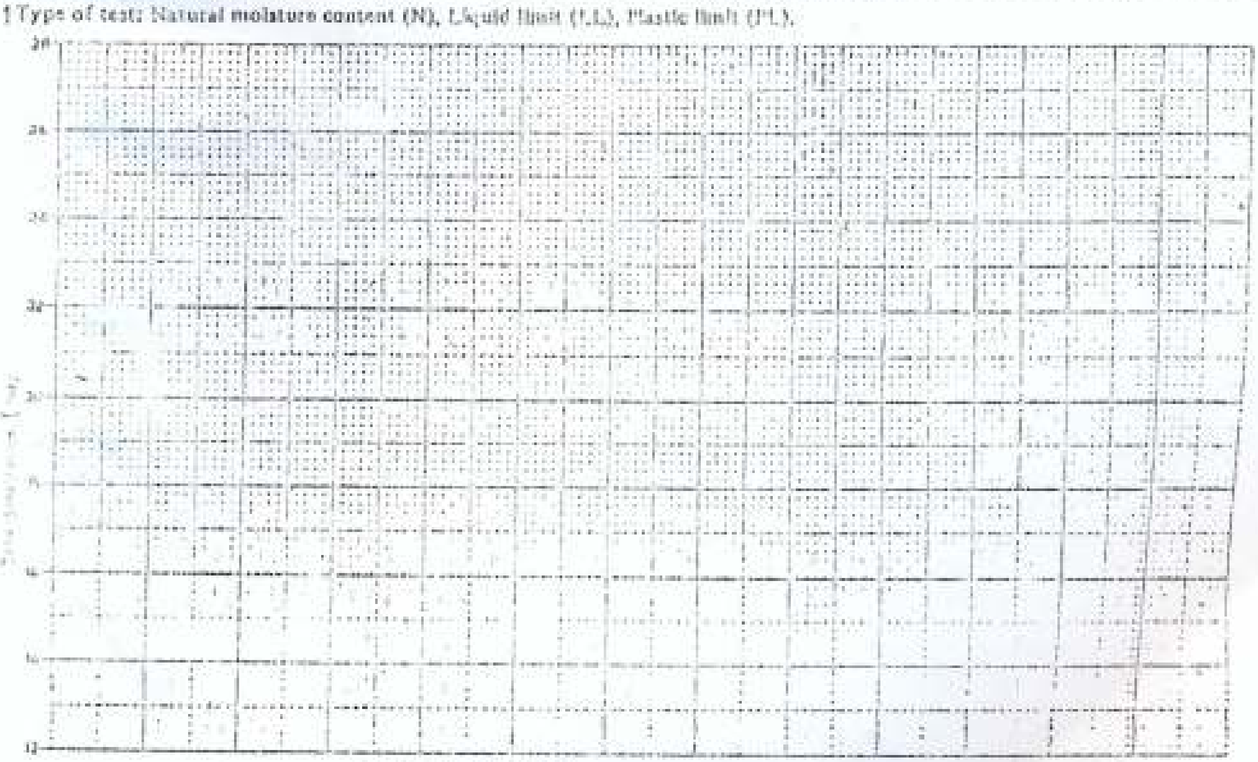

Results: Liquid limit (LL):
Plastic limit (PL) 22.8%
Plasticity index (PI)

Soil classification

Linear Shrinkage = $\frac{140-125}{140}$ = 11%